



POLITECNICO
MILANO 1863

SCUOLA DI INGEGNERIA INDUSTRIALE
E DELL'INFORMAZIONE

Polarons in P3HT: unravelling vibrational fingerprints of ordered and disordered doped phases in solids and solutions. IR and Raman study of the polymers and oligomers.

TESI DI LAUREA MAGISTRALE IN
MATERIALS ENGINEERING AND NANOTECHNOLOGY
INGEGNERIA DEI MATERIALI E DELLE NANOTECNOLOGIE

Author: **Sara Doti**

Student ID: 987461

Advisor: Luigi Brambilla

Co-advisor: Chiara Castiglioni

Academic Year: 2022-23

Abstract

Understanding the doping mechanism in conjugated polymers is of high importance for optimizing their electronic transport properties. In this work we delve into the study of the doping process of regioregular poly(3-hexylthiophene-2,5-diyl), or P3HT, with iodine (I_2) and F_4TCNQ , both in solution and through exposure to iodine vapours. The doping process in solution was carried out controlling the molar ratio of the dopant agent. Vibrational spectroscopy, both IR and Raman, is used as a tool to investigate the doping mechanism. The acquired vibrational spectra reveal the interaction between P3HT and the dopant showing significant differences when the system is in solution or in solid film. This observation led to the identification of several, and so far unknown features of the doping process, contributing to a richer comprehension of the mechanism.

Moreover, this work focuses on the characterization and study of the different charged defects that can be present in doped P3HT systems: ordered and disordered polaron phases and charge transfer complexes.

Since our aim is a deep study of the doping process several additional experiments were conducted involving model molecules (P3HT oligomers) and two different polymers (regiorandom P3HT and P3DT), which allow to understand the role of the backbone and of the alkyl side chains in the doping.

Key-words: poly(3-hexylthiophene-2,5-diyl), conjugated polymers, vibrational spectroscopy, polaron phase, charge transfer.

Abstract in italiano

La comprensione del meccanismo di doping nei polimeri coniugati riveste un'importanza fondamentale per ottimizzare le loro proprietà di trasporto elettronico. Questo lavoro si focalizza sullo studio del processo di doping del polimero regioregolare poli(3-esiltiofene-2,5-diyl), noto come P3HT, utilizzando iodio (I_2) e F_4TCNQ come droganti, sia in soluzione che attraverso l'esposizione ai vapori di iodio. Il processo di doping in soluzione è stato condotto controllando il rapporto molare dell'agente dopante. La spettroscopia vibrazionale, sia infrarossa (IR) che Raman, è stata utilizzata come strumento per investigare il meccanismo di doping. I dati spettrali vibrazionali acquisiti rivelano l'interazione tra il P3HT e il dopante, mostrando significative differenze quando il sistema è in soluzione o in forma solida. Questa osservazione ha portato all'identificazione di diverse caratteristiche non ancora note del processo di doping, contribuendo ad una comprensione più approfondita del meccanismo.

Inoltre, questo lavoro si concentra sulla caratterizzazione e lo studio dei differenti difetti di carica che possono essere presenti nei sistemi di P3HT dopati: fasi polaroniche ordinate e disordinate e complessi a trasferimento di carica.

Poiché il nostro obiettivo è uno studio approfondito del processo di doping, sono stati condotti diversi esperimenti aggiuntivi che coinvolgono molecole modello (oligomeri P3HT) e due polimeri diversi (P3HT regiorandom e P3DT), che consentono di comprendere il ruolo del backbone del polimero e delle catene alchiliche nel processo di doping.

Parole chiave: poli(3-esiltiofene), polimeri coniugati, spettroscopia vibrazionale, polarone, trasferimento di carica.

Contents

Abstract	i
Abstract in italiano	iii
Contents	v
Introduction	1
1 Doping of conjugated polymers: ICT and CTC	3
2 Experimental section	7
2.1 Materials preparation	7
2.2 Characterization	9
2.2.1 Vibrational spectroscopy of conjugated polymers	9
2.2.2 Characterization of liquid and solid samples	11
2.2.3 Characterization of pristine P3HT	12
2.2.4 Polaron vibrational signature in the literature	15
3 Results and discussion	19
3.1 FT-IR spectroscopy.....	19
3.1.1 FT-IR spectra of doped P3HT in solution	19
3.1.2 FT-IR spectra of doped P3HT solid film.....	30
3.1.3 Influence of the backbone conformation and the side alkyl chains in the doping process.....	38
3.1.3.1 FT-IR spectra of doped regiorandom P3HT in solution	38
3.1.3.2 FT-IR spectra of doped P3DT in solution	47
3.1.3.3 FT-IR spectra of doped oligothiophenes in solution	54
3.1.4 IR spectra of P3HT and rraP3HT doped by iodine vapours	65
3.2 FT-Raman spectroscopy	77
3.2.1 FT-Raman spectra of doped regioregular P3HT in solution	77
3.2.2 Influence of the backbone conformation and the side alkyl chains in the doping process.....	89
3.2.2.1 FT-Raman spectra of doped regiorandom P3HT: role of the backbone.	90
3.2.2.2 FT-Raman spectra of doped P3DT: role of the lateral alkyl chains.	93
3.2.2.3 FT-Raman spectra of doped oligothiophenes: role of the backbone length.	95
4 Conclusions and future developments	103

Bibliography	105
List of Figures	111
List of Tables	120
Acknowledgments	121

Introduction

Most polymers are typically insulators, for this reason they are not considered interesting material from the point of view of their electronic transport properties, but there is a family of polymers, conjugated polymers, that can exhibit semiconducting or even metallic properties. This is thanks to the alternating single and multiple bonds in the polymer backbone that results in π -electrons conjugation. [1] The simplest example of conjugated polymer is polyacetylene. The discovery in 1977 by Shirakawa et al. that polyacetylene can be doped after synthesis with many different dopants, draw the attention on the field of organic semiconductors (OSC). The possibility to tune their electronic structure, either by changing the polymer structure (e.g., through the choice of different chemical units) or doping, allows the development of low cost and flexible organic electronic devices. [2],[3],[4] OSC technology can offer prospects for the overcome of energy issues with their applications in light-emitting diodes (OLEDs), organic solar cells, and organic field-effect transistors (OFETs). [5]

It was shown that by suitable doping it is possible to increase by several orders of magnitude the conductivity of OSC thin films. For this reason, a complete understanding of the doping of organic semiconductors is an important step for the development of the field of organic electronics. [6]

The polymer of interest of this work is poly(3-hexylthiophene-2,5-diyl), or P3HT. The poly-alkyl-thiophenes family is one of the most widely studied between many conjugated polymers because of several features that distinguish them from other polyconjugated systems. For example, a first advantage is the possibility to be solubilized so that they can be processed by solution and they can be doped both chemically and electrochemically. [7] This allows these materials to be of much interest in application in organic electronics, like in the field of polymer-based photovoltaic devices. [8] In this work, doping of P3HT by both iodine and 2,3,5,6-tetrafluoro-7,7,8,8-tetracyanoquinodimethane (F_4TCNQ) is studied. In particular, the second one is a molecule that is highly used in organic-based electronics because of its properties as electron acceptor with a quite high electron affinity. For this reason, this molecule is widely used for increasing the conductivity in devices like OLEDs or OFETs but is also used for the doping of hole transporting materials in photovoltaics. [9] Two different doping process are studied: doping in solution and by exposure to vapours dopant. This last method has been the subject of recent reports and it allows to obtain film with a high conductivity, however, a problem could be how to control the amount of dopant added to the system. [10] Controlled processes have been adopted in this work,

starting from the doping in solution up to the deposition of the doped solution in thin films.

The aim of this study is to better understand the mechanism of P3HT doping. To this aim, also samples of doped regiorandomP3HT and of dodecyl-substituted, P3DT, were used to investigate the effect of conformational order and the influence on the doping process of the alkyl side chains. Finally, the behaviour of the polymer is also compared to three different P3HT oligomers: 8T, 13T and 21T, which have been subjected to doping.

1 Doping of conjugated polymers: ICT and CTC

Doping of organic semiconductors is not like doping of inorganic semiconductors where the dopants are impurity atoms with a different number of valence electrons from the host material. Chemical doping of π -conjugated materials consists of redox reactions between the host and dopant. Stable doping of OSCs is obtained by adding strong molecular donors or acceptors to conjugated polymers. Achieving a stable doping of OSCs is difficult and the mechanism of doping is still nowadays not completely understood for many dopants that are already widely used. [11] The doping molecules must have proper energy levels so that a charge transfer reaction can occur between the two partners, for example for p-type doping the LUMO of the dopant should be close or deeper than the HOMO of the conjugated polymer. [6] The doping process involves a random dispersion of the dopant in the polymer matrix that binds with the polymer chain thanks to weak noncovalent interactions. Several features limit the doping efficiency, for example, molecular doping allows to increase the charge carrier density but at the same time it can also affect the ordered polymer stacking structures, reducing the carrier mobility. [12] For these reasons, the optimization of the properties of the doped material requires a deep knowledge of the doping process and insight into the structure of the doped material.

There are two different models that are commonly used to describe the donor-acceptor interaction. The first one is the integer charge transfer model (ICT), where a hole (p-doping) is transferred from the dopant to the polymer chain resulting in a positively charged defect. [13] In case of the two dopants used in this work, since they are both strong acceptors, a positive charge is formed on the P3HT chain and a counter ion (I_3^- or F_4TCNQ^-) is generated. There is experimental evidence that the dopant molecules reside in the aliphatic side-chain regions. [11] If an electron is removed from the pristine P3HT, the positive charge which remains on the polymer chain is delocalized on several thiophene rings. There is a distortion of the backbone that locally changes the structure from aromatic towards a more quinoidal one, as showed in Figure 1. The unpaired electron that remains on the polymer chain together with the distorted backbone structure, forms a polaron. [14],[15] There are different theories on the extension of the polaron on the P3HT chain, but the polaron length is considered to be between 7 and 4 thiophene rings.

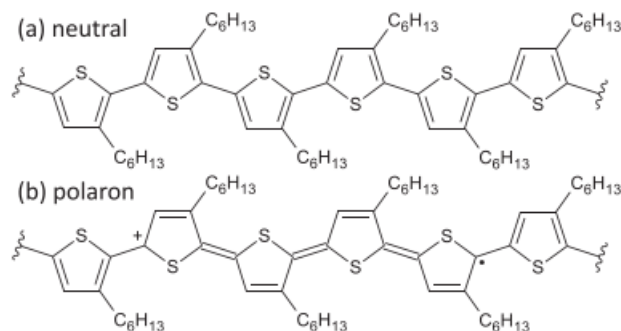


Figure 1: Chemical structures of a) neutral P3HT, b) P3HT polaron [14]

Due to the formation of the polaron two localized electronic states are present in the gap of the pristine polymer, which creates two new allowed optical transitions, showed in Figure 2. [14],[15]

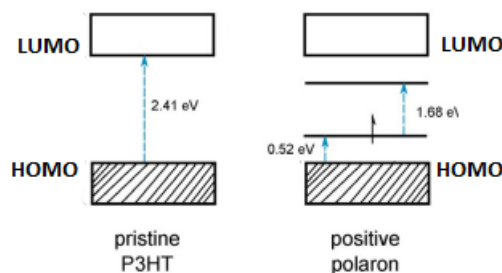


Figure 2: schematic representation of the energy level diagrams of pristine P3HT and positive polaron after chemical p-doping. The possible electronic transitions are highlighted by the blue arrows. The black arrow on the first localized state in the gap of the p-doped polymer represents an unpaired electron. [14]

Experimental and theoretical studies during the past years have shown that in some cases the interaction of host and dopant can result in formation of a charge-transfer complex (CTC), in which the consequence of the interaction is a partial charge transfer. While in ICT ionic species are formed, CTCs should be considered tightly bounded pairs electrically neutral. [11] These two different mechanisms are represented in Figure 3.

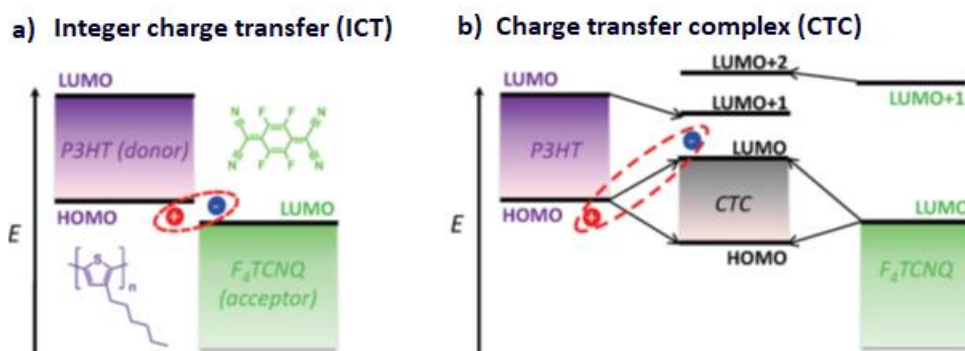


Figure 3: schematic representation of the different models to describe the charge transfer between P3HT and F₄TCNQ: a) integer charge transfer (ICT) where a hole electron is transferred resulting in a charged defect; b) charge transfer complex (CTC) in which there is a partial charge transfer between polymer and dopant. [13]

The ICT model fully fit the theoretical description of the polaron defect, where the two net charges resulting upon doping are weakly interacting, so with the name “polaron” we will specifically indicate ICT state. When doping, CTCs are not desired since they increase the polymer conductivity much less than ICT. CTCs have a low dissociation rate and the energy required to break the bond between ionized dopants and generated charges is very high due to the strong Coulombic forces created between the charges. For this reason, the charge generation efficiency (CGE), defined as the ratio between the free charge carriers generated and the numbers of dopant molecules participating in the doping, is significantly lower. [16] Fortunately, ICT is the favoured mechanism, while CTCs are rarer. This is due to the kinetic of the two processes: dopants molecules prefer to reside in the polymer lamellar spacing along the polymer side chains since the energy barrier to insert between the side chains is smaller than the one required to break the π -stacking of the polymer chains. The first case leads to the formation of ICT because the wave function overlap between the donor and acceptor is not sufficient for the formation of CTC. On the other hand, the second case, less favoured, leads to the formation of CTC species, where the dopant is able to form π -stacked complex with the conjugated polymer. [17] By the use of vibrational spectroscopy the signatures of these structures were recognised and assigned in this work.

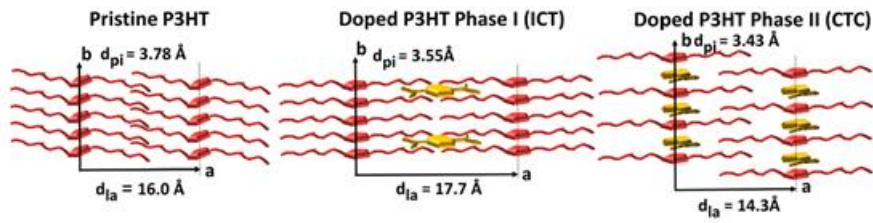


Figure 4: schematic representation of a) pristine P3HT crystal structures; b) ICT structure of doped P3HT where the dopant resides in the lamellar region; c) CTC structure where the dopant resides in the π -stacking of the polymer chains [17]

2 Experimental section

2.1 Materials preparation

The aim of the experiments done in this work is to study the effect of doping of regioregular poly(3-hexylthiophene-2,5-diyl), or P3HT, ($M_w=50000-65000$ g/mol, polydispersity index < 6.0 , $RR \geq 90\%$).

In addition, for a wider understanding of the process, are analysed samples of:

- i) regiorandom poly(3-hexylthiophene-2,5-diyl), or rraP3HT;
- ii) Poly(3-decylthiophene-2,5-diyl), or P3DT, (average $M_w=42000$ g/mol; regioregular);
- iii) oligothiophenes (OTs) with 8, 13 and 21 monomer units, respectively named 8T, 13T and 21T.

All the polymers' samples are purchased from Sigma Aldrich, while the oligomers were synthesized by Felix P. V. Koch and Paul Smith (Eidgenössische Technische Hochschule (ETH) Zürich).

The polymers are doped with iodine and F_4 TCNQ in solution with chloroform by gradually increasing the level of doping. I_2 (in form of flakes with a purity $\geq 99\%$), F_4 TCNQ (crystalline powder and/or chunk with a purity $\geq 97\%$) and chloroform (stabilized with amylenes, purity $\geq 99.5\%$) are purchased by Sigma Aldrich. Different solutions of P3HT polymer doped with iodine and F_4 TCNQ were prepared with an increasing molar ratio between polymer and dopant. Three different levels of doping were analysed: the less doped case is the 25:1 meaning that in the system there is one molecule of the dopant agent for every 25 hexyl thiophene unit, then the medium doping regime is the 5:1, one dopant molecule for every five thiophene rings, and, finally, the highly doped one, the 1:1, with one molecule of dopant for each monomer unit. The doping ratio and the solutions used are shown in Table 1 and Table 2. The final solutions were obtained by mixing a solution with fixed concentration of P3HT in chloroform, with solutions of the dopant agent in suitable concentration to obtain the final desired molar ratio.

Doping ratio	Thiophene rings	I_3^-	Solution of P3HT in $CHCl_3$	Solution of I_2 in $CHCl_3$
25:1	25	1	5 mg in 1 ml	1.3 mg in 15 ml
5:1	5	1	5 mg in 1 ml	2.3 mg in 5 ml
1:1	1	1	5 mg in 1 ml	1.8 mg in 2 ml

Table 1: doping ratio and concentration of the solutions of pristine P3HT in $CHCl_3$ and of I_2 in $CHCl_3$

Doping ratio	Thiophene rings	F_4TCNQ	Solution of P3HT in $CHCl_3$	Solution of F_4TCNQ in $CHCl_3$
25:1	25	1	5 mg in 1 ml	1.5 mg in 23 ml
5:1	5	1	5 mg in 1 ml	2 mg in 6.5 ml
1:1	1	1	5 mg in 1 ml	1 mg in 8 ml

Table 2: doping ratio and concentration of the solutions of pristine P3HT in $CHCl_3$ and of F_4TCNQ in $CHCl_3$

The doped solutions have been made by adding 0.5 ml of the dopant solution in 0.5 ml of the P3HT solution and leaving them for 10 minutes at room temperature. Immediately after the mixing of the two solutions it can be noticed a significant change in colour proving that the doping process is taking place. Since the efficiency of the reaction isn't known, the exact number of dopant molecules that will actually interact with the polymer chain can't be predicted, so the following representation of the doping ratio is just an indication of the level of doping obtained in the different solutions. Assuming an efficiency of the doping process of 100%, the situation that we have in each of the three cases, considering an extension of the polaron of about five P3HT monomer units, is represented in Figure 5. In the 25:1 few isolated polarons might be anticipated, in the 5:1 adjacent polaron and, finally, in the 1:1 an excess of dopant should be expected (the sketch in Figure 5.c could be quite unrealistic as in this case some amount of unreacted dopant molecules could be present in the solution).

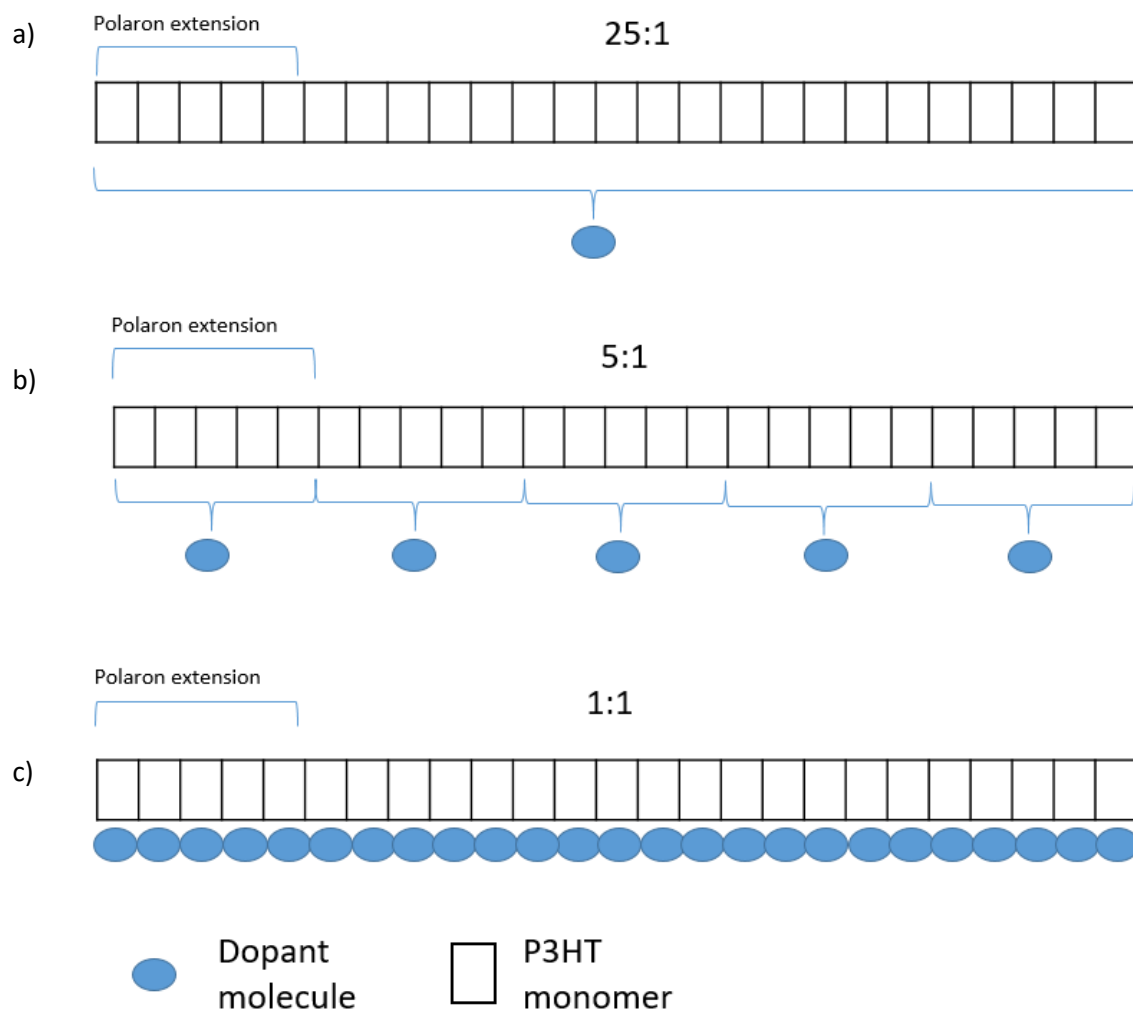


Figure 5: illustration of the three levels of doping a) low level of doping with one dopant molecule every 25 P3HT monomer unit; b) medium level of doping with one dopant molecule every 5 P3HT monomer unit; c) high level of doping with one dopant molecule for each P3HT monomer unit

2.2 Characterization

2.2.1 Vibrational spectroscopy of conjugated polymers

Thanks to the strong electron-phonon coupling, alteration in the electronic structure of π -conjugated polymers results in significant modification in the nuclear structure and dynamics. Vibrational spectroscopy (IR and Raman) is sensitive to variations of

the local dipole moments and the polarizability, and, for this reason, it has become a highly valuable tool for understanding the electronic and molecular structure within these systems. [18] In π -electron conjugated polymers in the crystalline phase, characterized by translational symmetry, collective oscillations in which the bond length alternation varies in phase are Raman-active normal modes but not IR-active. Indeed, the Raman spectra of these materials are characterized by strong peaks around $1600\text{-}1400\text{ cm}^{-1}$ that can be assigned to such collective skeletal vibration involving the whole chain. [19] These vibrations are assigned to the simultaneous stretching of the C=C and the shrinking of the C-C, usually coupled with CH wagging. These oscillations, called Effective Conjugation Coordinate (ECC) modes, are sensitive to the electronic structure and in particular to the conjugation length, which is affected by the overlapping between neighbouring $2p_z$ orbitals and so by the geometry of the system. Increasing the delocalization of π -electron there is a decrease in the energy of these vibrational transitions and a higher Raman intensity. [18],[20],[21]

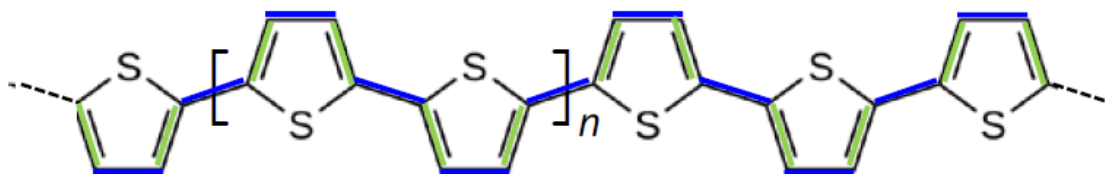


Figure 6: Schematic illustration of the vibrational displacements associated to the collective ECC coordinate for polythiophene. Green and blue segments represent respectively simultaneous stretching and shrinking of the CC bonds [20]

These Raman-active modes become active also in the IR if the π -electrons system is polarized. This happens when charges are injected in the polymer backbone by chemical doping, for this reason, strong features, called IRAV (IR active vibrations), rise in the IR spectra of doped conjugated polymers. [18][20] From a theoretical perspective, the activation of the IRAV modes was initially explained by Horovitz et al., [22] who described the dynamics of the IRAV modes in the frame of the Amplitude Mode Theory, also introducing the effect of a pinning potential describing the interaction of the doped polymer and the dopant. This was later further explored by Zerbi et al. [23] that developed a theory based on the effective conjugation coordinate (ECC). In more recent times, the activation of IRAV modes has been elucidated through the use of Density Functional Theory (DFT) calculations. DFT has proven to be a valuable tool in understanding and predicting the behaviour of these modes in doped conjugated polymers. [18]

For the reasons just explained vibrational spectroscopy is widely employed in many studies to investigate organic semiconductors and their doping process, in particular

in thin films samples. [18] In this work, IR and Raman spectroscopy are used to investigate and monitor the doping process of P3HT from the doped solution to its deposition in thin films.

2.2.2 Characterization of liquid and solid samples

In this study, both liquid and solid samples are analysed. Doping the polymer in solution provides a higher degree of control and reproducibility over the doping process allowing precise regulation of the dopant concentration. At the same time, studying doping in solution allows to understand more about the doping process revealing differences between doping in solution and in solid film, as later demonstrated.

The FT-IR spectra are recorded using a Nicolet 6700 FT-IR spectrometer with a resolution of 4 cm^{-1} and collecting 128 scans. For the characterization of the liquid solutions a KBr sealed liquid cell is used. Chloroform, used as solvent for the solutions, exhibit high absorption in the following spectral regions: between 3040 cm^{-1} and 3005 cm^{-1} ; between 1240 cm^{-1} ; 1190 cm^{-1} ; between 810 cm^{-1} and 655 cm^{-1} . For this reason, these regions are hidden and provide no information about the polymer solutions. As a result, these regions are not considered for the analysis and are not shown in the IR spectra of solutions.

On the other hand, when characterizing the solid samples, thin films are deposited from the solutions on a KBr substrate. However, due to the high reflectivity of the doped solid films, recording good quality absorption spectra, without encountering additional optical phenomena was not so easy. Although, also films on glass and ZnSe substrate were analysed, the best quality of the spectra was obtained with a KBr substrate.

FT-Raman spectra are collected using an Nicolet NXR FT-Raman Module with a Nd:YAG 1064 nm exiting laser, 100 mW power, 4 cm^{-1} resolution and 1024 scans. For the characterization of the thin film, the solutions are deposited on aluminium foil. The complexity of the Raman spectra is not in the experimental set up but mainly concerns the interpretation of the results. As a matter of fact, we obtained significantly lower intensity in the spectra of charged species compared to neutral ones. For this reason, the signal of the polaron shows a lower vibrational intensity in respect to the neutral chain, not influenced by the charged defect.

Both IR and Raman spectra are analysed using the OMNIC software.

2.2.3 Characterization of pristine P3HT

In this section the Raman and IR spectra of pristine P3HT both in solid and liquid state are discussed. By the observation of the vibrational spectra of this polymer it was possible to suggest that in the solid state three different phases in which P3HT coexist: a first phase or hairy-A phase, that is the most ordered phase where the thiophenes in the backbone are coplanar and the polymer chains form an ordered 3D structure; a second phase, or hairy-B phase, where the backbone is slightly distorted without a regular packing of the chains; a third phase, “amorphous” phase, characterized by conformational disorder that is observed in solution characterized by conformational disorder of both the backbone and alkyl chains as it can be observed in solution or for melt sample. [19],[24] By looking at the Raman spectra, the ECC mode vibration (ν_1) is sensitive to the structure of the polymer: the peak is around 1445 cm^{-1} when the polymer backbone is planar, while it shifts to 1475 cm^{-1} in case of distorted backbone. In fact, looking at the Raman spectra of P3HT in solid film and in solution reported in Figure 7, it can be noticed that in the first case the frequency of the peak is at 1445 cm^{-1} (ν_1^S) as expected for the ordered phase, while it shifts to higher frequency (ν_1^L) when the sample is in solution, and so in a disordered conformation. [25] Another feature of the Raman spectra of pristine P3HT is the presence of another band of smaller intensity (ν_2) at around 1380 cm^{-1} . From calculated spectra, this band is assigned to an ECC-like vibrations coupled with CC stretching of the alkyl chains. Differently from ν_1 , this frequency does not vary a lot with the changing in the conjugation length, in fact it stays unaltered going from solid to liquid sample. [19]

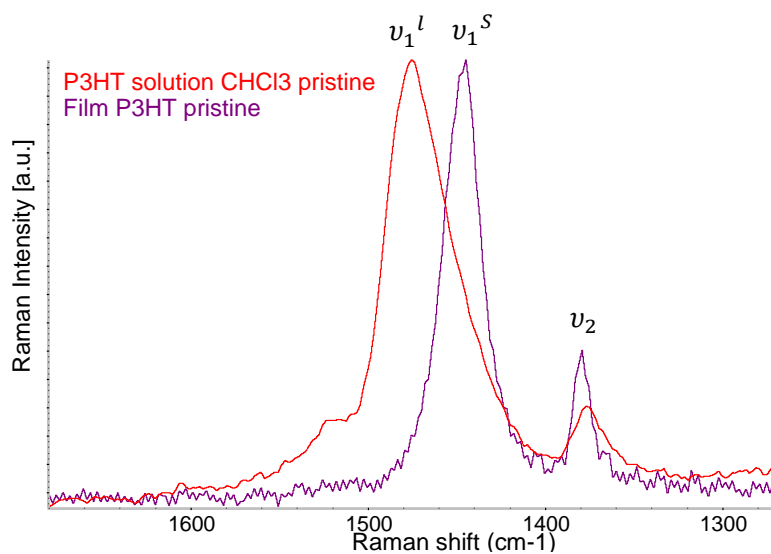


Figure 7: FT-Raman spectra of liquid solution of P3HT in chloroform (red line) compared to solid P3HT thin film (purple line)

In Figure 8 are reported the IR spectra of pristine P3HT in chloroform solution and in solid film. No significant differences can be seen from the spectra in the two different states: the two spectra show similar features, many of them ascribed to vibrational modes localized on the alkyl chains. Focusing on the most relevant features it can be observed between 3000 and 2800 cm^{-1} four bands corresponding to the stretching vibrations of $>\text{CH}_2$ and $-\text{CH}_3$ groups in the region:

- Band 1, attributed to antisymmetric $-\text{CH}_3$ stretching.
- Band 2, attributed to antisymmetric $>\text{CH}_2$ stretching.
- Band 3, attributed to symmetric $-\text{CH}_3$ stretching.
- Band 4, attributed to symmetric $>\text{CH}_2$ stretching.

The shape of these bands is similar to that observed for amorphous n-alkanes thus indicating a conformational disorder of the lateral hexyl chains of the P3HT. [19]

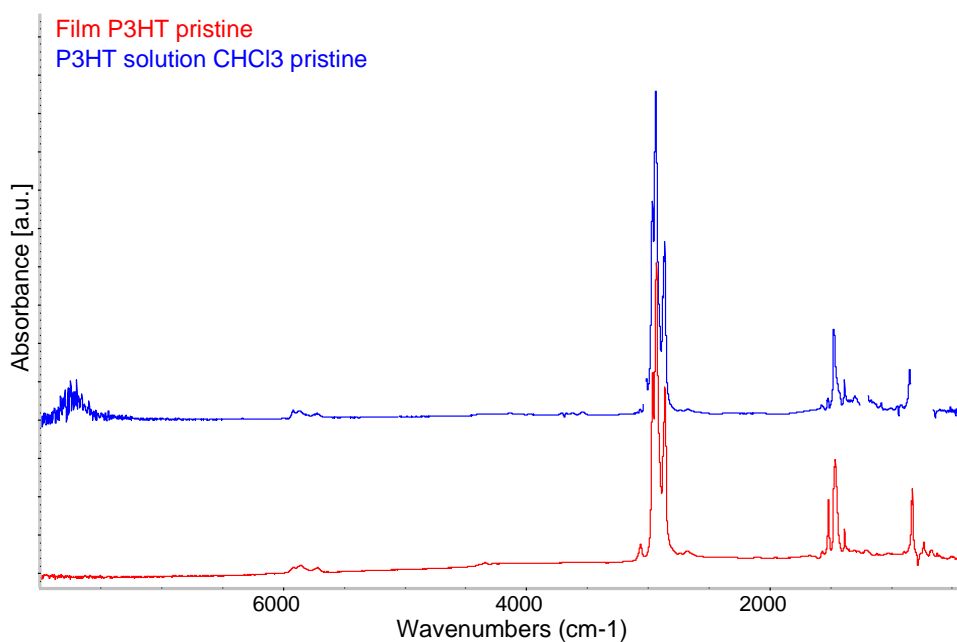


Figure 8: IR spectra of pristine P3HT solid film (red line) compared to pristine P3HT in chloroform solution (blue line)

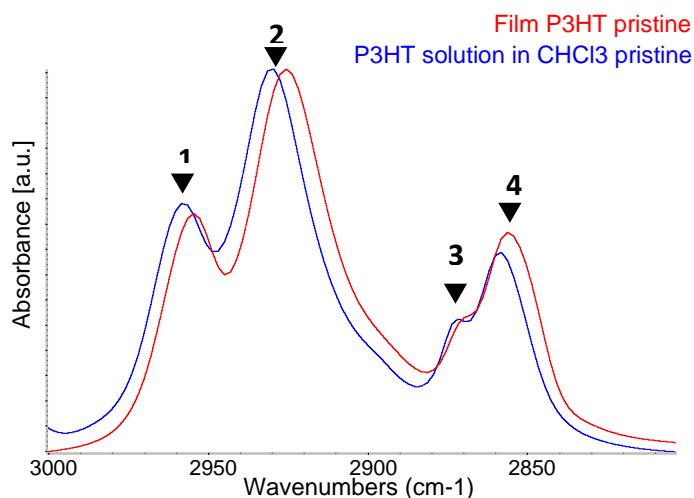


Figure 9: $>CH_2$ and $-CH_3$ absorption of solid pristine P3HT (red line) and liquid solution of pristine P3HT (blue line)

In the spectral region $1500-1300\text{ cm}^{-1}$ we observe modes involving CC stretching vibrations of the aromatic rings and vibrations of the lateral chains. The band associated to the $>CH_2$ bending (band 5) and $-CH_3$ umbrella (band 6) vibrations can be seen respectively at around 1460 cm^{-1} and 1378 cm^{-1} . The shape and the width of these bands can give information on the conformational order of the alkyl chains. In case of conformational order (all trans configuration) the two peaks are sharp, while in case of disorder of the chains an asymmetrical and structured broad band appears from 1480 to 1400 cm^{-1} and, in addition, the $-CH_3$ umbrella band shifts slightly at higher wavenumbers, as it can be seen in the spectra of P3HT in solution (Figure 10). [19]

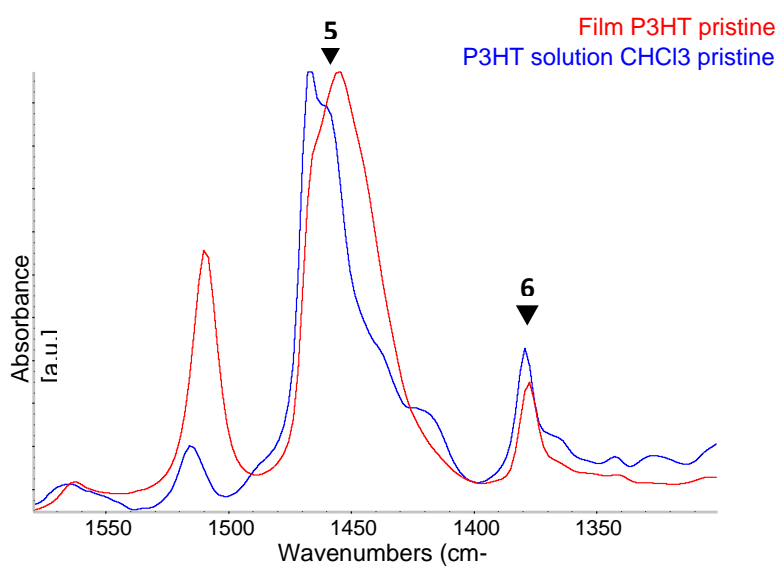


Figure 10: IR spectra in the region between 1560 cm^{-1} and 1300 cm^{-1} of solid pristine P3HT (red line) and liquid solution of pristine P3HT (blue line)

2.2.4 Polaron vibrational signature in the literature

The large interest that conjugated polymers have recently gained has led to many studies focused on the understanding of their properties and, in particular, of their doping process. The research is mainly focused on solid P3HT rather than doping in solution. In this chapter are reported some of the evidence of the polaron signature which has been documented in the literature.

By looking at the Raman spectra, the doping and the formation of polaron in P3HT lead to an evident downshift in the frequency and broadening of the peak that originally appears at 1445 cm^{-1} in the pristine polymer, as reported in many studies. [26],[27] It was also shown that this shift increases with increasing the level of doping, as reported in Figure 11.

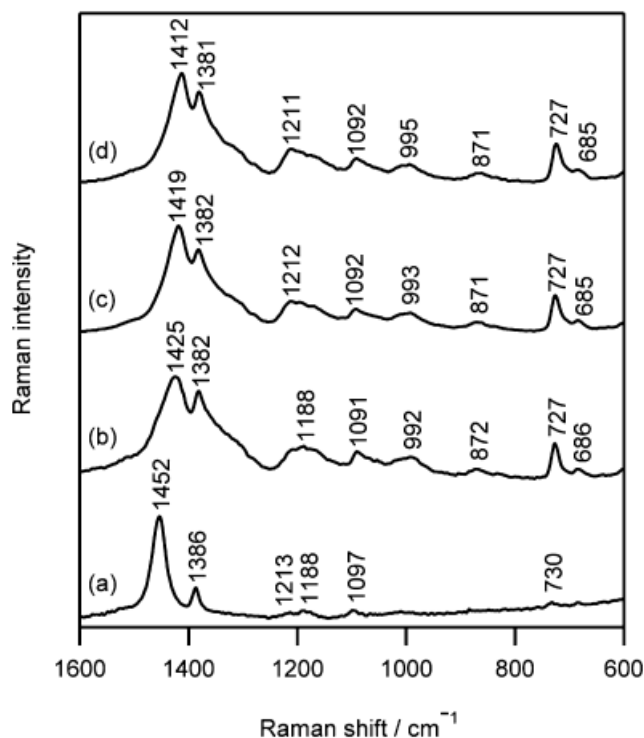


Figure 11: Raman spectra (exiting laser 830 nm) of (a) neutral P3HT solid film and (b,c,d) P3HT film doped with an acetonitrile solution of FeCl_3 . The doping level increases from (b) to (d). [27]

The bands in the spectral region from 1425 to 1412 cm^{-1} are assigned to the ECC modes of polarons and they correspond to the ECC vibration band at 1452 cm^{-1} in pristine P3HT. [27]

The presence of the polaron is also detected by the use of IR spectroscopy, leading to characteristic spectral features of the charged polymer (IRAV). In literature are

reported many examples of these IRAV features in P3HT, especially for solid film doped by sequential doping or by vapour, with different dopants. [27], [28]

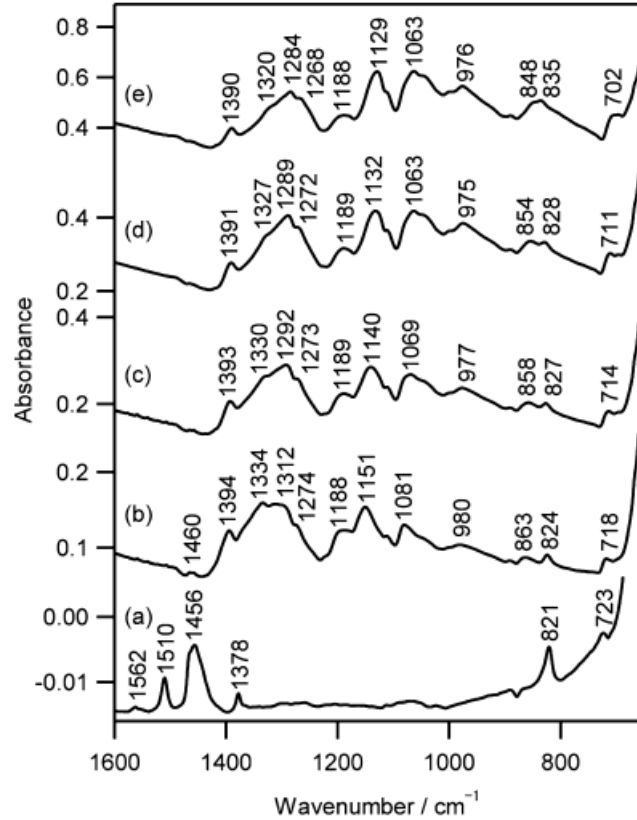


Figure 12: IR absorption spectra of (a) pristine P3HT film and (b-e) P3HT film doped FeCl₃ by solution doping with increasing doping level from (b) to (e). [27]

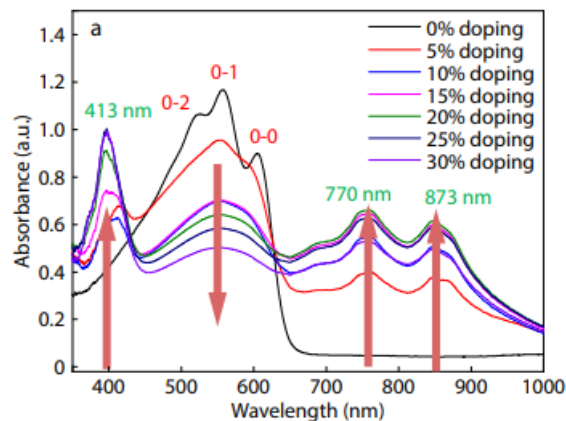


Figure 13: UV-Vis-NIR absorption spectra of P3HT undoped and doped F₄TCNQ solution in TCE with increasing doping level [28]

These evidences are consistent also with the spectra calculated theoretically by DFT calculation, as showed in Figure 14. [29]

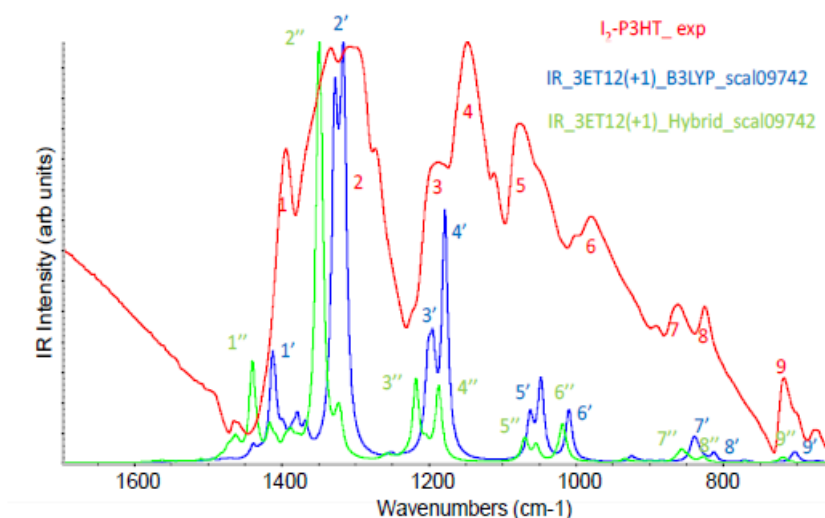


Figure 14: B3LYP (blue line) and hybrid (CAM-B3LYP//B3LYP) (green line) approach IR spectra of the dodecamer of 3-ethyl thiophene compared to the experimental spectrum of P3HT doped by I₂ (red line). [29]

From these studies, it can be asserted that a “universal” IR spectral signature of the polaron in P3HT emerges from the spectra, irrespective of the dopant used. These “universal” IRAVs are ascribed to the ordered ICT structure (Figure 4.b) and their appearance will be followed in this work starting from the analysis of the spectra of the doped solution. Spectra of doped samples in solution will be compared to those obtained after the deposition as a solid film and with the solid film doped by vapour. In many studies on doped P3HT it was demonstrated the coexistence of CTC and ICT complexes. [30] The presence of CTC or ICT holds direct implications for the effectiveness of the system since CTC contribute less to the increase of conductivity in the conjugated polymer. [30],[17] For this reason is relevant to understand in which conditions the formation of these kind of complexes is favoured in respect to the formation of CTC, as it will be done in this work.

Finally, another innovative aspect will be discovered in this study: the observation of a peculiar kind of ICT complex, different from that commonly referred as “polaron”, which can be detected within specific systems and conditions.

3 Results and discussion

In this Chapter are reported the results obtained from the vibrational analysis of P3HT, rraP3HT, P3DT and of the oligomers doped with iodine and F₄TCNQ both in solution with chloroform and in film obtained depositing the doped solutions.

3.1 FT-IR spectroscopy

In this section are reported the results of the analysis carried out by FT-IR spectroscopy of:

- doped P3HT in solutions at three doping ratios with both dopants and thin films deposited from the previous solutions;
- doped rraP3HT in solution at doping ratio 5:1 with both dopants and thin film deposited from the previous solution;
- doped P3DT in solution at doping ratio 5:1 with both dopants and thin film deposited from the previous solution;
- doped 8T, 13T and 21T in solution doping ratios 5:1 with both dopants and thin films deposited from the previous solutions.

3.1.1 FT-IR spectra of doped P3HT in solution

In Figure 15 are reported the spectra in solution of P3HT pristine and doped with iodine at the three doping ratios. The differences between the pristine and doped spectra can be clearly seen due to the high intensity IRAV bands that rise in the spectra of doped P3HT.

In Figure 17 and Figure 18 are reported the spectra of P3HT solutions doped respectively with iodine and F₄TCNQ. It can be noticed that, depending on the level of doping, different patterns are obtained. The main differences as a function of the P3HT/dopant ratio can be seen in the region between 1450 cm⁻¹ and 1250 cm⁻¹, which we called region α and highlighted in grey in Figure 16. Here the bands change strongly both in intensity and in peaks frequency, while in the other regions, β

(between 1170 cm^{-1} and 1090 cm^{-1}) and γ (between 1090 cm^{-1} and 900 cm^{-1}), the bands seem to be more stable in frequency, even if they undergo some changes. For this reason, in this work the discussion will be focused mostly on the region α .

In region α , there is a sharp band A that remains almost unaltered in frequency at all three doping levels. Then, in the same region, other three main components can be seen: the band C_1 at 1340 cm^{-1} , much broader than the others and dominant in the 1:1 doping; P_1 at 1300 cm^{-1} for the 5:1 and I_1 for the low doping ratio 25:1. It can be noticed that, differently from band A, the three bands C_1 , P_1 and I_1 , typical of different doping regimes, show a significant separation in frequency. Moving to region β , a single band for each doping ratio can be observed: C_2 and P_2 at almost the same frequency (1155 cm^{-1}) for the 1:1 and 5:1 samples respectively, and I_2 at lower wavenumbers (1135 cm^{-1}) for the lowest doping level. Finally, in region γ , the 25:1 doping gives again the most different spectrum in respect to the other two cases, showing three bands: I_3 observed also in the other two doping levels at a bit higher wavenumbers, I_4 is seen also in the 5:1, and I_5 (975 cm^{-1}) that is not present in the other two cases.

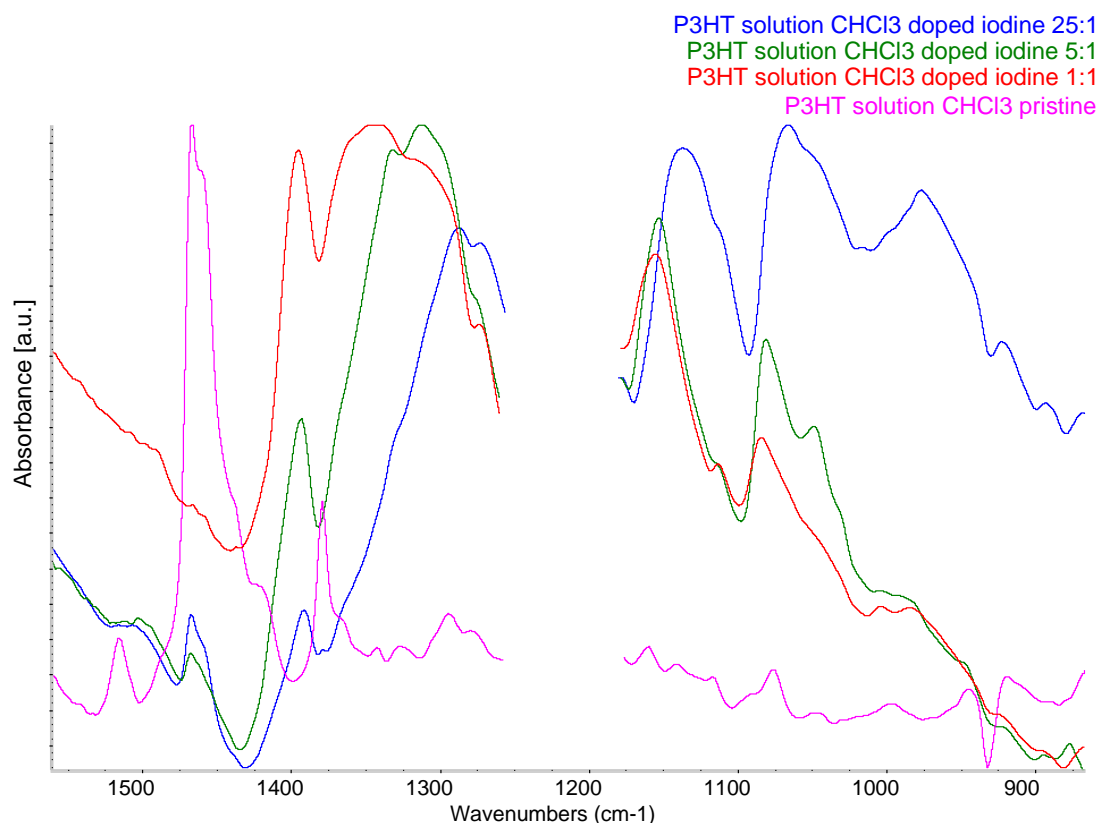


Figure 15: FT-IR spectra in the region between 1600 cm^{-1} and 900 cm^{-1} of solution of P3HT in CHCl_3 pristine (pink line) and doped with iodine in different molar ratios: 25:1 blue line, 5:1 green line, and 1:1 red line.

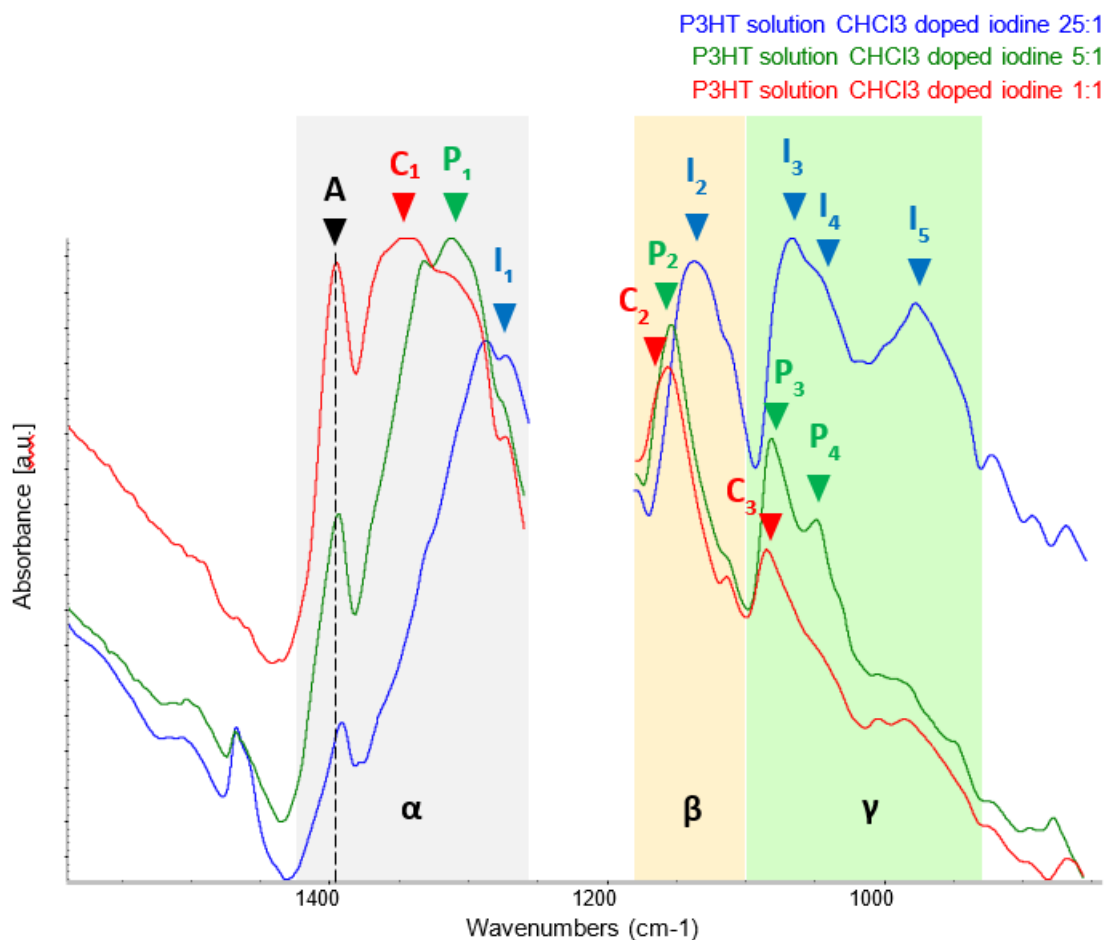


Figure 16: FT-IR spectra in the region between 1600 cm^{-1} and 900 cm^{-1} of solution of P3HT in CHCl_3 doped with iodine: 25:1 blue line, 5:1 green line, 1:1 red line. The grey, pink and green areas identify respectively the region α , β and γ of the spectra.

Doping ratio	Component	Band A (cm^{-1})	Band 1 (cm^{-1})	Band 2 (cm^{-1})	Band 3 (cm^{-1})	Band 4 (cm^{-1})	Band 5 (cm^{-1})
25:1	I	1392	1270	1135	1067	1046	975
5:1	P	1393	1300	1152	1081	1048	-
1:1	C	1393	1340	1156	1080	-	-

Table 3: wavenumbers of the three components I, C and P observed in the IR spectra of P3HT solution doped $\text{I}_2/\text{F}_4\text{TCNQ}$ at the three doping ratio.

In Figure 19 are reported the spectra of P3HT solutions doped with iodine and with F_4TCNQ normalized in respect with the intensities of the CH stretching bands that are not affected by the doping process. From these spectra the relative intensities of the IRAV bands increase with increasing the doping ratio, meaning that, as expected, the

level of doping increases when more dopant is added to the polymer solution. It can also be noticed that in the low doping level are still present some spectral features of the pristine polymer (highlighted with a blue arrow in Figure 17 and Figure 18), which means there are some chains that remain undoped.

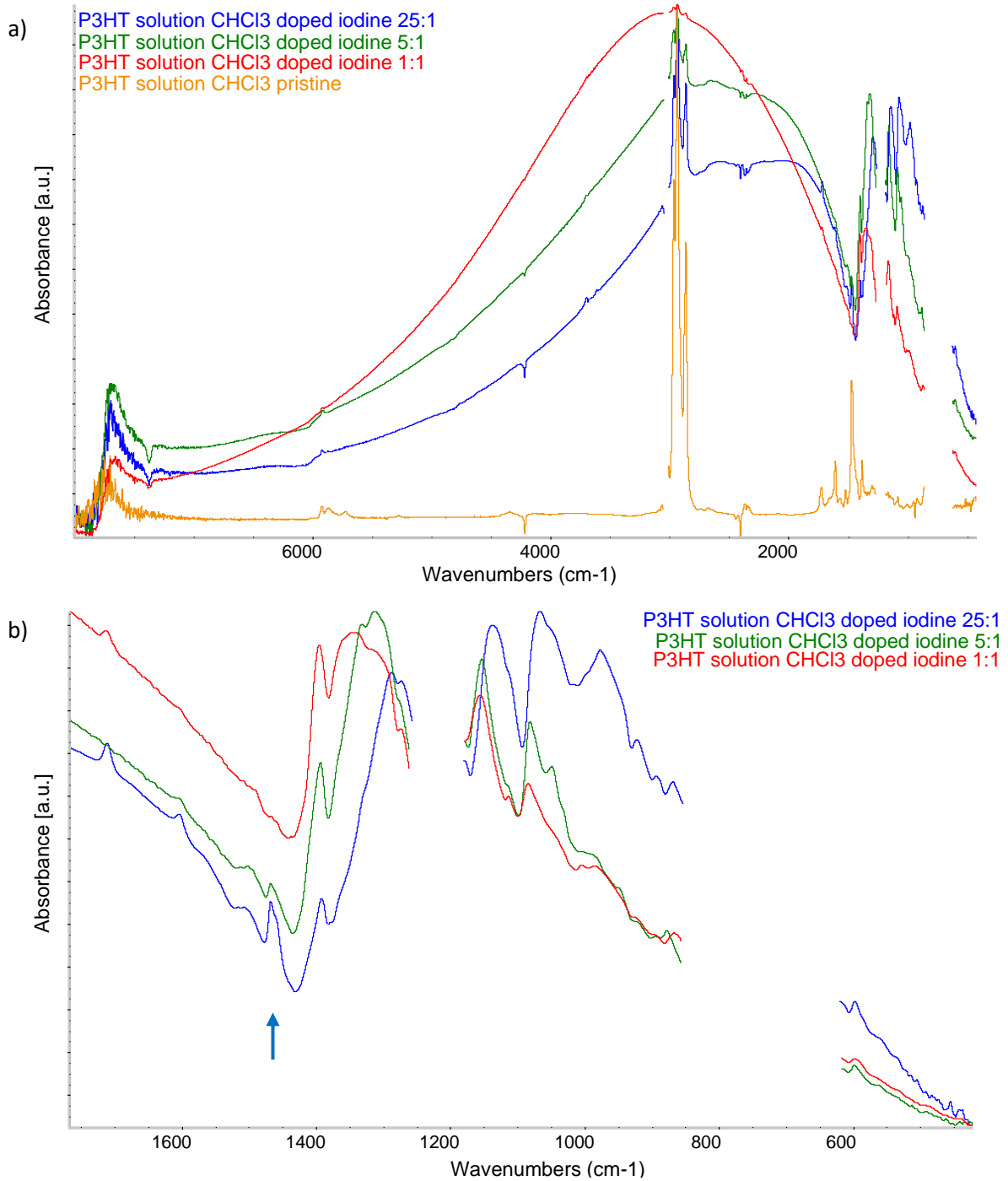


Figure 17: FT-IR spectra of a) solution of P3HT in CHCl₃ pristine (brown line) and doped with iodine: 25:1 (blue line), 5:1 (green line), 1:1 (red line); b) solution of P3HT in CHCl₃ doped

with iodine in the region between 1700 cm^{-1} – 500 cm^{-1} . The blue arrow highlights the signals of pristine P3HT.

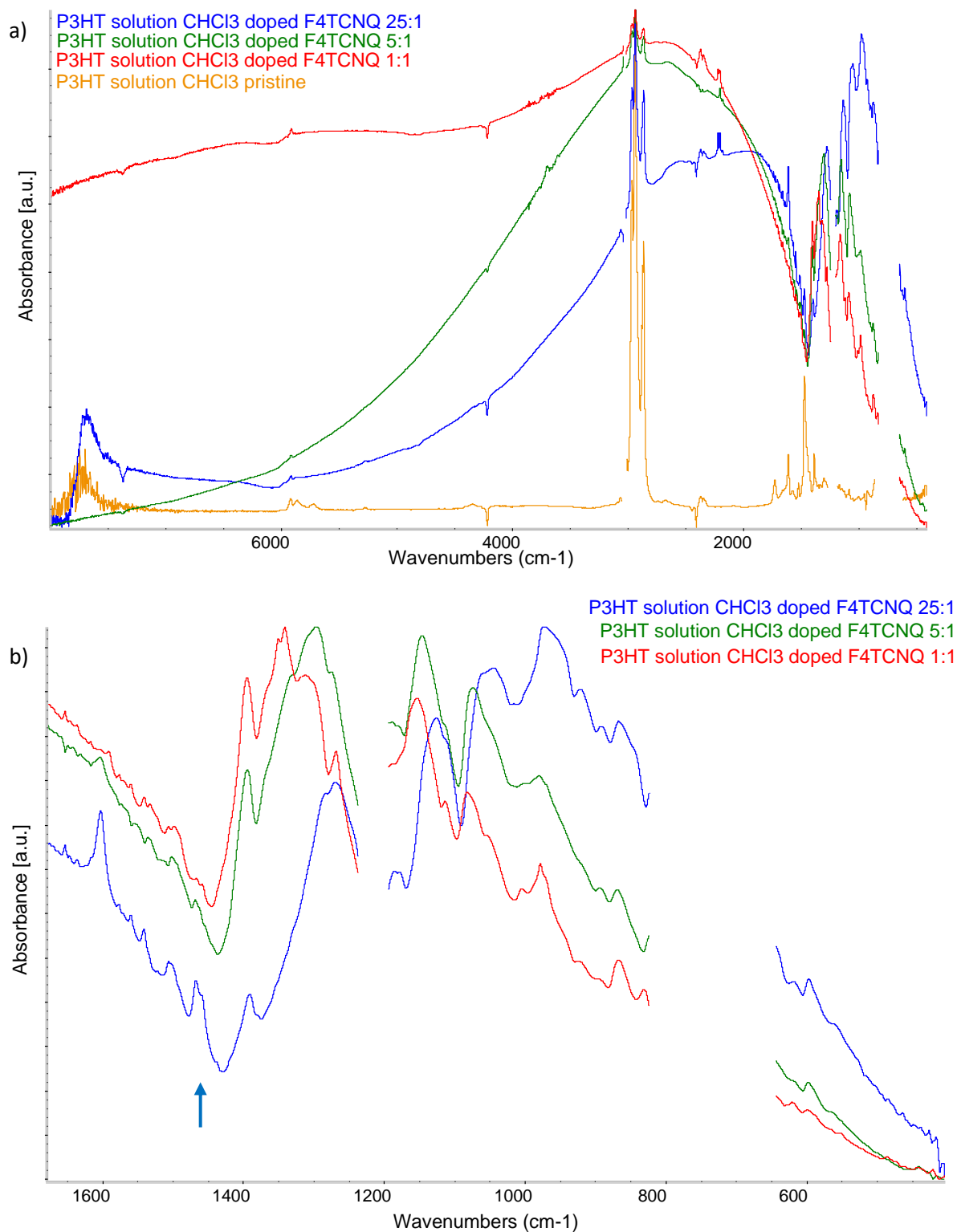


Figure 18: FT-IR spectra of a) solution of P3HT in CHCl_3 pristine (brown line) and doped with F_4TCNQ : 25:1 (blue line), 5:1 (green line), 1:1 (red line), b) solution of P3HT in CHCl_3 doped

with F₄TCNQ in the region between 1600 cm⁻¹– 500 cm⁻¹. The blue arrow highlights the signals of pristine P3HT.

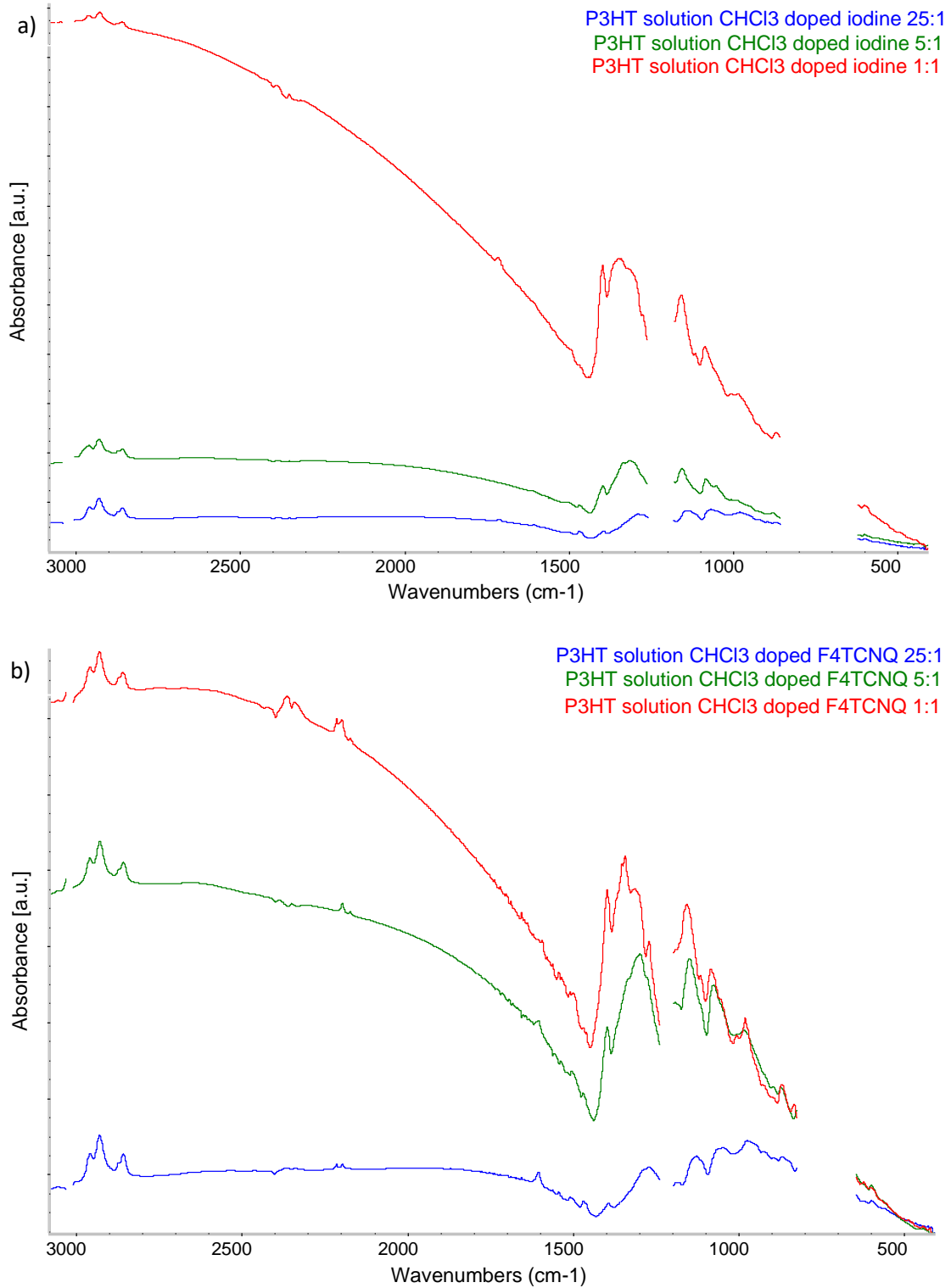
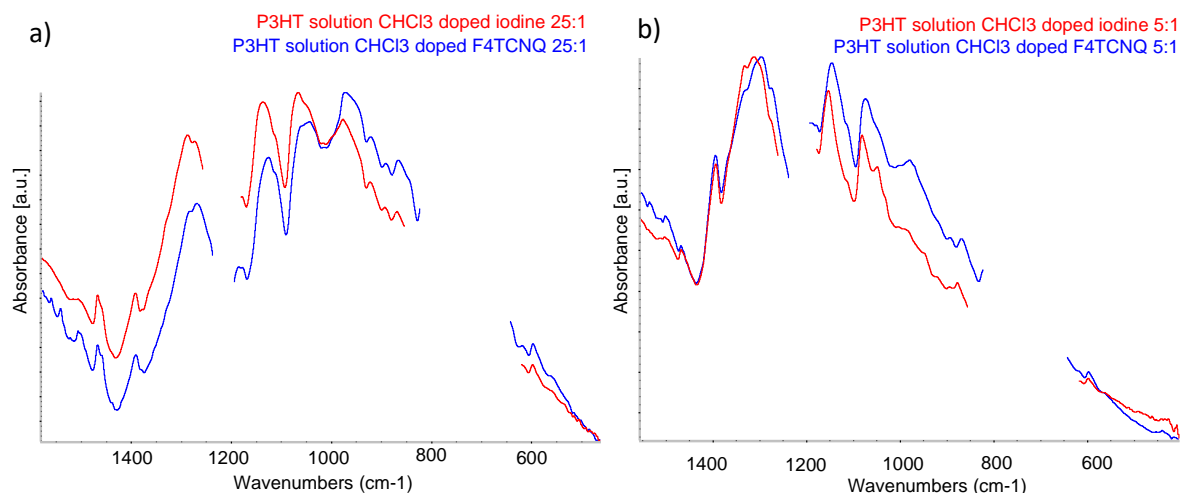


Figure 19: FT-IR spectra of solution of P3HT in CHCl₃ doped with iodine (a) and F₄TCNQ (b):

blue line 25:1; green line 5:1; red line 1:1; normalized in respect with the intensity of the CH stretching.

The three different patterns identified in the spectra of the three doping ratios suggest the presence of different species in the doped polymer solutions that depend on the level of doping, meaning that there could be different interactions between the dopant and P3HT depending on the quantity of dopant that is added to the solution. In the 25:1, where a small number of dopant molecules are present and so, in principle, few and isolated polarons can be formed, we observe the four I bands (see Figure 16) systematically shifted at lower wavenumbers with respect to those appearing for solutions at medium and high doping ratios. Since the 25:1 sample gives the most different IR pattern among the three cases, its spectrum could be the signature of an incipient stage of formation of doping induced defects, while a possibly more stable configuration is obtained at higher doping. Indeed, as the level of doping is increased other components at higher frequencies rise in the spectra: in the 5:1 solution, where ideally, we should have polarons one close to each other, the four P bands can be observed, and the three C bands in the 1:1 where we have a very high concentration of doping agent. These three distinct IR patterns are present in the spectra of both P3HT doped with iodine and with F₄TCNQ, as showed in Figure 20: this indicates that the two dopants behave in a similar way when doping the polymer chain.



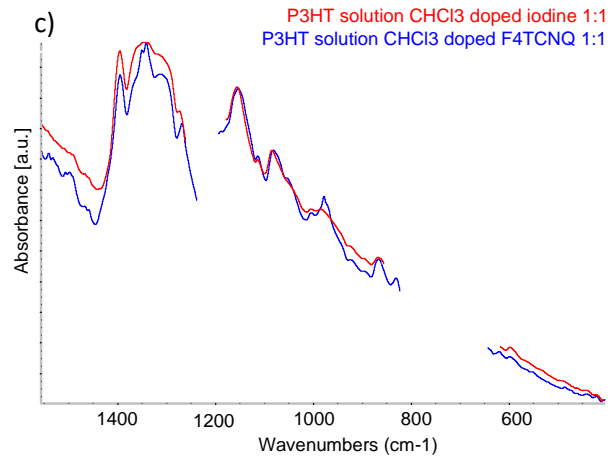


Figure 20: FT-IR spectra in the region between $1500\text{ cm}^{-1} - 500\text{ cm}^{-1}$, comparison between P3HT solution doped with iodine (red lines) and doped with F_4TCNQ (blue lines): a) 25:1; b) 5:1 and c) 1:1

In F_4TCNQ doped polymer solutions, differently from the case of iodine doping, also vibrational transitions of the dopant molecules can be seen in the IR spectra allowing to understand more about the dopant/polymer interaction. There are two different IR active modes of this molecule in the region between 1800 cm^{-1} and 2500 cm^{-1} , the symmetric and the antisymmetric stretching modes of the CN groups, that are highly sensitive to the charge state of the dopant (F_4TCNQ vs. F_4TCNQ^-) and to the intermolecular interactions. In particular, the vibrational frequencies of the F_4TCNQ anion in this region depend highly on the local environment, shifting to lower wavenumbers as the local electron density increase. These two modes are symmetric and antisymmetric $C\equiv N$ stretching with symmetry B_{1u} and B_{2u} , respectively at higher and lower wavenumber, as represented in Figure 21. [31][32]

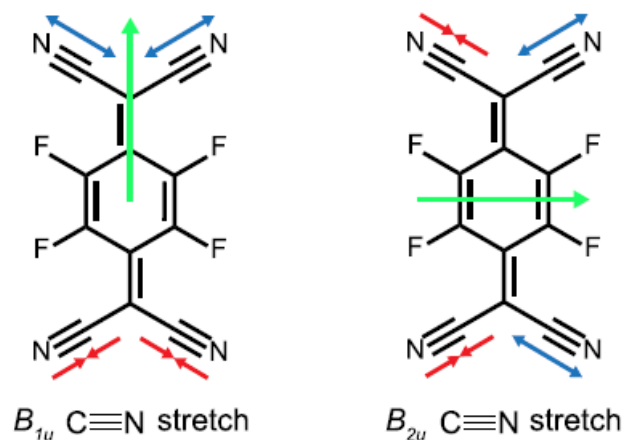


Figure 21: Representation of the two vibrational modes of $C\equiv N$ stretching with B_{1u} and B_{2u} symmetry. The atomic displacement vectors are represented in the figure: compression of the

C≡N bonds is represented with red arrows, while the expansion with blue arrows. The green arrows represent the dipole moments of the two modes. [31]

Looking at the C≡N stretching region in the samples at the three different levels of doping, reported in Figure 23, compared to the molecule F₄TCNQ in solution with chloroform, the following observations can be made and the different peaks that can be observed in the four cases are summarized in Table 4.

Doping ratio	N ₁	N ₂	A _D	A ₂
F₄TCNQ	2213 cm ⁻¹	2192 cm ⁻¹	-	-
25:1	2213 cm ⁻¹	-	2194 cm ⁻¹	2173 cm ⁻¹
5:1	-	-	2194 cm ⁻¹	2171 cm ⁻¹
1:1	2213 cm ⁻¹	-	2196 cm ⁻¹	2170 cm ⁻¹

Table 4: peaks corresponding to the C≡N stretching modes in neutral F₄TCNQ in CHCl₃ and in the three P3HT doped solutions.

In the lower doping level (25:1) it is evident that there are still many dopant molecules non interacting with the polymer chains; indeed, an intense N₁ band can be observed as in F₄TCNQ/CHCl₃ solution. In addition, other two bands can be seen: A_D and A₂. Comparing with some results in the literature, showed in Figure 24, these two bands can be attributed to the presence of the anion F₄TCNQ⁻ implying that some molecules of the dopant are interacting with the polymer with a complete charge transfer mechanism. [17] These features indicate that, at this low level of doping, some of the dopant molecules are free in solution and have not interacted with the P3HT chain. This suggests that there is an equilibrium between formation and dissolution of the charged defects. [6] Inspired by ref [6] we can argue that some amount of the dopant molecules remains neutral in solution, while others form charged defects, promoting the formation of clusters of doped polymer chain, as represented in Figure 22.

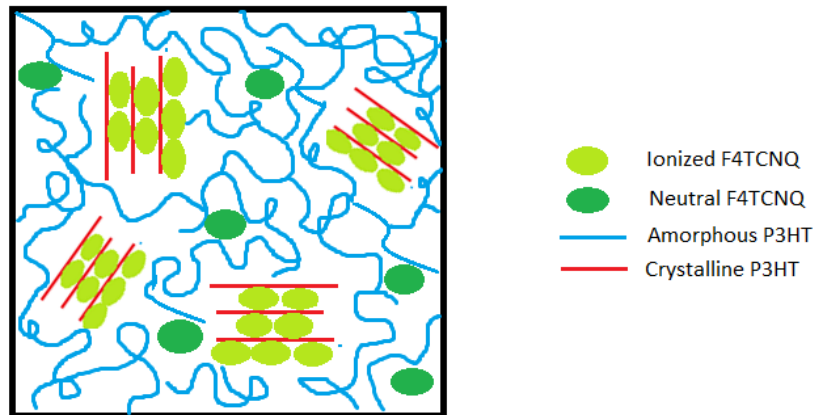
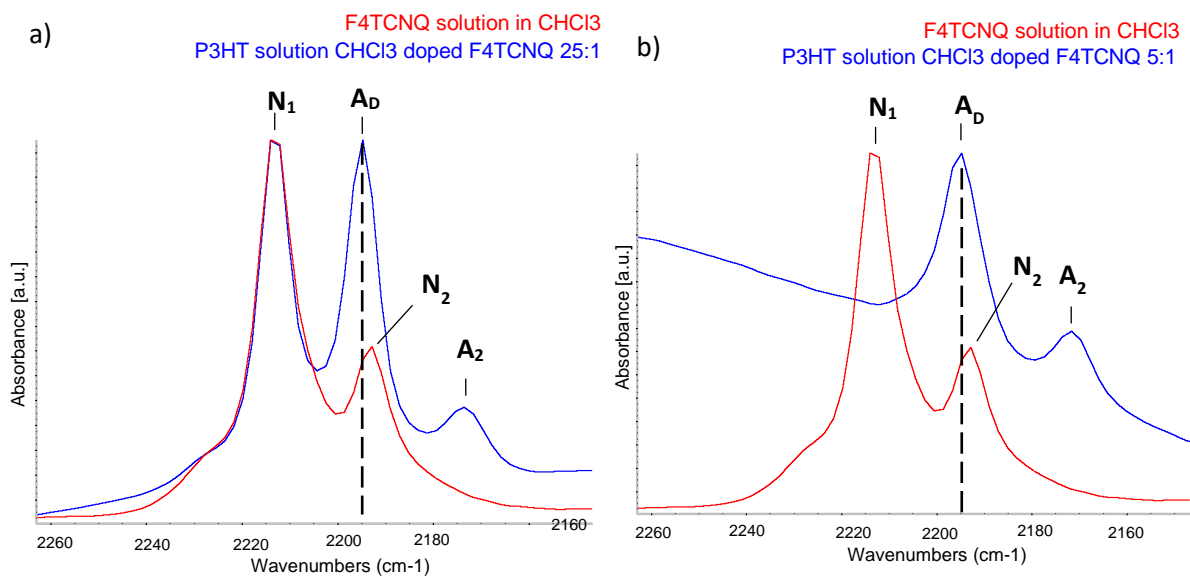


Figure 22: schematic representation of the morphology of P3HT doped F_4TCNQ^- solution 25:1. The blue lines represent the amorphous polymer, red lines and light green dots are domains of crystalline polymer with incorporated dopant molecules and dark green dots are neutral dopant molecules that are not interacting with the polymer chain. Figure adapted from ref. [6]

In the medium doping level (5:1) the band N_1 can no more be seen; this may suggest that almost all the dopant molecules are interacting with the polymer. Indeed, we only see the presence of F_4TCNQ^- anion. Finally, in the highly doped case (1:1) free molecules of F_4TCNQ are present again in solution, probably because of the excess of dopant, and, at the same time, there are other molecules that are forming charged complexes with the polymer chain.



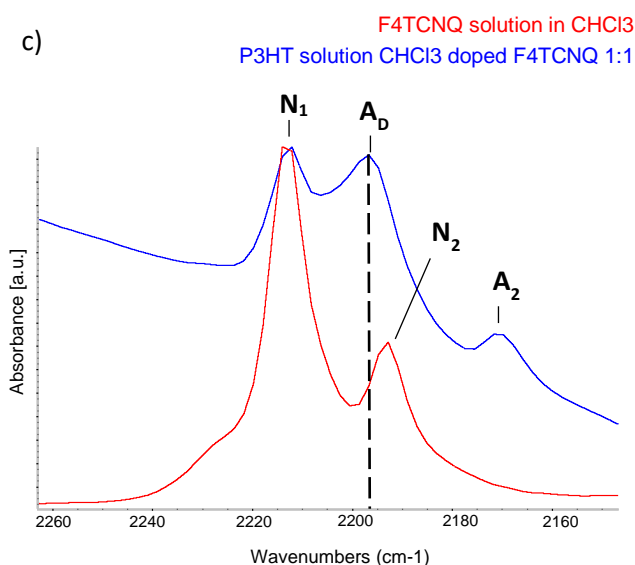


Figure 23: FT-IR spectra in the C≡N stretching region (from 2260 cm⁻¹ to 2160 cm⁻¹) of F₄TCNQ in solution with CHCl₃ (red line) compared to solutions of F₄TCNQ doped P3HT (blue line) a) 25:1; b) 5:1; c) 1:1.

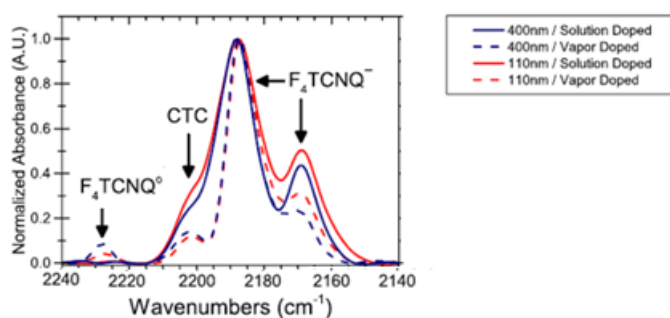


Figure 24: FT-IR spectra of 400 nm-thick (blue curves) and 110 nm-thick (red curves) doped P3HT samples. Continuous lines correspond to films treated by sequential solution doping with F₄TCNQ; dotted lines correspond to vapor phase doping. Figure adapted from ref. [17]

By comparing the height of the F₄TCNQ N₁ band and the F₄TCNQ⁻ band A_D a qualitative estimation of the quantity of dopant interacting with the polymer can be obtained. The results are reported in Table 5 and showed in the graph in Figure 25. It can be noticed that in the 25:1 case the dopant molecules that do not form charged complex with the polymer are about 49.7% of the total F₄TCNQ molecules added in solution. This means that, at low doping level, almost half of the dopant remains neutral. On the other hand, when too much dopant is added to the system, there are extra F₄TCNQ molecules that cannot interact with the polymer. The 1:1 ratio is an excess of dopant: the polymer is not able to interact with all these dopant molecules and about the 44.2% of them remains neutral. However, this is just an approximation, to have precise values requires the knowledge of the absolute absorption intensity of

each CN stretching band, while in our calculation we assumed that it remains constant, irrespective to the charge state of F₄TCNQ.

Doping ratio	N ₁ peak height	A _D peak height	% F ₄ TCNQ	% F ₄ TCNQ ⁻
25:1	0.00733	0.00741	49.7	50.3
5:1	0	0.0151	0	100
1:1	0.0053	0.0067	44.2	55.8

Table 5: height of the band N₁ (corresponding to neutral F₄TCNQ) and A_D (corresponding to anion F₄TCNQ⁻); % of F₄TCNQ and F₄TCNQ⁻ for solution of F₄TCNQ-doped P3HT in the three different doping levels.

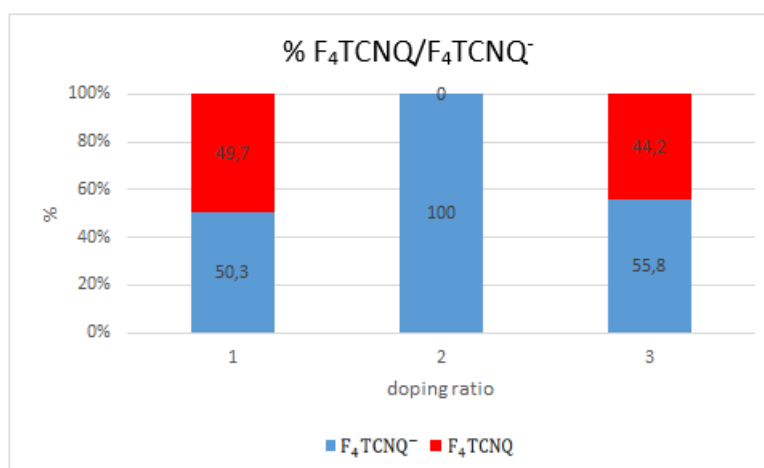
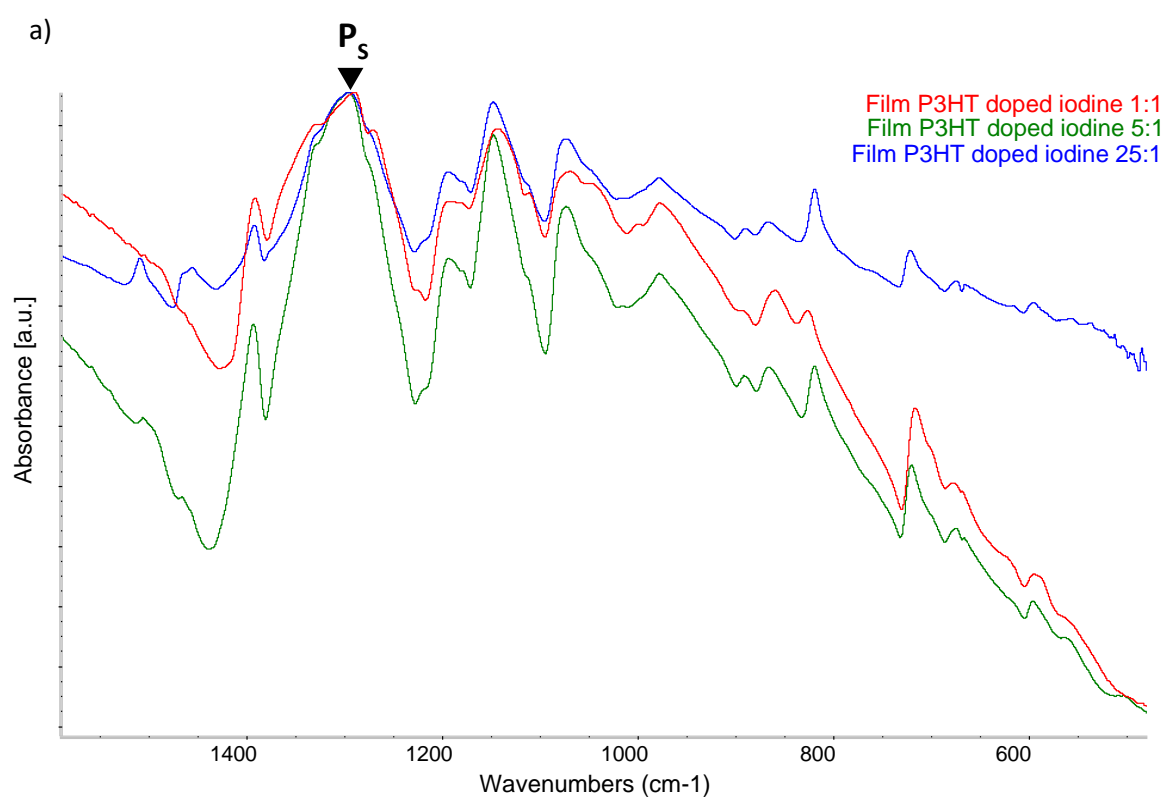


Figure 25: graph representing the % of F₄TCNQ neutral molecules (red) and anions (blue) for F₄TCNQ-doped P3HT solutions in the three different doping levels.

3.1.2 FT-IR spectra of doped P3HT solid film

The spectra of doped P3HT solid film are shown in Figure 26. As it can be seen from the IR spectra all the three levels of doping, for both dopants, show a similar pattern in solid state. There are no more different components depending on the doping ratio as in solution, but all the spectra show the same IR pattern in the α region with a band P_s at around 1295 cm⁻¹. This may suggest that when the solutions are deposited and the solvent is removed, P3HT and dopant molecules rearrange forming the most stable complexes. The resulting IR spectrum could be the vibrational signature of this stable doped state and could be taken as the signature of the polaron in solid and highly ordered state. In fact, by comparing these results with those previously reported from

the literature, this pattern seems to be “universal” - it is shared also by electrochemically doped P3HT samples - and is commonly reported as the IR evidence of polarons formation in solid P3HT. In the following, we will label this ordered doped phase as “polaron_OA”, meaning that it occurs in domains which develop a crystal-like ordered architecture, which signature is the appearance of the P IRAV bands. According to the literature, the denomination “polaron” will be used for any kind of ICT defects (see Chapter 1) possibly occurring also in disordered environments; when clearly identified, defects from partial charge transfer, namely charge transfer complexes, will be indicated as CTC.



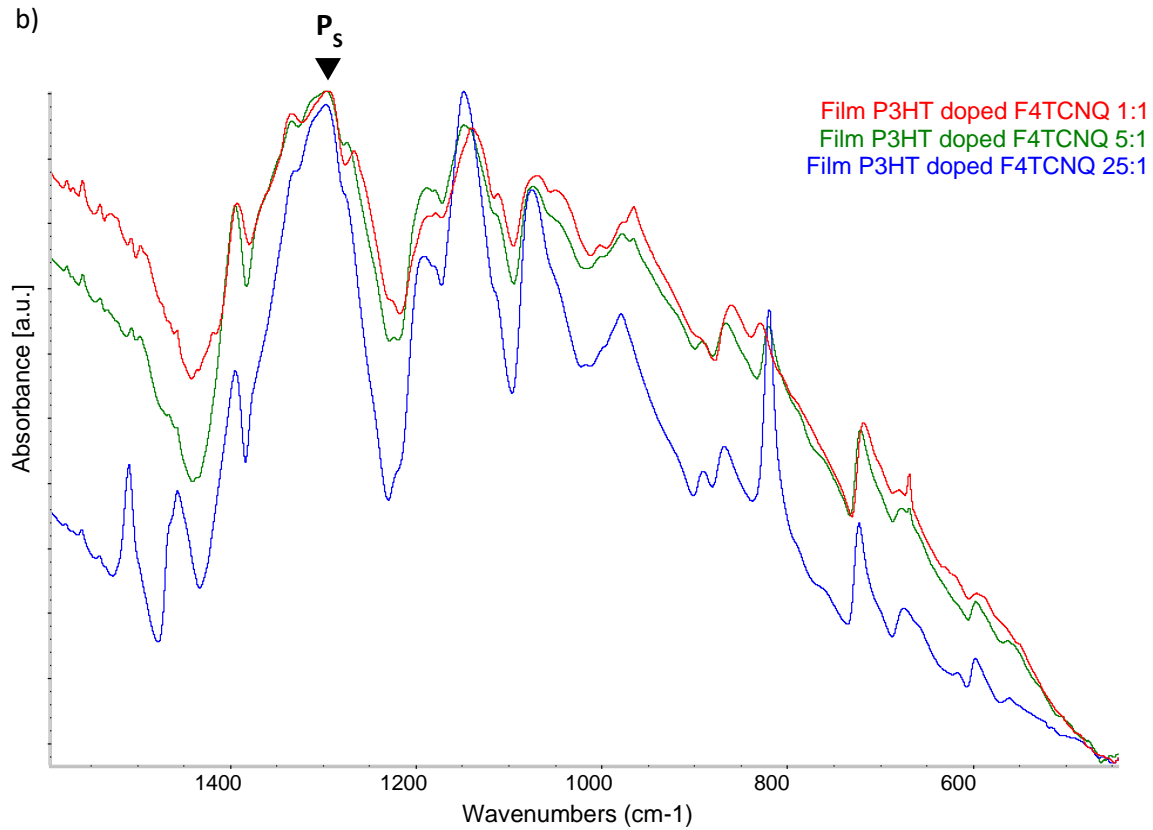


Figure 26: FT-IR spectra in the region between 1500 cm^{-1} - 500 cm^{-1} of P3HT thin films doped 25:1 (blue lines), 5:1 (green lines) and 1:1 (red lines) with a) iodine, b) F₄TCNQ.

As expected, and parallel to what seen in solution, also in thin films the two dopants act in a similar way, indeed, as reported in Figure 27 the IR pattern obtained in the two cases is very similar.

Interestingly, Figure 28, shows that, with both dopants at a doping ratio 5:1, the pattern obtained for the spectra in solution and in the film are very similar. This may suggest that this doping ratio allows the formation of pre-ordered polaronic structures by clustering of doped chains in solution, thus obtaining a stable, ordered configuration that does not change in the solid state when the solution is deposited on a substrate. This could be also confirmed by the fact that, as previously seen, no neutral dopant molecules were observed in solution at such relative concentration.

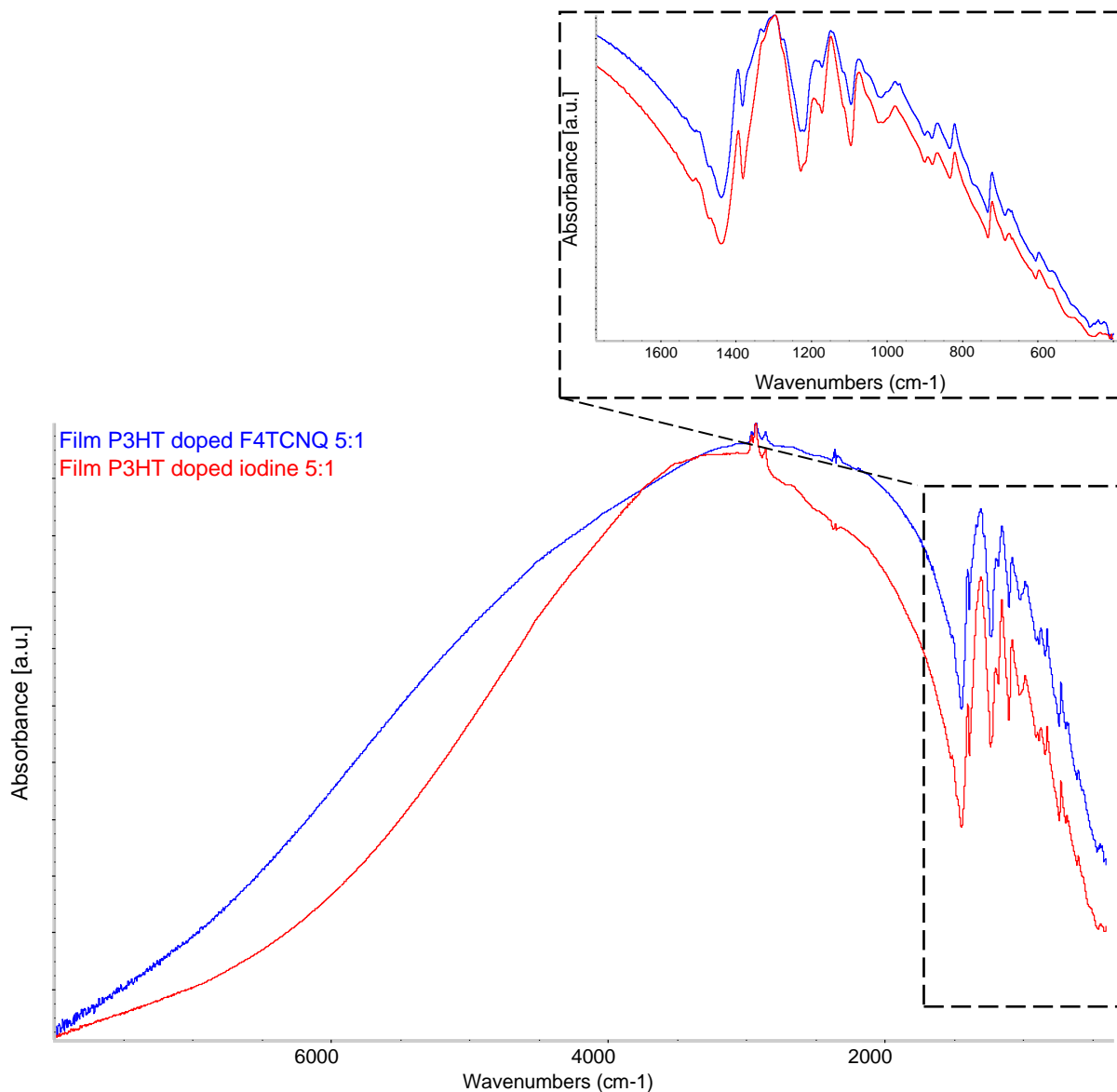


Figure 27: IR spectra of P3HT thin films from iodine (red line) and F₄TCNQ (blue line) doped polymer solution 5:1 deposited on a KBr substrate.

| Polarons in P3HT: unravelling vibrational fingerprints of ordered and disordered doped phases in solids and solutions. IR and Raman study of the polymers and oligomers.

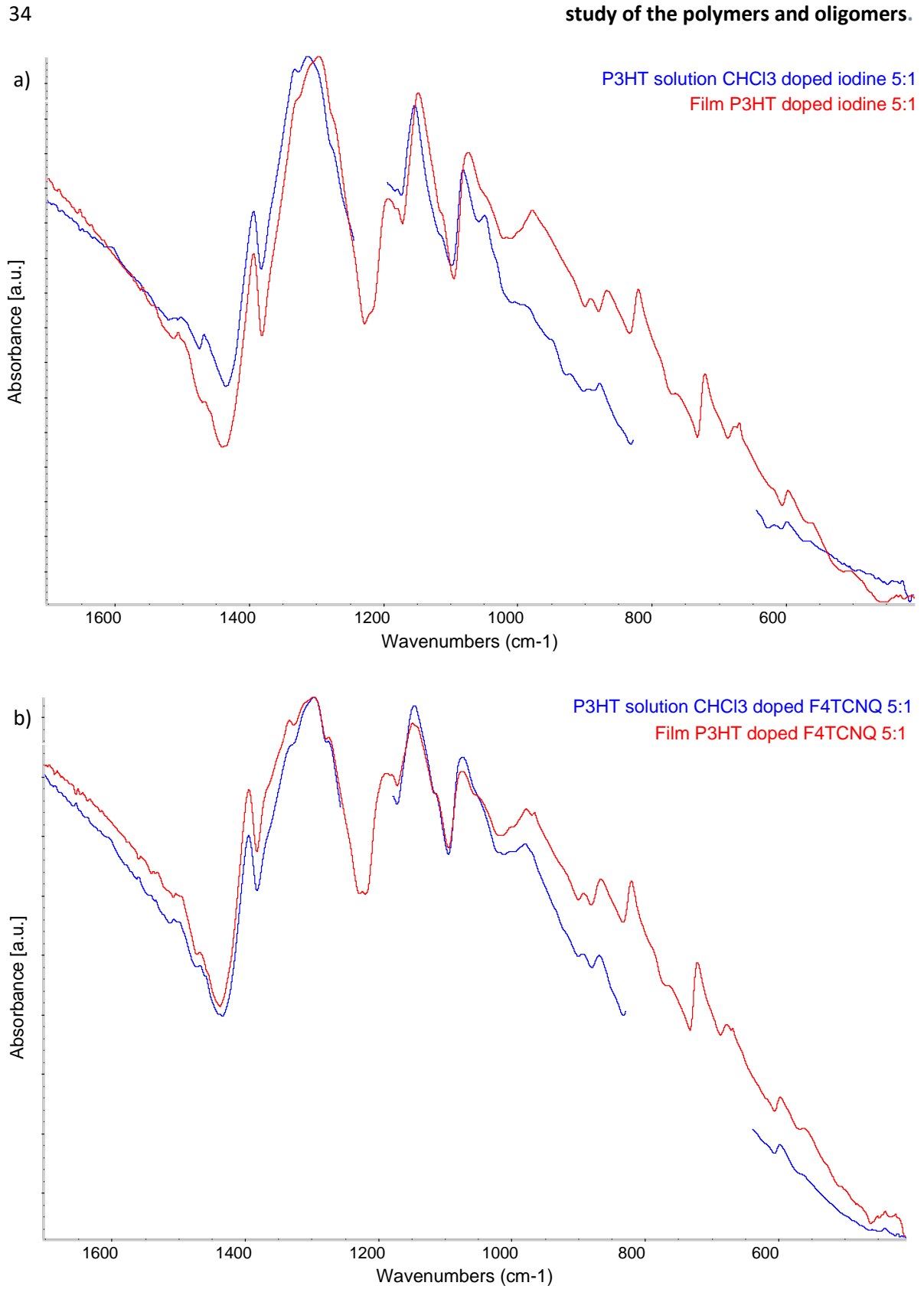


Figure 28: FT-IR spectra in the region between 1600 cm^{-1} - 600 cm^{-1} of P3HT in solution (blue lines) and film (red lines) doped 5:1 with a) iodine; b) F4TCNQ.

Looking at the vibrations of the CN groups in the P3HT film doped at the three doping levels, showed in Figure 29, no neutral dopant molecules are present in the films, but only the presence of dopant anions can be inferred looking to IR spectra. The frequency shift of the different peaks will be discussed later in section 3.1.3.2.

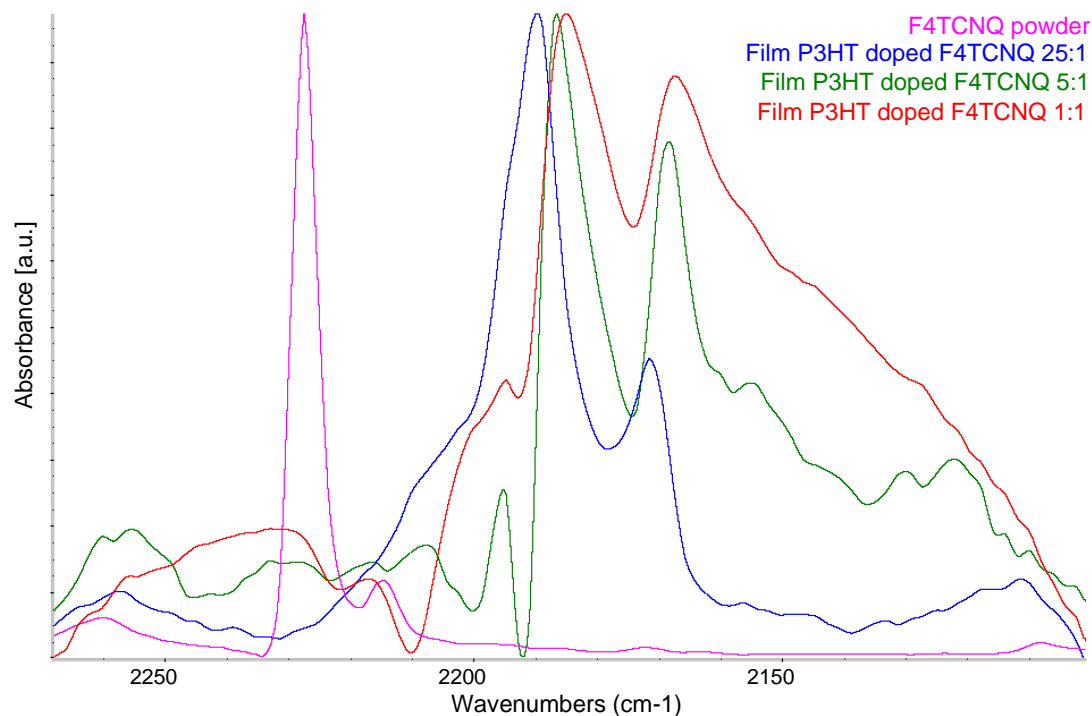


Figure 29: stretching bands of the CN groups of film casted from solution of P3HT doped F_4TCNQ 25:1 (blue line), 5:1 (green line) and 1:1 (red line) compared to F_4TCNQ in powder (pink line). The spectra are reported with a baseline correction.

The main difference observed between doping with iodine and F_4TCNQ is that the first one is more volatile and so the doping with iodine is less stable in time than doping with F_4TCNQ . This is confirmed by the fact that leaving the iodine doped films at room temperature the IRAV bands slowly decrease in intensity (Figure 30), meaning that the system is undergoing to a de-doping process. On the contrary, F_4TCNQ doped P3HT films remain stable in time (Figure 31) and they even rearrange better (slightly stronger IRAVs) if energy, in form of heat, is given to the system (Figure 32).

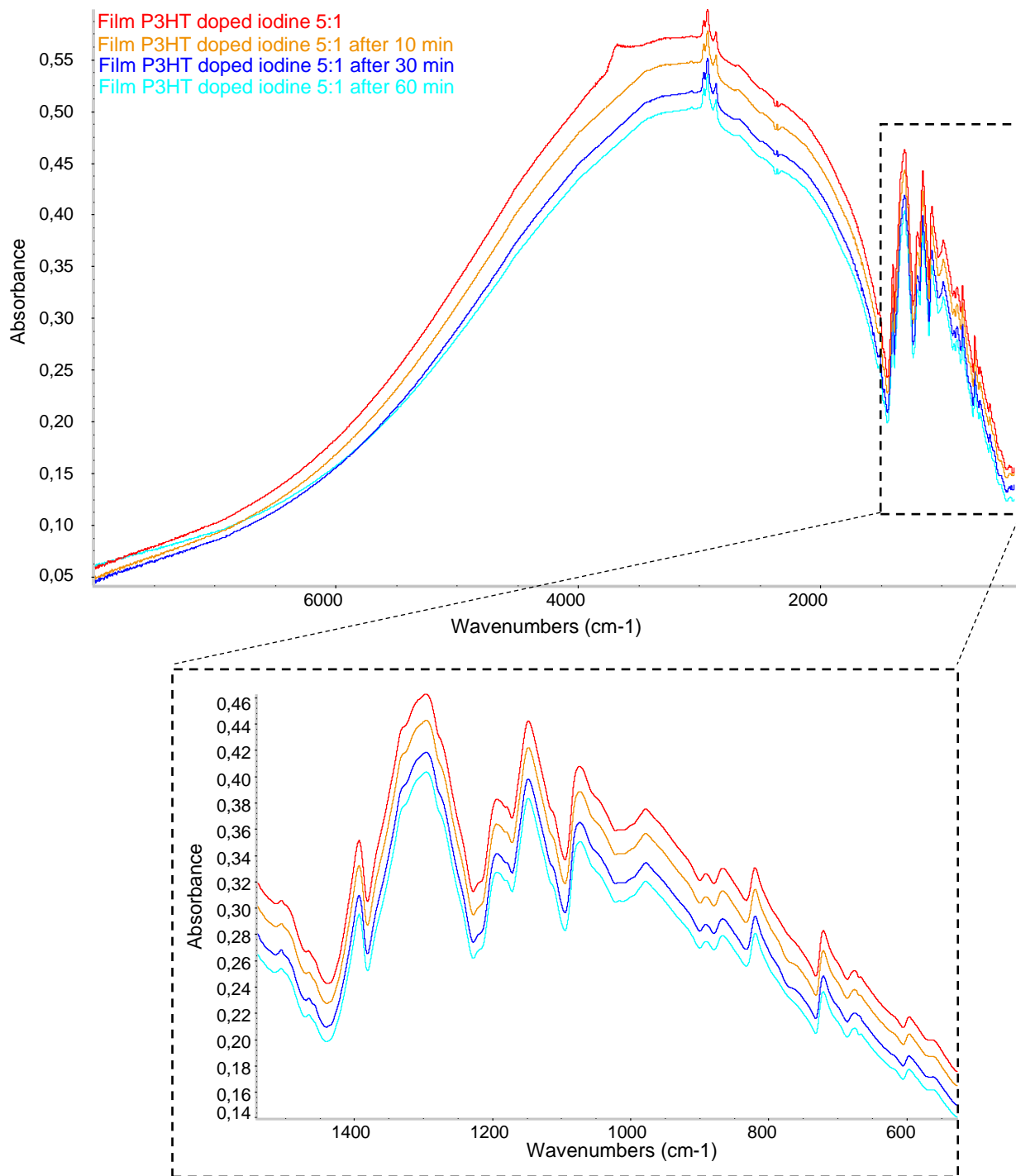


Figure 30: FT-IR spectra reported in common scale of thin film P3HT from iodine doped polymer solution 5:1 measured at different times: just after casting (red lines); after 10 minutes (orange lines); after 30 minutes (blue lines) and after 60 minutes (light blue lines).

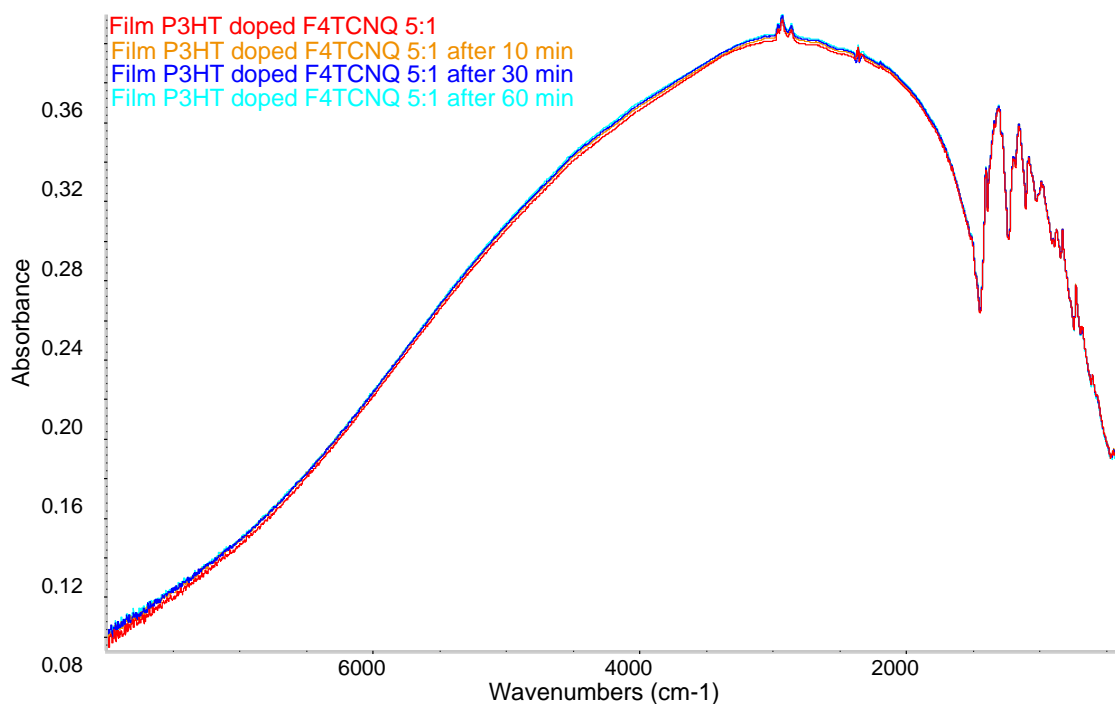


Figure 31: FT-IR spectra reported in common scale of thin films of P3HT from F₄TCNQ doped polymer solution 5:1 measured at different times: just after casting (red line); after 10 minutes (orange line); after 30 minutes (blue line) and after 60 minutes (light blue line).

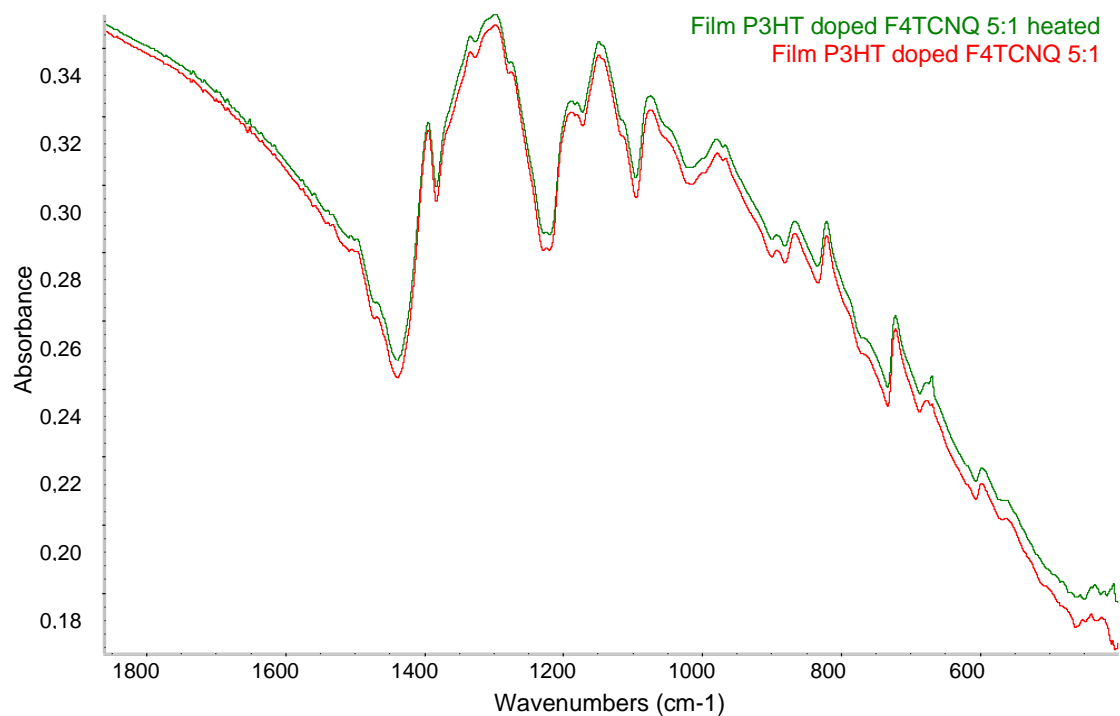


Figure 32: FT-IR spectra reported in common scale of thin film P3HT from F₄TCNQ doped solution 5:1 (red line) and the same film heated for 2 minutes (green line)

To summarize, differences were observed in the doped solutions in respect with the doped thin films.

- 1) In solutions, evidence of the presence of different IR components were identified depending on the level of doping: an incipient polymer/dopant species (bands I) was observed in the low doping case, a pre-ordered polaronic structure (bands P) in the 5:1 and a third phase (bands C) when the doping level is higher.
- 2) In solids film obtained by drop casting from solutions, for all three doping levels the spectra converge to the same pattern (bands P) that was attributed to the polaron in an ordered solid state, namely to polaron_OA phase.
- 3) The analysis of the spectra in solution suggests that there is an optimal concentration (5:1) that should facilitate the formation of the polaron_OA phase after deposition, by formation of stable doped pre-aggregates already in solution.

3.1.3 Influence of the backbone conformation and the side alkyl chains in the doping process

Focusing on the charge defects in this Chapter will be analysed the role on the doping process of different factors, including:

- P3HT backbone conformations;
- length of the alkyl side chains;
- length of the backbone.

To explore the role of distorted backbone, the study will involve regiorandom P3HT (hereafter referred as rraP3HT) samples. For the second case, samples of doped P3DT will be analysed both in solution and in solid film. Lastly, the role of the length of the backbone is analysed using three different oligomers (8T, 13T and 21T).

3.1.3.1 FT-IR spectra of doped regiorandom P3HT in solution

In this Section the effect of a disordered backbone on the doping process in solution is analysed by the use of rraP3HT samples. In the following the name P3HT without any prefix will be used for the regioregular polymer, while the prefix “rra” identifies regiorandom samples.

rraP3HT differs from regioregular P3HT because of a higher degree of structural disorder due to insertion defect head-tail of the monomer on the polymer backbone. Due to this characteristic in rraP3HT the thiophene units cannot form extended

sequences of coplanar units thus preventing an ordered 3D chains aggregation. This suggest that polaron_{OA} cannot be formed; for the same reasons, CTCs are expected to be the main products of the doping process in solution. [11]

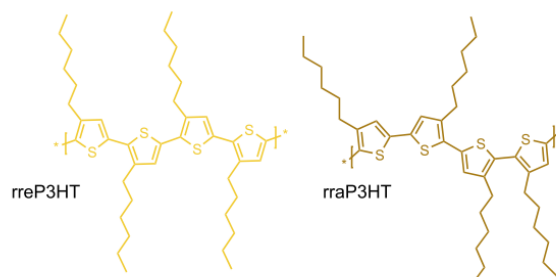


Figure 33: representation of the chemical structure of P3HT and rraP3HT. [11]

Regioregular and regiorandom P3HT show practically the same IR spectrum in the pristine state (solution), as can be seen in Figure 34, but the spectra for the doped polymer solution are strongly different in the two cases. Indeed, IR absorption spectra of doped rraP3HT reveal significant differences compared to the results obtained with P3HT. Iodine is not able to dope rraP3HT in solution at the doping ratio 5:1, while F₄TCNQ seems to be more efficient in doping the regiorandom polymer in solution at the same doping level. The presence of chains that remained undoped can be inferred from the presence of the band at 1460 cm⁻¹, highlighted in Figure 36. However, also with F₄TCNQ, the IR spectrum of doped rraP3HT obtained is very different from the one of P3HT. Indeed, looking at the C≡N vibrations of the dopant molecules (Figure 37), it can be noticed that only the bands associated to neutral F₄TCNQ in solution, slightly shifted in frequency, can be seen, accompanied by a small band at wavelength typical of the neutral solid dopant. In fact, there is no evidence of the presence of dopant anions meaning that no complete charge transfer (i.e., no ICT complexes) occurs between F₄TCNQ and rraP3HT in solution.

40

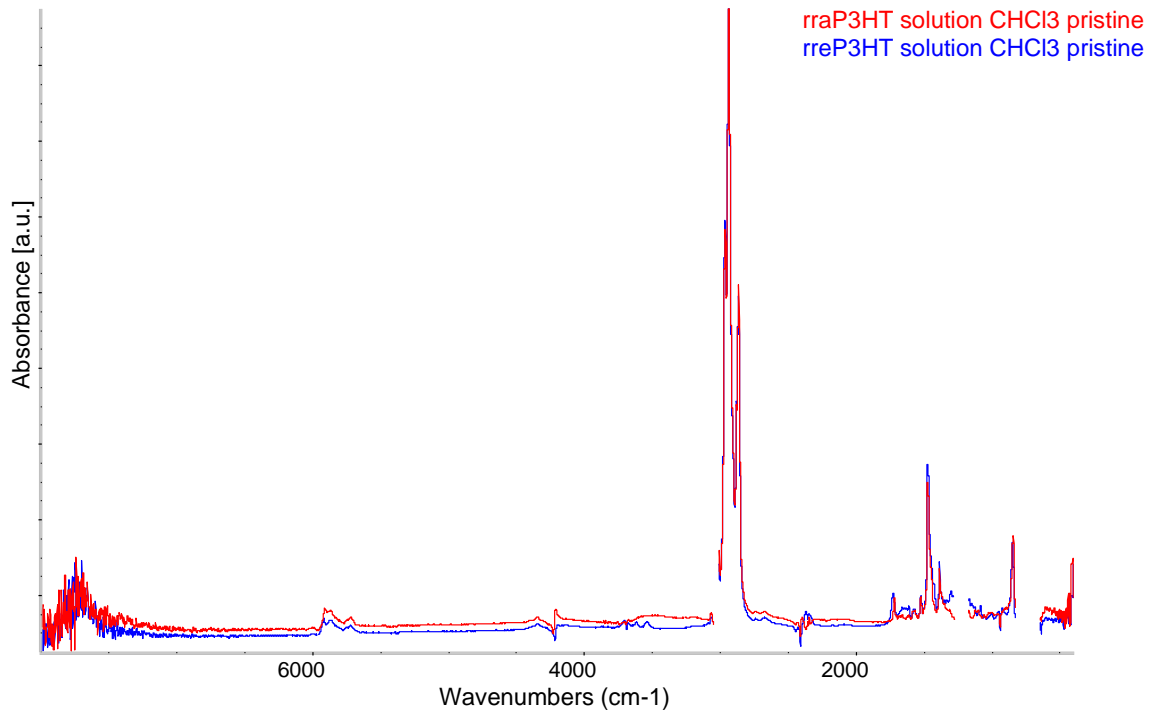


Figure 34: FT-IR spectra of pristine rraP3HT in solution (red line) and pristine (regioregular) P3HT in solution (blue line).

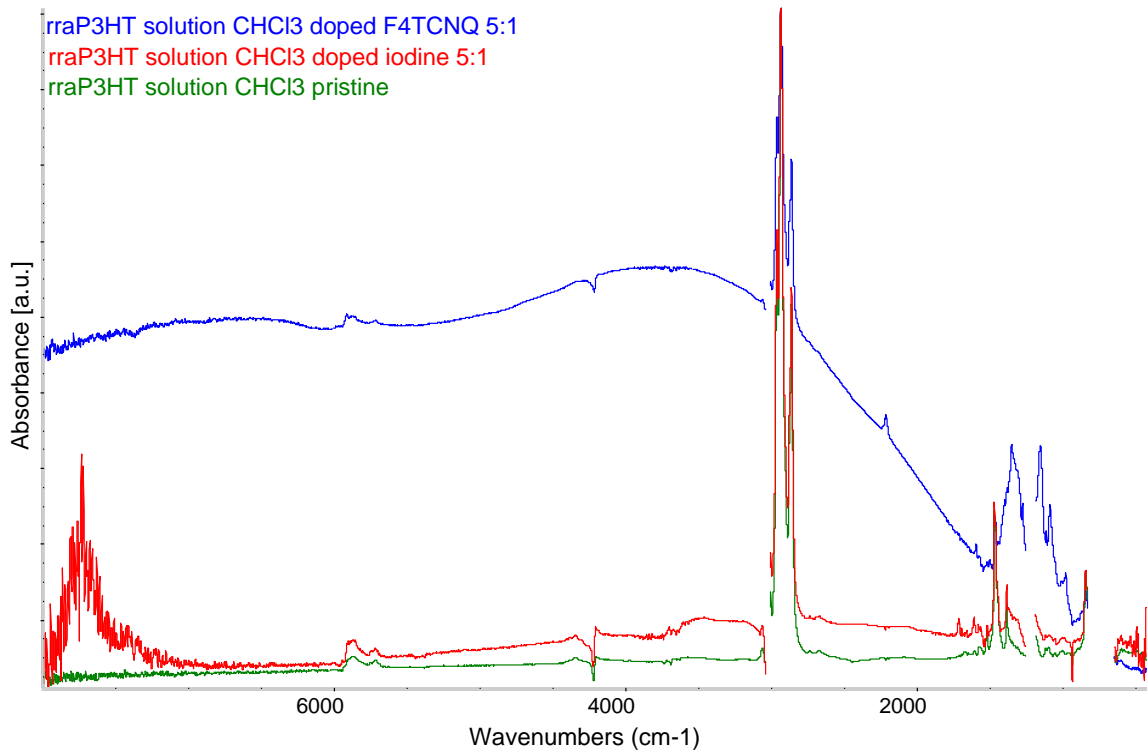


Figure 35: FT-IR spectra of rraP3HT in solution doped with iodine 5:1 (red line); doped with F4TCNQ 5:1 (blue line) and pristine rraP3HT in solution (green line).

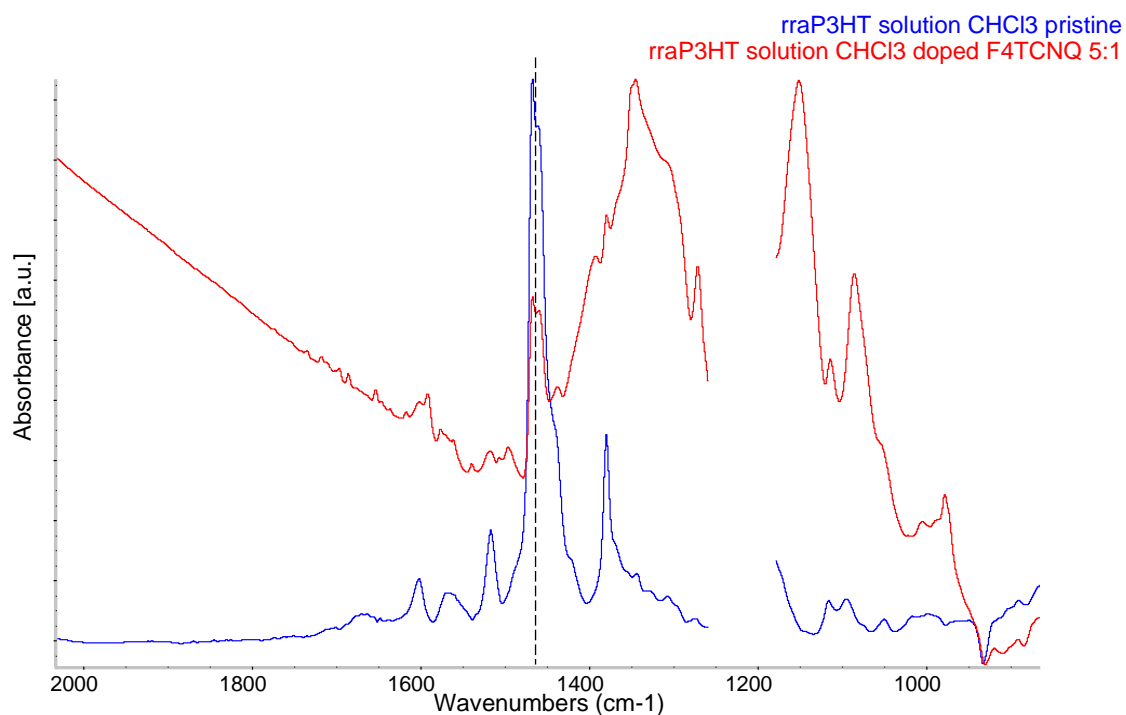


Figure 36: FT-IR spectra of rraP3HT in solution doped with F₄TCNQ 5:1 (red line) and pristine rraP3HT in solution (blue line). The black dotted line highlights the signal of pristine P3HT.

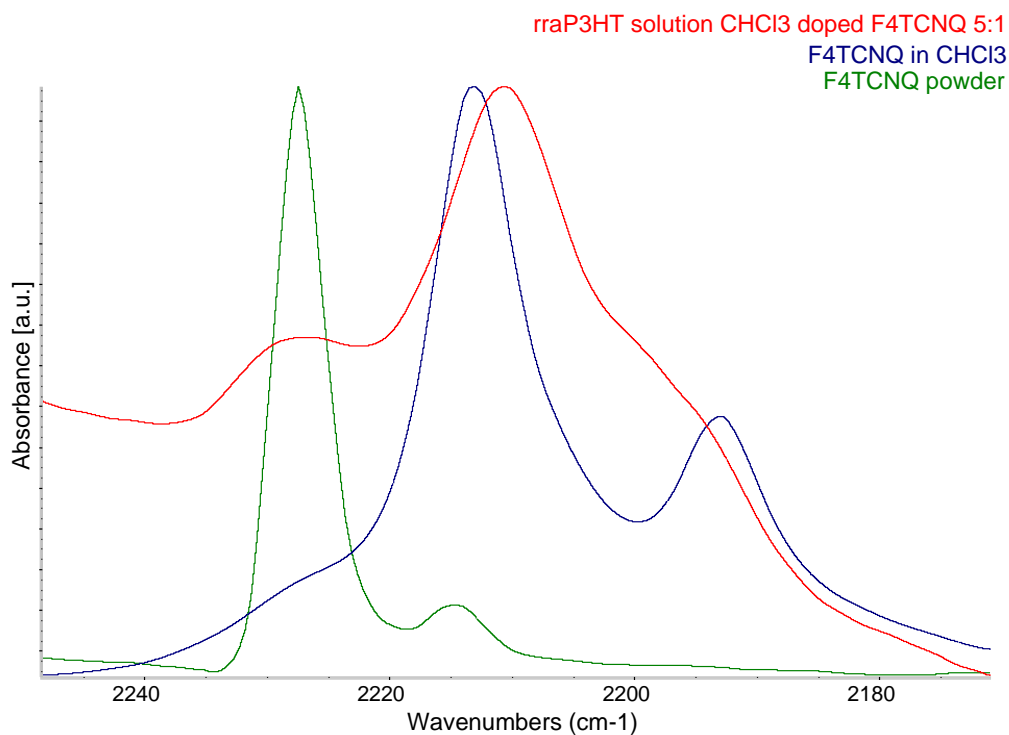


Figure 37: FT-IR spectra in the C≡N stretching region of rraP3HT in solution doped with iodine 5:1 (red line) compared to F₄TCNQ in solution (blue line) and in solid state (green line).

However, once the solutions are deposited in thin films with both dopants, ICT defects in rraP3HT samples are obtained. In Figure 39 are reported the spectra of the thin films of rraP3HT casted from solutions doped 5:1 compared to doped P3HT film. It can be noticed that the IR spectral features of the regiorandom polymer film differ both in position and in shape from those seen in doped regiorgular polymer. There is an evident shift towards higher wavenumbers in respect with the spectral feature that was considered the marker band of the polaron_{OA} (P_s bands). This may confirm the fact that rraP3HT is not able to form ordered phases as consequence of the doping process also in the solid state.

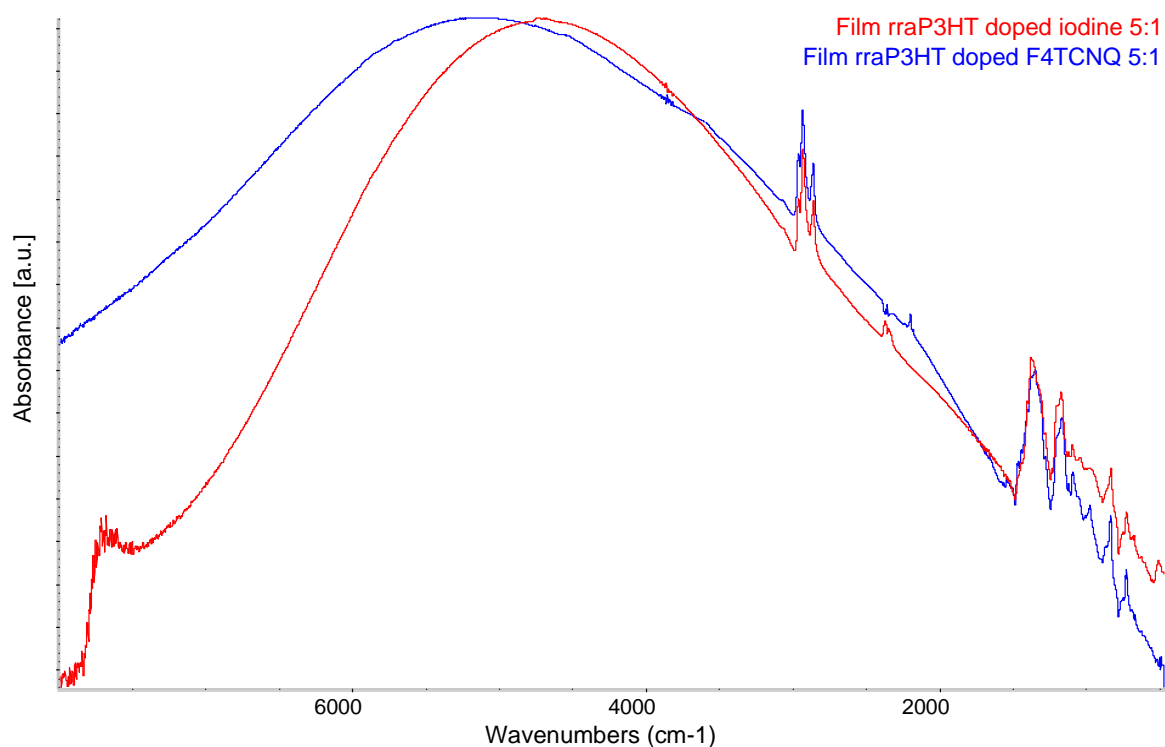


Figure 38: FT-IR spectra of rraP3HT film casted from solutions doped 5:1 iodine (red line) and F_4TCNQ (blue line) 5:1.

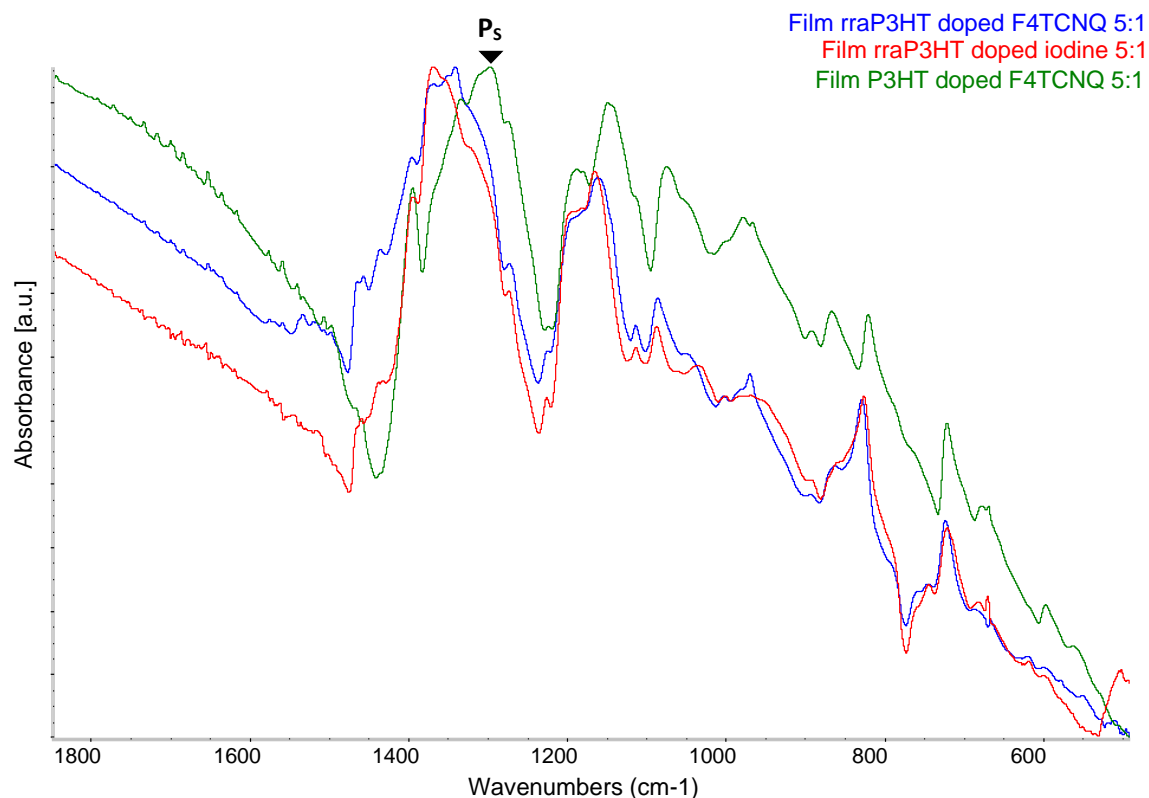


Figure 39: FT-IR spectra in region between 1800 cm⁻¹ and 600 cm⁻¹ of rraP3HT films casted from solutions doped iodine (red line) and F₄TCNQ (blue line) 5:1 compared to P3HT film casted from solution doped F₄TCNQ 5:1 (green line).

As for P3HT, in the spectral region between 1800 and 2500 cm⁻¹ of rraP3HT doped F₄TCNQ the stretching of the CN groups can be seen and they are reported in Figure 40. The appearance of a band at around 2230 cm⁻¹ (S) suggest the presence of solid dopant that has not reacted with the polymer, but also the presence of dopant anion can be supposed because of the two bands A_s and A₂ that are attributed to F₄TCNQ⁻ vibrations. This implies an interaction with the polymer with a complete charge transfer from the F₄TCNQ molecules to the P3HT chain, i.e., formation of ICT defects, but this interaction does not guarantee the formation of a polaron_{OA} phase, as previously observed looking at the IR_{AV} of doped rraP3HT. This behaviour is certainly due to the disordered morphology of the rraP3HT backbone, which hinders the formation of crystalline domains where the polarons can form an ordered structure. Importantly, F₄TCNQ is still able to form a different kind of ICT complex with the polymer. In addition, from Figure 40, it can be also seen a small shoulder at 2205 cm⁻¹ that, according to the literature, can be assigned to the formation of CTCs also in solid phase [17]

In figure 41 are reported the IR spectra registered at different times after the deposition of the rraP3HT film: from these results it can be noticed that the 2205 cm^{-1} band disappear slowly as time goes on. This may suggest that the CTCs in the solid state are not stable and the system rearrange in another configuration. Comparing the film right after casting and the film after heating it, almost all CTCs seem to be disappeared. The spectral features of CTCs and their evolution with heating can be highlighted by spectra subtraction, as shown in Figure 42.

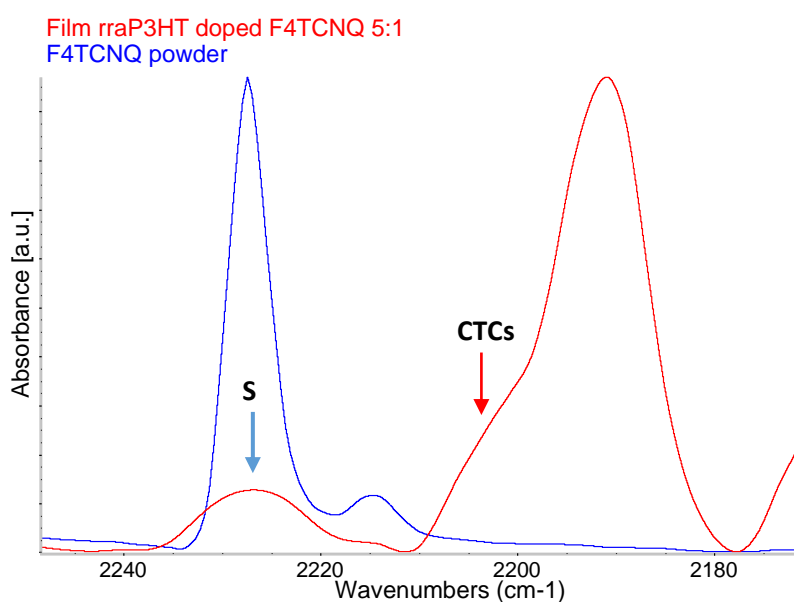


Figure 40: FT-IR spectra of the CN modes of film casted from solution of rraP3HT doped F_4TCNQ 5:1 (red line) compared to the CN modes of F_4TCNQ powder (blue line). The red arrow and the blue arrow highlight respectively the band attributed to the formation of the CTCs and the presence of neutral dopant molecule in the doped film.

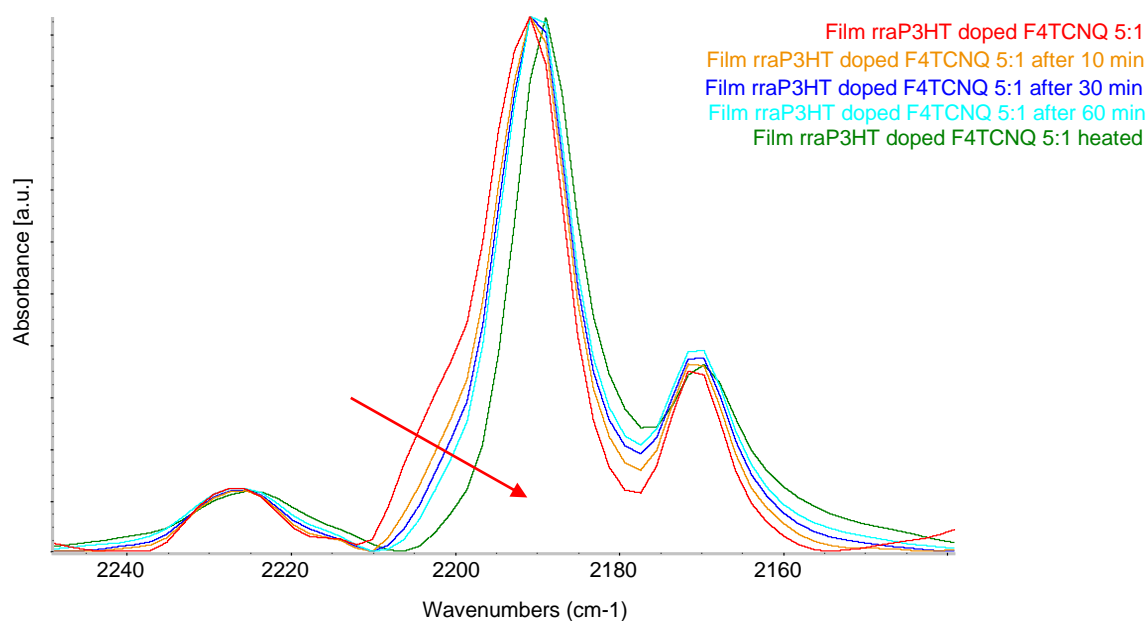


Figure 41: FT-IR spectra of CN modes of film casted from solution of rraP3HT doped F₄TCNQ 5:1 immediately after deposition (red line); after 10 minutes (orange line); after 30 minutes (blue line); after 60 minutes (light blue line) and after heating it (green line). The red arrow points out the decreasing of the CTCs band at about 2205 cm⁻¹.

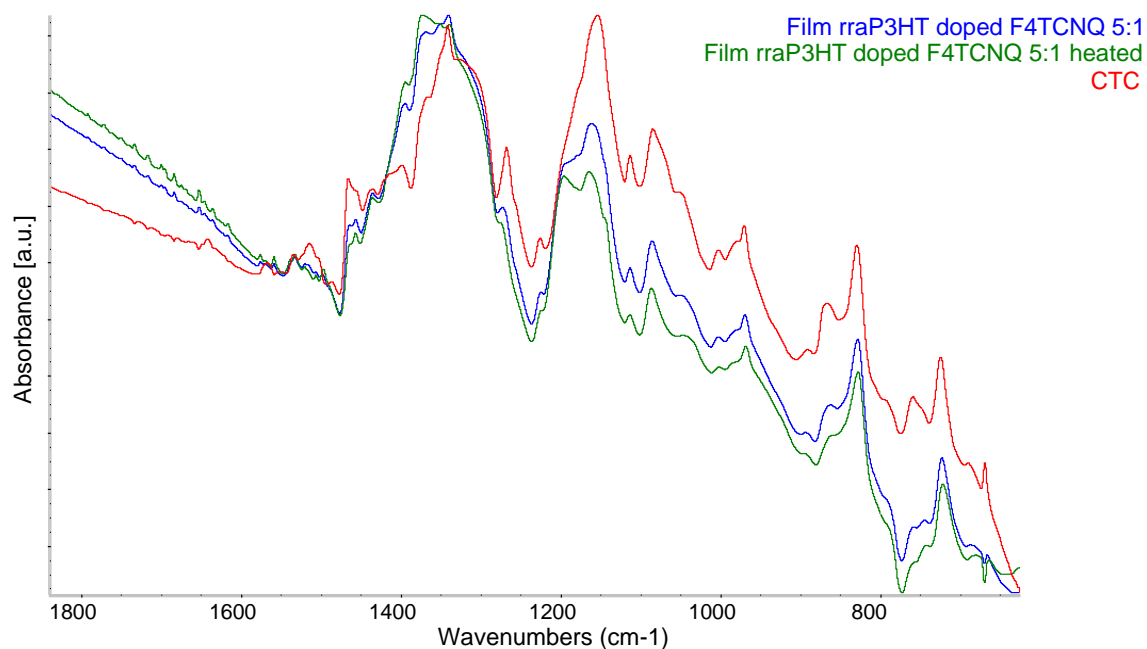


Figure 42: FT-IR spectra between 1800 cm⁻¹ and 700 cm⁻¹ of rraP3HT film doped F₄TCNQ in solution 5:1 right after casting (blue line), after heating (green line) and the subtraction spectra obtained by subtracting the spectrum of the heated film from that of the film after casting (red line).

Comparing these IR features in the IRAV region of the CTC with the different components that were observed for the doped regioregular P3HT in solution at different doping ratio it can be noticed that the IRAV features displayed by the solutions with a doping ratio 1:1 are similar to the one obtained for the CTCs. This may suggest that, in solution, when too much dopant is added, the excess of F₄TCNQ or iodine, promotes the formation of CTCs. The comparison between the IRAV of CTC and P3HT highly doped solutions is shown in Figure 43.

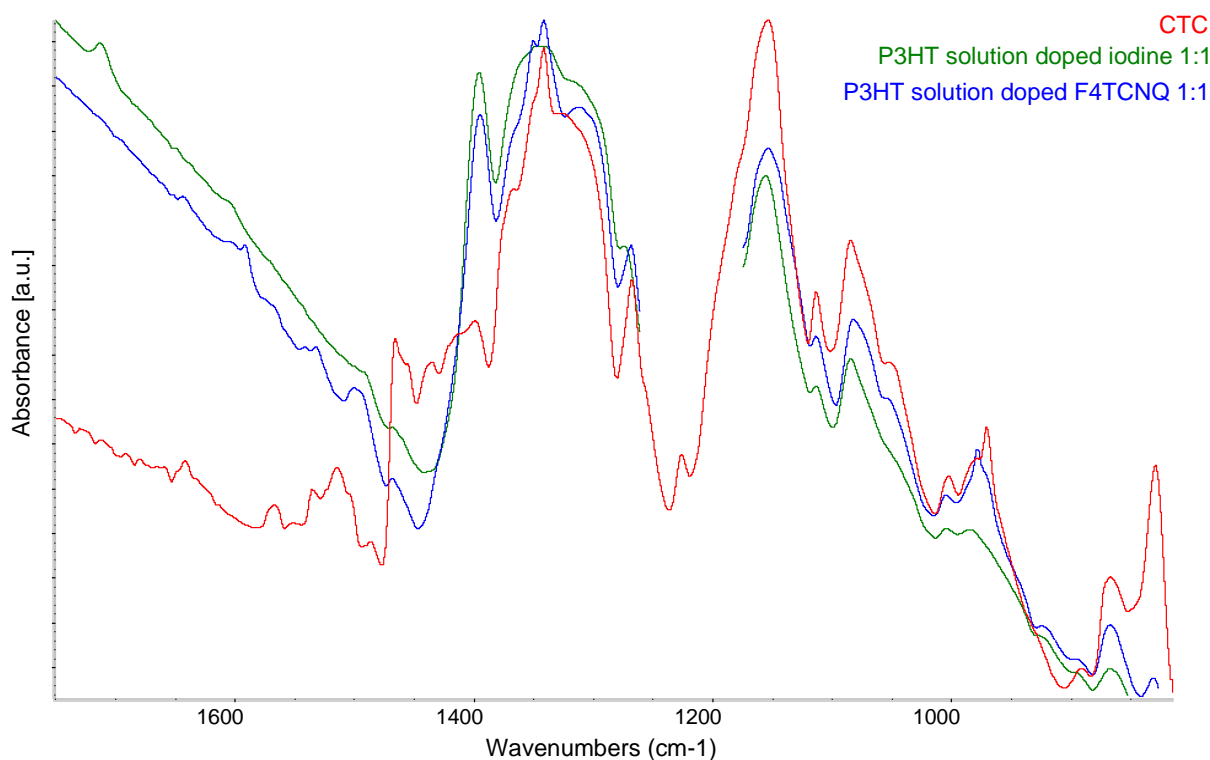


Figure 43: FT-IR spectra between 1700 cm⁻¹ and 800 cm⁻¹ of P3HT iodine doped solution 1:1 (green line); P3HT F₄TCNQ doped solution 1:1 (blue line) compared to the CTC IR features obtained by the subtraction spectra of rraP3HT doped film after casting and the heated film (red line).

These results confirm the coexistence of both kind of donor-acceptor interaction, ICT and CTC: the first one mainly forms polaron_{OA} of regioregular P3HT in film, but also in solution if the doping ratio is not too high. The CTC, on the other hand, is prevalent in amorphous region of the polymer, like in rraP3HT. [33] This is also suggested by a study developed by Neelamraju et al. on F₄TCNQ-doped P3HT films. It was shown that if the degree of disorder of dopant-polymer systems traditionally exhibiting ICT, like P3HT film, is increased the integer charge transfer mechanism is replaced by CTCs formation, like in the case of rraP3HT, thus suggesting that a high degree of conformational order in the host material is required for having an efficient

ICT between the polymer and the dopant. [34] Also in films of regioregular P3HT there could be small amounts of amorphous domains that may lead to the formation of CTC state, but in a much smaller quantity in respect with the dominant ICT mechanism. [33]

In addition, a different kind of ICT mechanism was observed in rraP3HT/F₄TCNQ systems at the solid state, giving rise to disordered polaron phase, which is well distinguishable, from its IR/V pattern in region α . Moreover, the presence of F₄TCNQ⁻ anions confirm the existence of these peculiar kind of polymer/dopant complexes.

3.1.3.2 FT-IR spectra of doped P3DT in solution

In this section the effect of the length of the side chains on the doping process in solution is analysed. P3DT differs from P3HT because of the length of the side alkyl chains made by a sequence of 10 carbon atoms (while in the P3HT are shorter and only made of 6 carbon atoms).

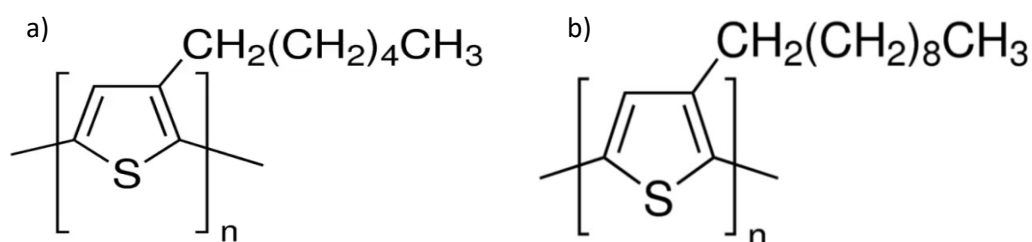


Figure 44: representation of the chemical structure of a) P3HT and b) P3DT. [35], [36]

P3HT and P3DT have the same IR pattern in the pristine state both in solution and in film, as seen in Figure 45. However, some important differences can be spotted out when looking at the spectra of the doped samples. In the previous sections it was observed that P3HT in solution can be doped at all the three doping ratios considered in this work and that, after depositing the solution into a film they all converge to the polaron_{OA} solid phase. As it can be noticed looking at the spectra, P3DT has a different behaviour. This may suggest that the length of the side chains actually affects the doping process, at least in solution. In fact, it can be noticed that, in solution and with a doping ratio of 5:1 (optimal for P3HT doping), iodine is not able to dope P3DT, while with F₄TCNQ a slight change of the IR spectra can be observed, as in the rraP3HT. This may be due to the fact that the higher steric hindrance of the longer alkyl chains hinders the interaction between the dopant and the polymer chain and possibly prevent the formation of stable aggregates in solution. In fact, if the spectra

of P3DT and rraP3HT doped 5:1 in solution are compared a similar pattern can be observed in the IR/V region, as showed in Figure 48.

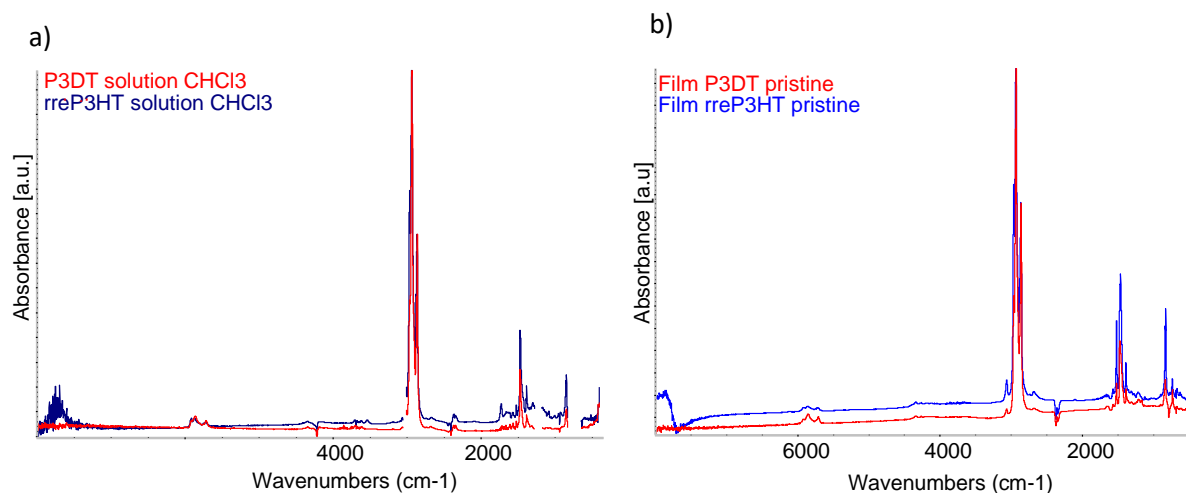


Figure 45: comparison of FT-IR spectra of pristine P3DT (red lines) and P3HT (blue lines) in solution (a) and in film (b).

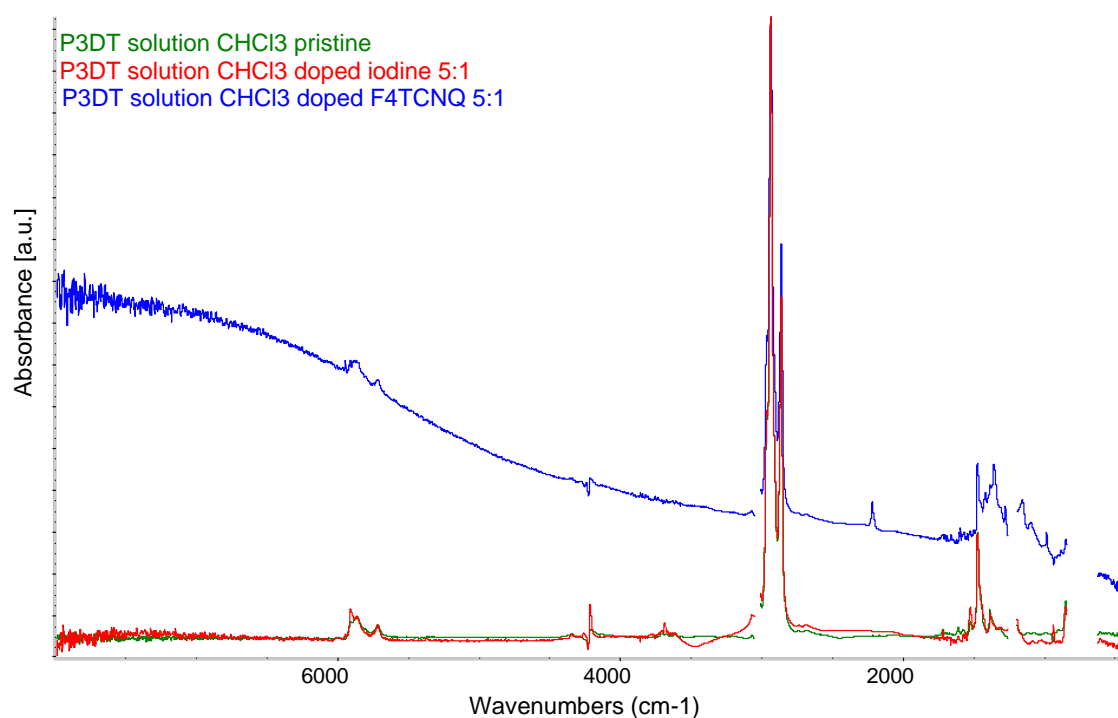


Figure 46: FT-IR spectra of P3DT solutions doped 5:1 with iodine (red line) and F4TCNQ (blue line) compared to pristine P3DT in chloroform (green line).

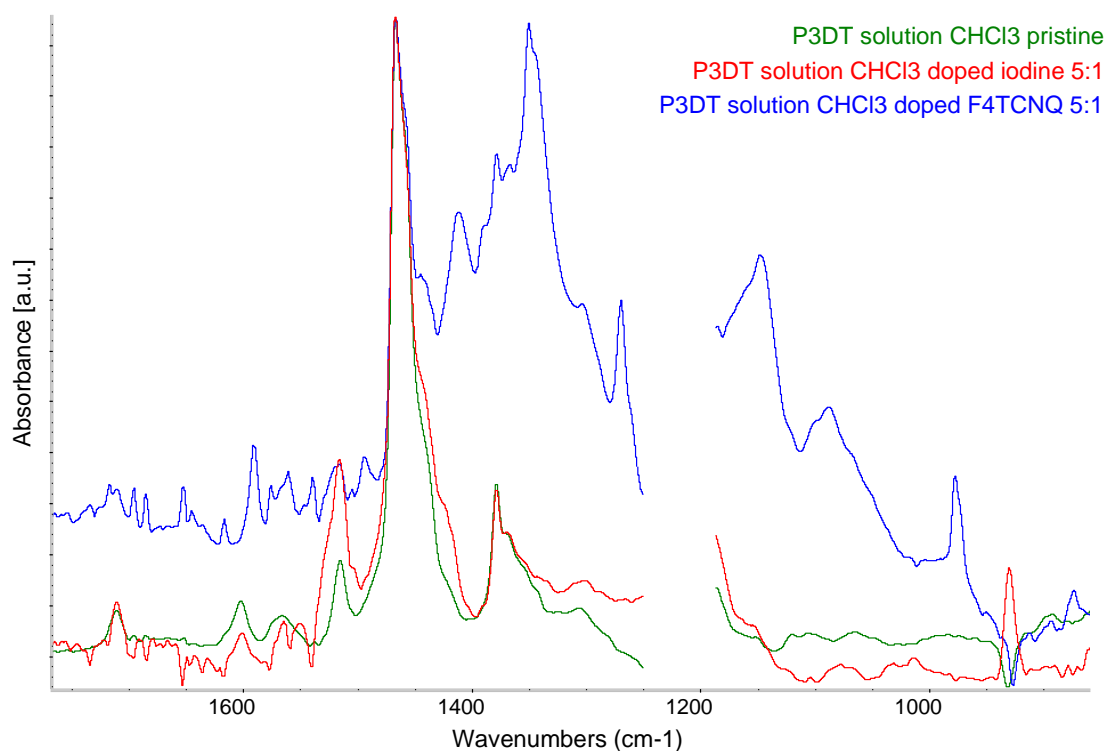


Figure 47: FT-IR spectra of P3DT solutions doped 5:1 with iodine (red line) and F₄TCNQ (blue line) compared to pristine P3DT in chloroform (green line) in the IRAV region.

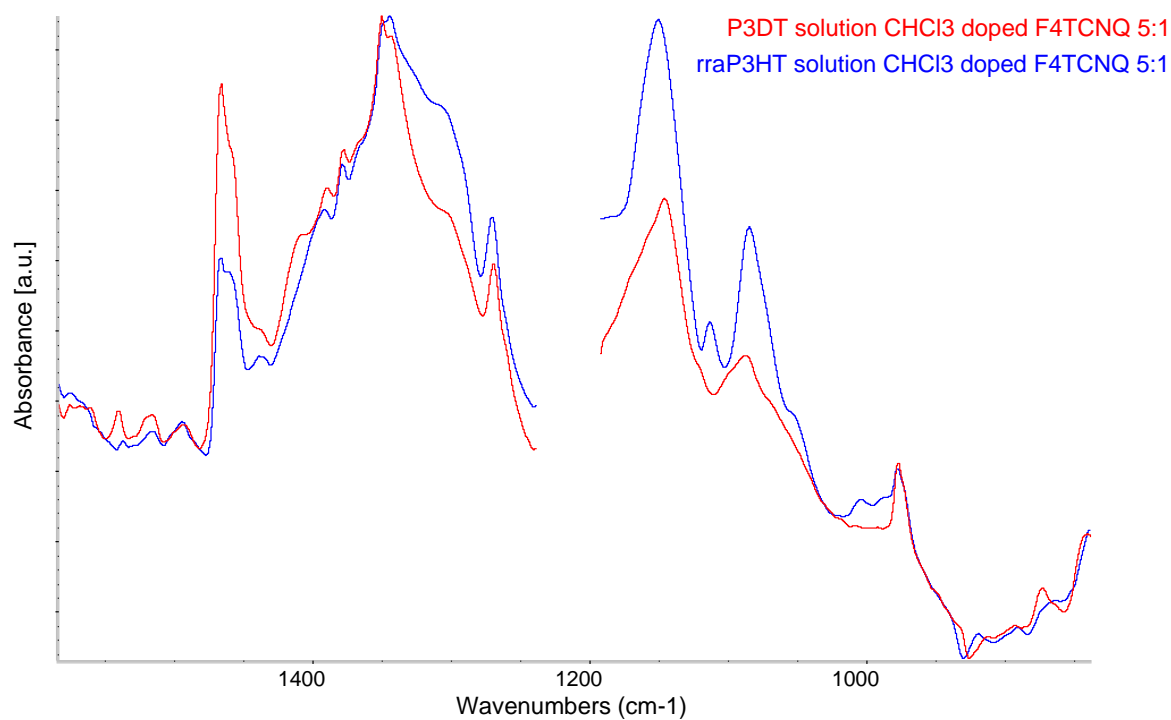


Figure 48: FT-IR spectra of P3DT solution doped 5:1 with F₄TCNQ (red line) and rraP3HT solution doped 5:1 with F₄TCNQ (blue line) in the IRAV region.

Once the solutions are deposited on a substrate, the IR spectra of both iodine and F₄TCNQ doped P3DT shows IRAVs as reported in Figure 49. Looking at the region α of doped P3DT films it can be noticed a similarity with the pattern seen in rraP3HT where polaron_OA does not form due to the disordered backbone structure. Indeed, comparing the spectra of P3DT and P3HT films, two different IR pattern can be seen in this spectral region. This may suggest that also in P3DT ordered polaron structures are not present in the doped film, due to the length of the alkyl chains. However, a closer look at the F₄TCNQ doped P3DT film shows a IRAV component at lower wavenumbers, closer to the polaron band P_s. In fact, comparing the spectra of P3DT, rraP3HT and P3HT (Figure 51) it can be seen that P3DT shows a component shifted towards that of regioregular P3HT. This observation suggests that doping with F₄TCNQ is more efficient than Iodine doping in forming a polaron_OA phase, even if in a small quantity, also on P3DT. This hypothesis can be confirmed by the Raman spectroscopy results reported in the next chapter.

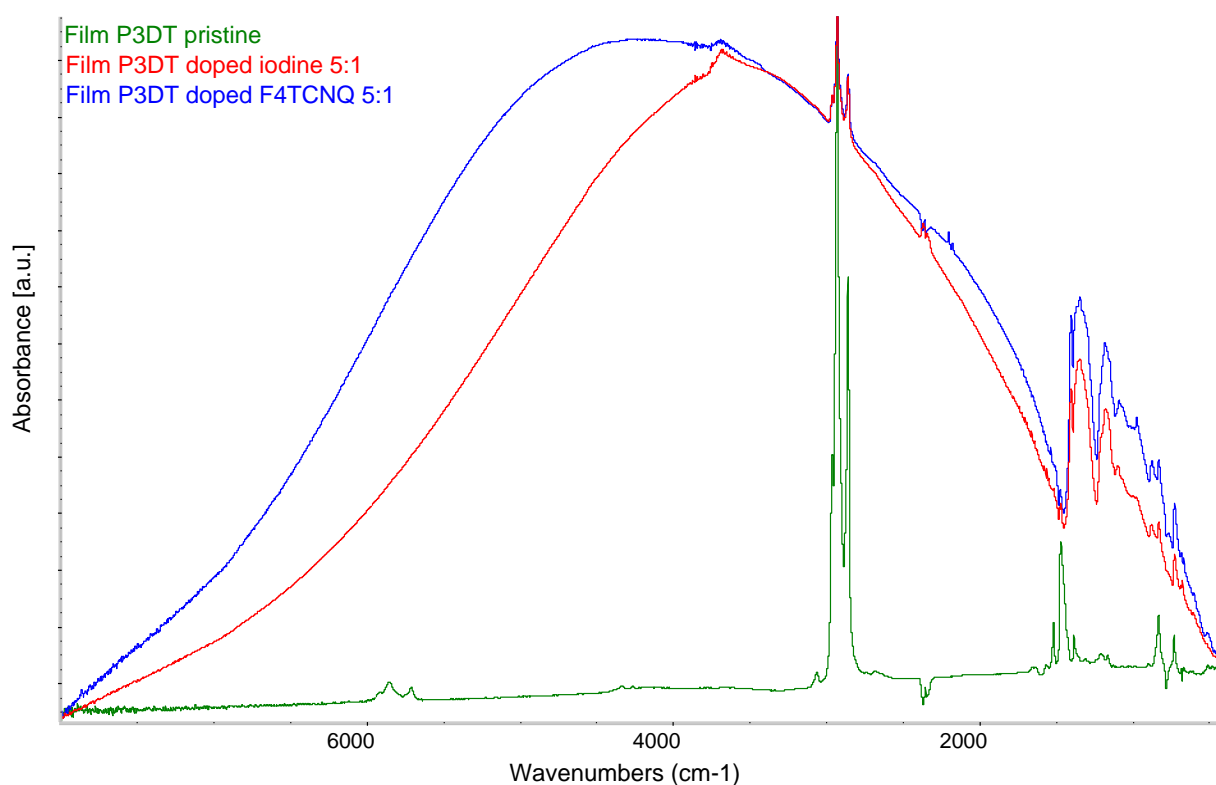


Figure 49: FT-IR spectra of P3DT films doped in solution 5:1 with iodine (red line) and F₄TCNQ (blue line) compared to pristine P3DT film (green line).

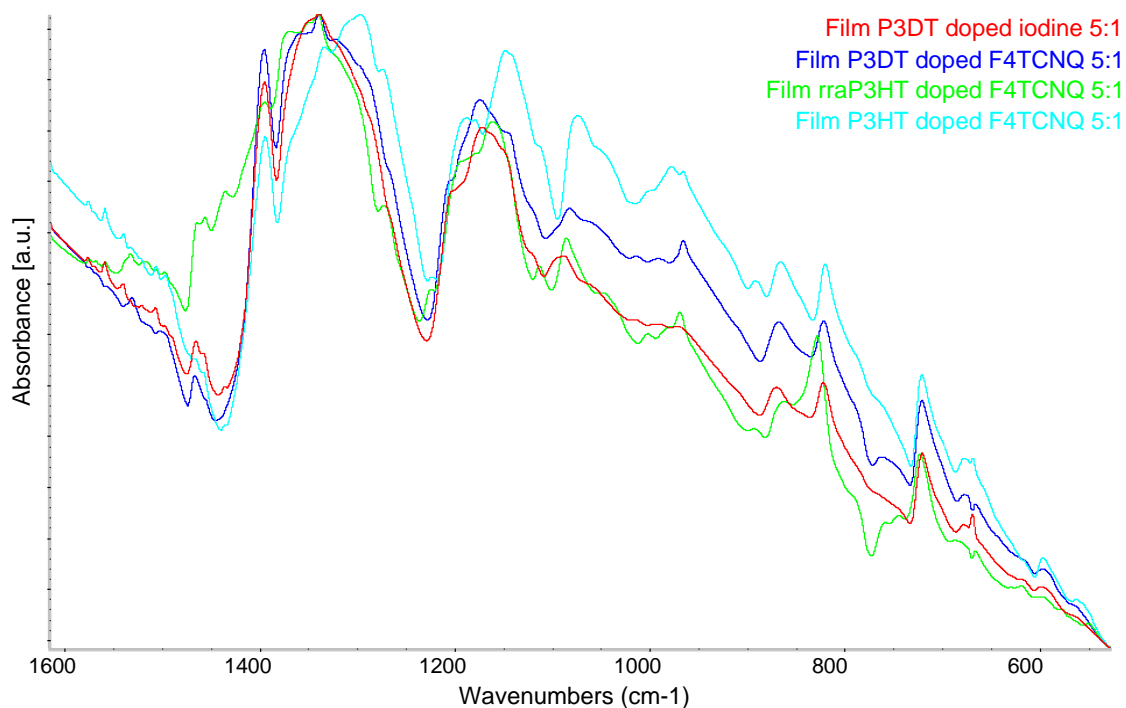


Figure 50: FT-IR spectra of P3DT films doped in solution 5:1 with iodine (red line) and F₄TCNQ (blue line) compared to rraP3HT film (light green line) and P3HT film (light blue line) in the IRAV region (between 1600 cm⁻¹ and 600 cm⁻¹).

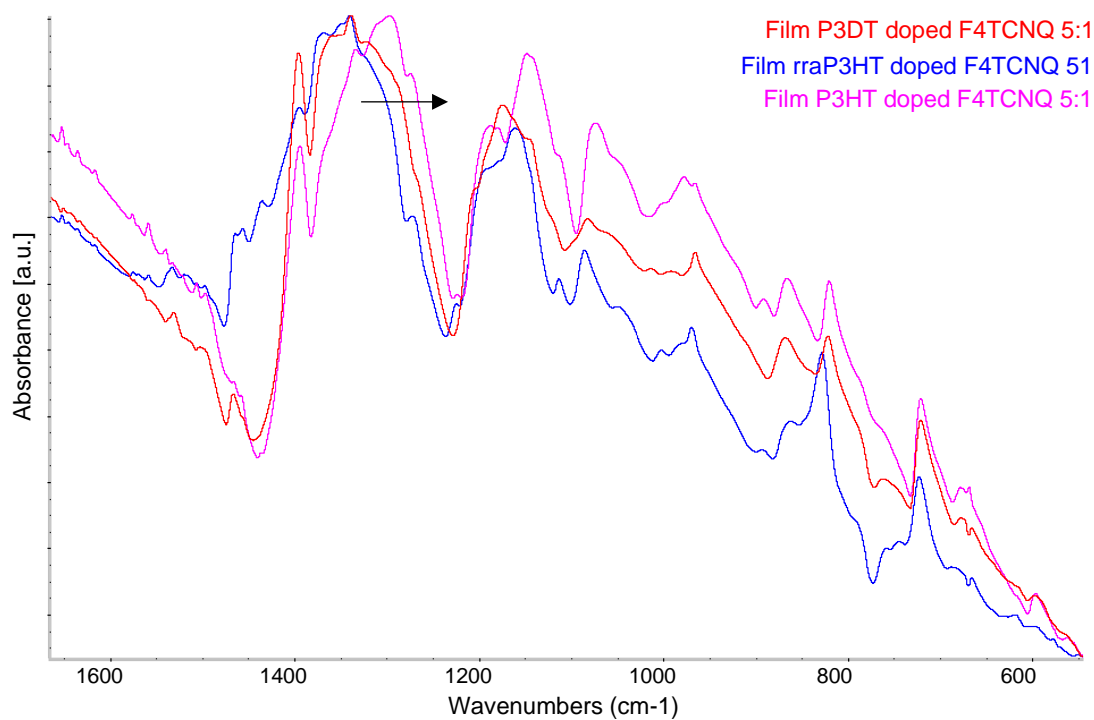


Figure 51: FT-IR spectra of P3DT (red line), rraP3HT (blue line) and P3HT (pink line). The black arrow highlights the shift towards lower wavenumbers.

Looking at the vibrations of the CN groups (Figure 52) we observe that: i) the band at 2205 cm^{-1} assigned to the CTC can't be identified, and ii) the band A_S of the F_4TCNQ^- anion, usually observed at 2190 cm^{-1} in P3HT solid film, is slightly shifted towards higher wavenumbers (A_D band, at 2194 cm^{-1}). Comparing P3DT doped film with P3HT film at the three different doping ratios it can be noticed that the band A_S progressively shift to lower wavenumbers from the film at lowest doping to the highest doping one. A high wavenumber band A_D was seen also in the P3HT doped solutions. This may imply that when the dopant form ICT complexes with the polymer, the amount of defects has a non-negligible effect on the spectrum of the anion and the wavenumber of the dopant anion band is higher for more diluted defects. In a similar way, the presence of more disordered polymer chains in the P3DT, due to an increase in the length of the side chains, can hinder an effective chain packing resulting in the blue shift to 2194 cm^{-1} of the A_S band of the anions.

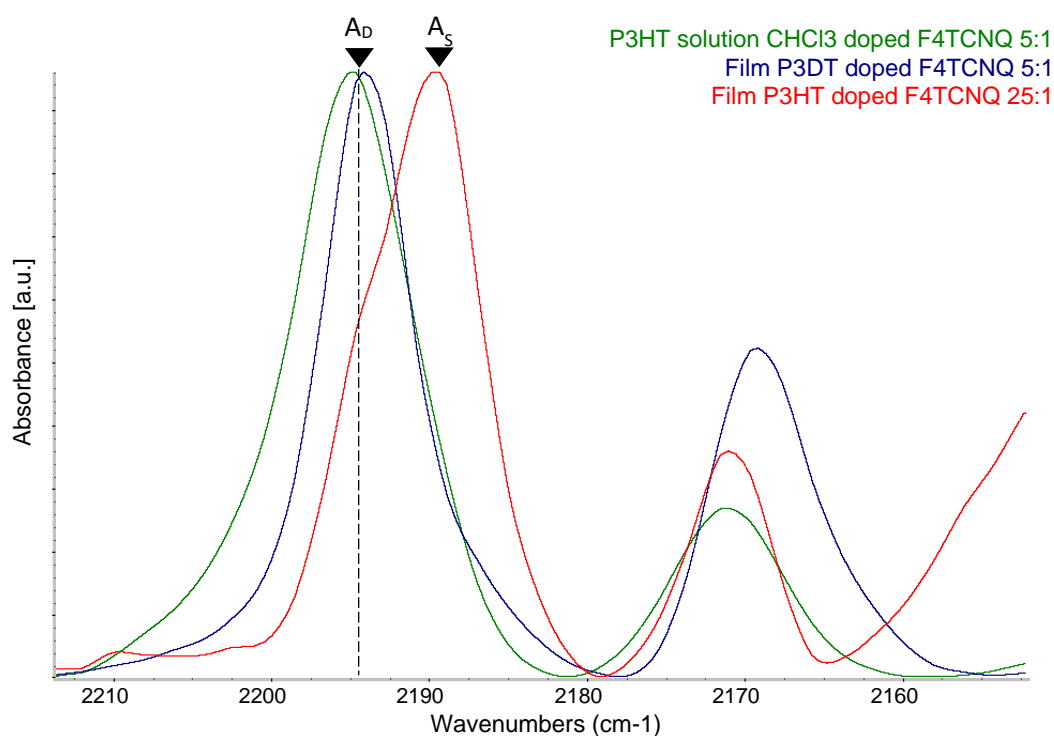


Figure 52: stretching modes of the CN groups of film casted from solution of P3DT doped F_4TCNQ 5:1 (blue line) compared to P3HT doped F_4TCNQ 25:1 solution (green line) and film (red line). The spectra are reported with a baseline correction.

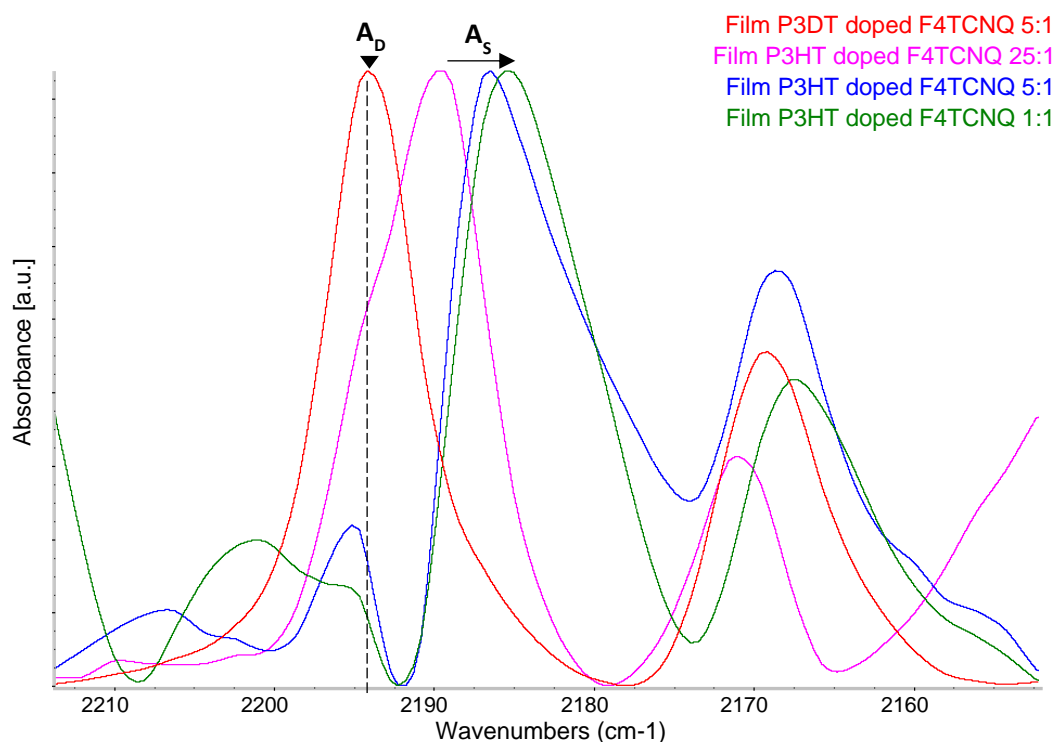


Figure 53: stretching modes of the CN groups of film casted from solution of P3DT doped F_4TCNQ 5:1 (red line) compared to film of P3HT doped F_4TCNQ 25:1 (pink line), 5:1 (blue line) and 1:1 (green line). The spectra are reported with a baseline correction.

Looking at CN groups vibrations in doped P3HT films it can be seen that in the 25:1 doping level the band attributed to the dopant anion A_S is at 2190 cm^{-1} , but a component A_D is still present as a shoulder, while for the films doped 5:1 and 1:1 the A_S bands are shifted to 2186 cm^{-1} and 2185 cm^{-1} respectively. Also in these two cases the band A_D can be seen, but with much lower intensity in respect with the other one. If, as seen before, higher wavenumbers are associated to more disordered configurations, this shift can be due to an increase of the amount of polaron_{OA} domain with respect to polarons in more disordered regions. Some chains can still remain in a disordered configuration even in the doped P3HT films and for this reason the band A_D can be seen in all three cases, but with a much lower intensity than in case of P3DT film or P3HT solution.

To sum up, the effect of longer alkyl side chains is to hinder the doping of the polymer in solution, but also hampering the formation of extended ordered polarons domains in the solid state. However, integer charge transfer (ICT) was observed, suggesting the possibility of the formation of a more disordered polaronic structures in P3DT films.

3.1.3.3 FT-IR spectra of doped oligothiophenes in solution

In this section the effect of the length of the backbone on the doping process in solution is analyzed. For this study, three different oligothiophenes are used: 8T, 13T and 21T.

Polymeric materials are characterized by large dispersion of molecular weights, for this reason, the study of their properties can be complicated. Therefore, oligomers, consisting in a finite and known number of monomeric units, are often used as models to study the property of the infinite chain polymers. [37] In many studies oligothiophenes (OTs) have been used as models to understand and predict the spectroscopy of polythiophene, both in the pristine and doped state. [38] For this reason, in this work the behavior of different $(3HT)_n$ with an increasing number of thiophene units ($n=8,13,21$) is compared with the one of P3HT.

Solutions of the oligomers in chloroform were prepared and doped with F_4TCNQ , since it seems to be more efficient than iodine and can give more information thanks to the $C\equiv N$ group vibrational modes. The doping ratio used is the 5:1, being this level of doping, as observed before, the most effective both in solution and in film.

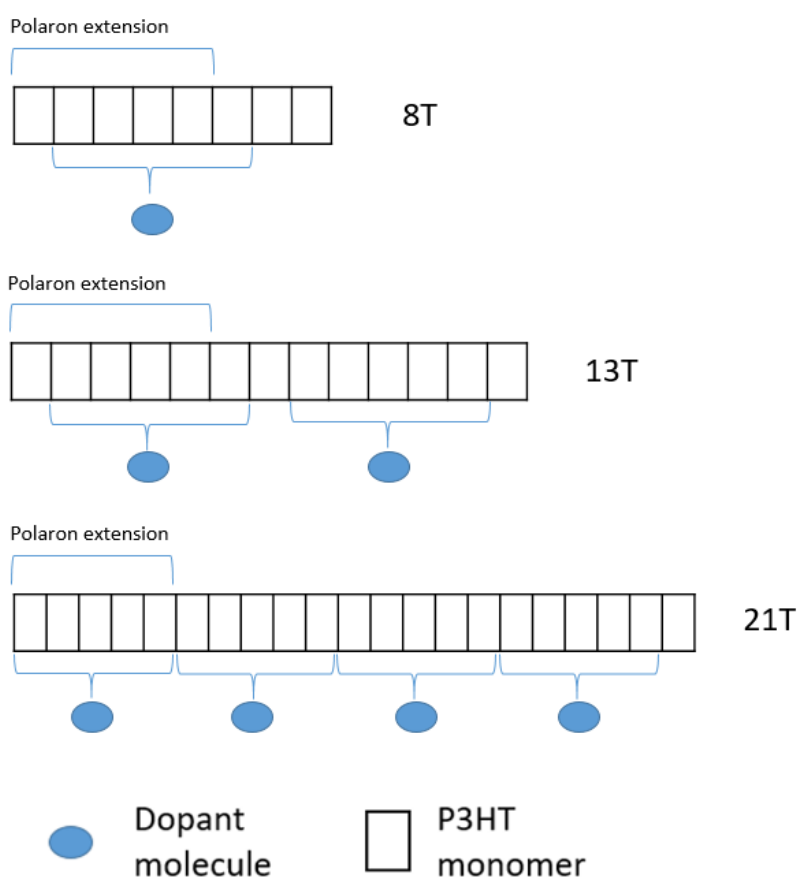


Figure 54: schematic representation of the doping ratio 5:1 in the different oligomers.

The comparison between the FT-IR spectra of the three pristine oligomers in solution and in film with the pristine polymer shows the same behavior of the different materials, as shown in Figure 55.

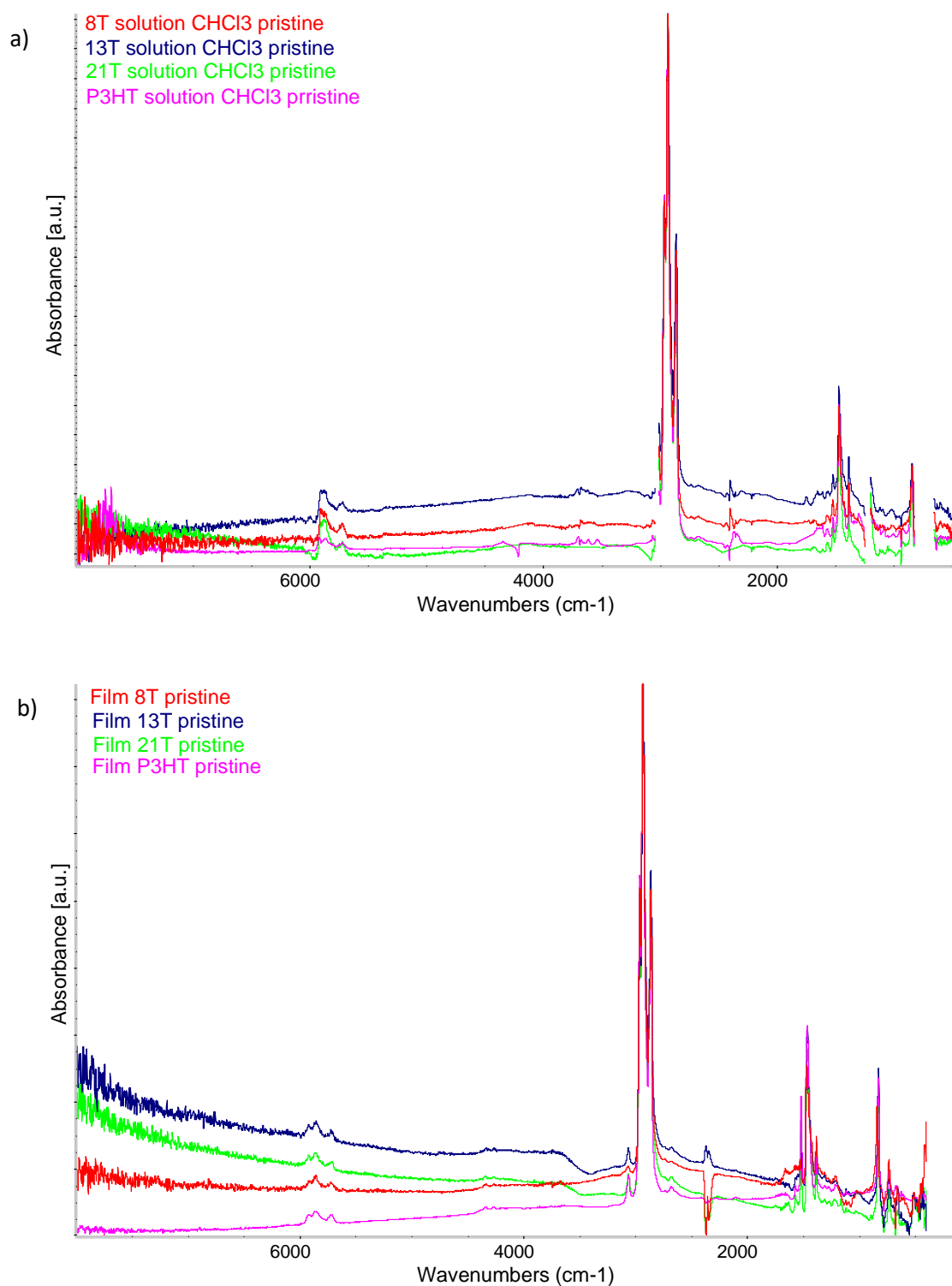
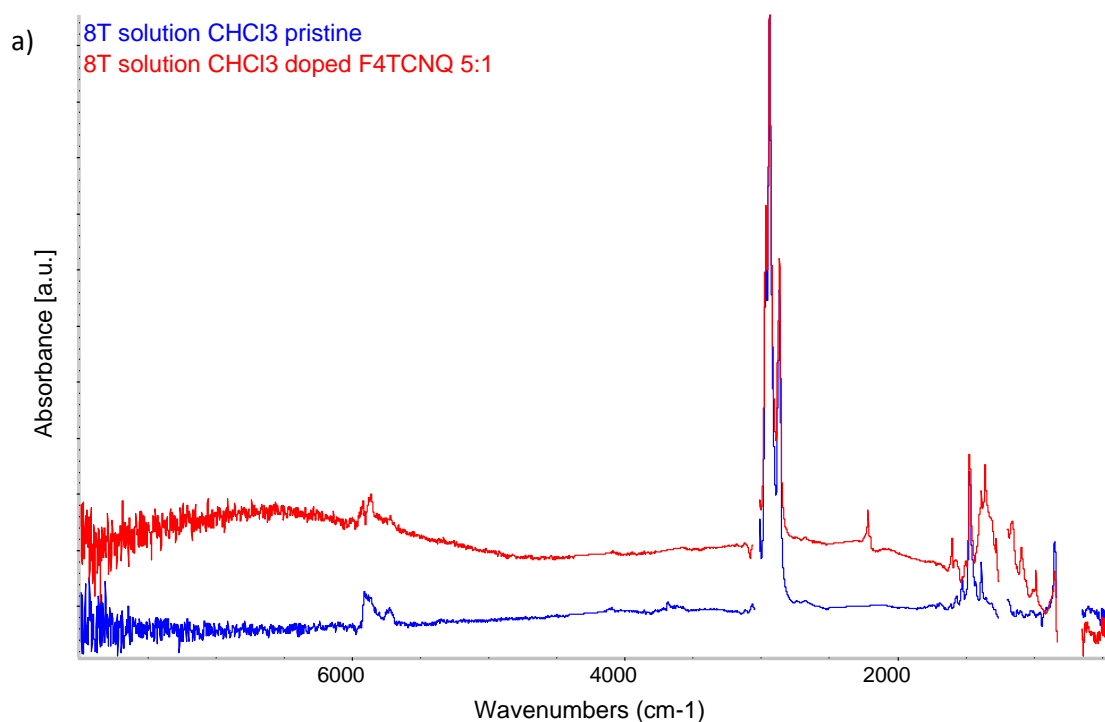


Figure 55: FT-IR spectra of P3HT (pink lines), 21T (green lines), 13T (blue lines) and 8T (red lines) pristine in solution (a) and in solid film (b).

In Figure 56 the spectra of the three pristine oligomers are compared to the doped ones in solution. It can be immediately noticed that the behavior in solution is quite different from the one of P3HT: only small changes in the spectral patterns of oligomers can be observed between pristine and doped solutions. This may suggest that oligomers in solution, due to their short length are not able to form polarons. If the spectra of the doped oligomers in solution are compared with the one of doped rraP3HT in solution a similar pattern can be seen, as shown in Figure 58.



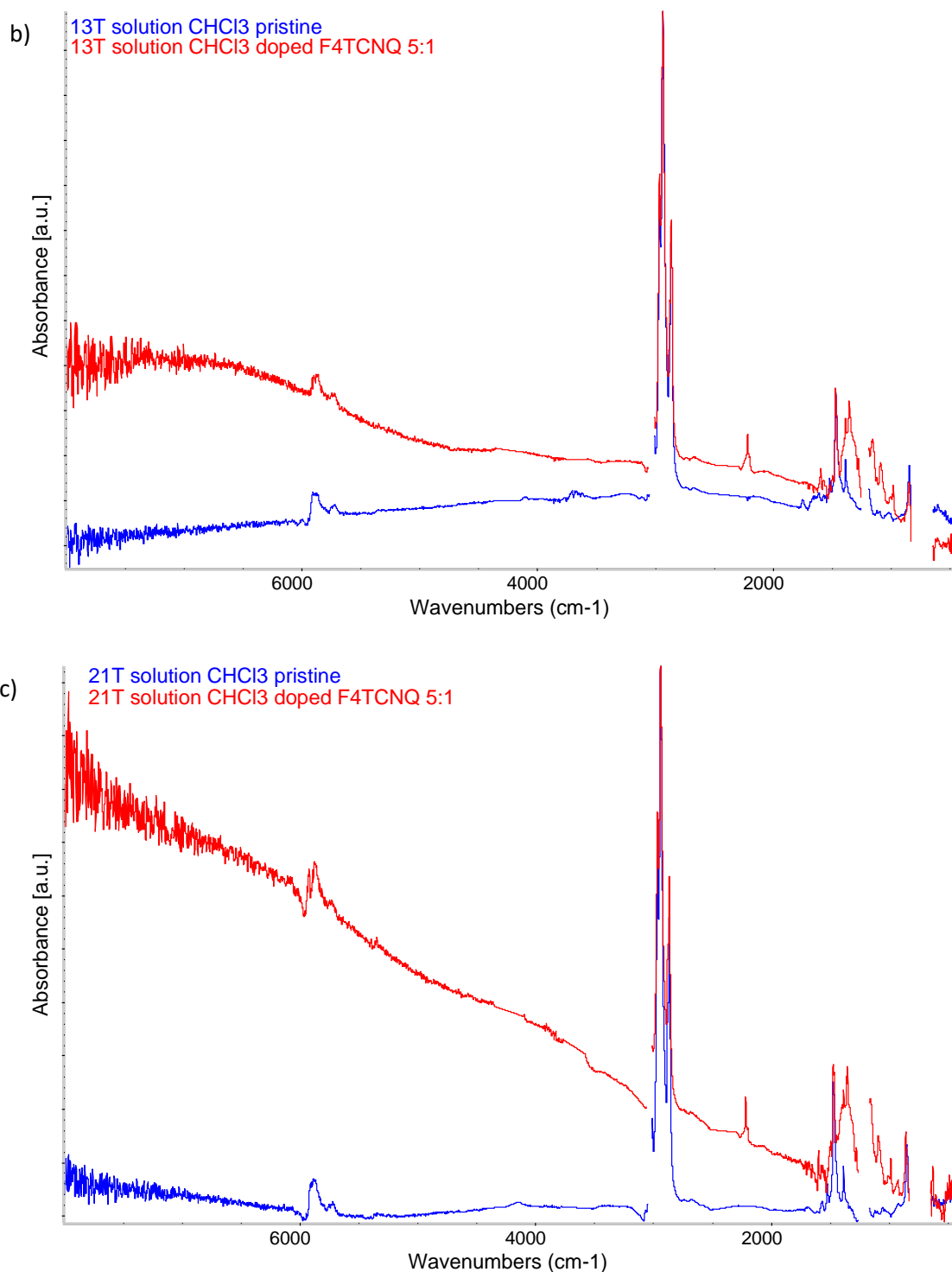


Figure 56: FT-IR spectra of a) 8T in solution doped 5:1 with F₄TCNQ (red lines) compared to the pristine 8T in solution; b) 13T in solution doped 5:1 with F₄TCNQ (red lines) compared to the pristine 8T in solution; c) 21T in solution doped 5:1 with F₄TCNQ (red lines) compared to the pristine 8T in solution.

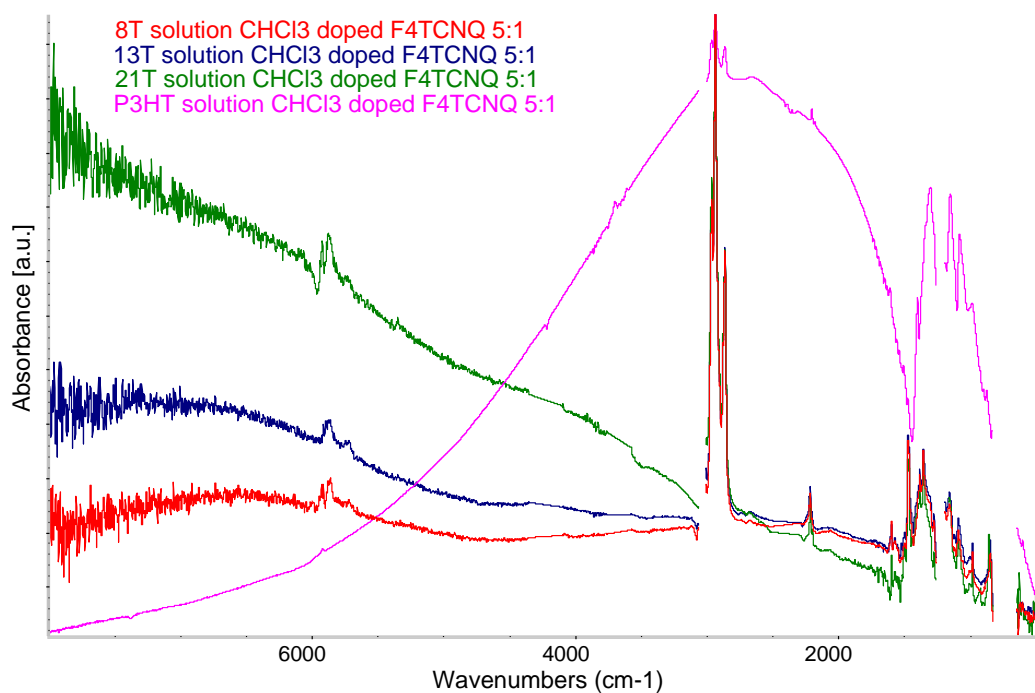


Figure 57: FT-IR spectra of 8T (red line), 13T (blue line) and 21T (green line) in solution doped 5:1 with F₄TCNQ compared to P3HT in solution doped 5:1 with F₄TCNQ (pink line).

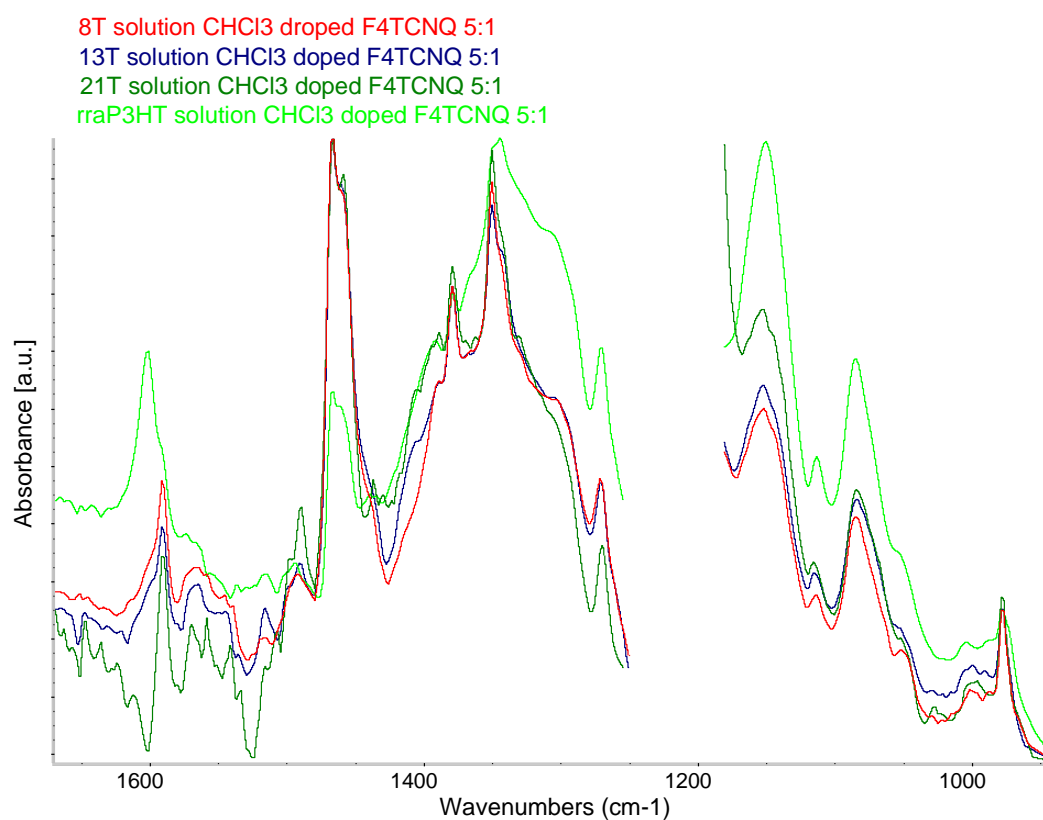


Figure 58: FT-IR spectra of 8T (red line), 13T (blue line) and 21T (green line) in solution doped 5:1 with F₄TCNQ compared to rraP3HT in solution doped 5:1 with F₄TCNQ (light green line).

By looking at the vibrations of the $C\equiv N$ groups it can be noticed that in all three cases only neutral molecules of F_4TCNQ are present in the solution, while there aren't evidence of anionic species (F_4TCNQ^-), meaning that a complete charge transfer from the dopant to the oligomers is hampered, confirming the inability of the $(3HT)_n$ to form polarons in solution (see Figure 59). This observation suggests that the few interactions between dopant and oligomers, if present, are in form of CTC only, maybe because of the difficulty to form clusters containing different $3HT_n$ molecules in solution.

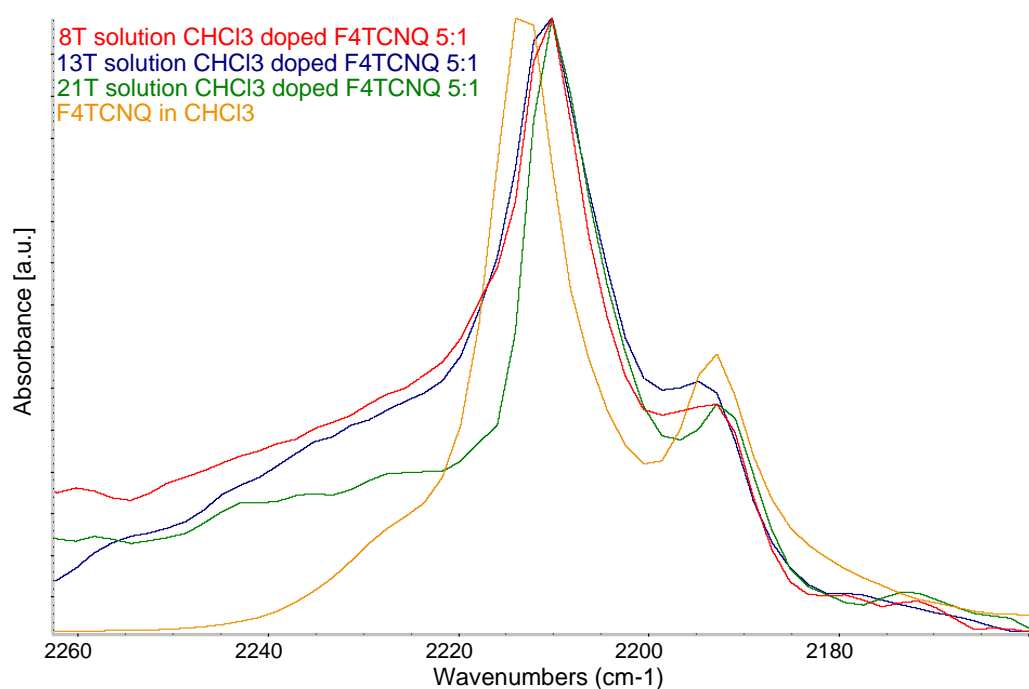
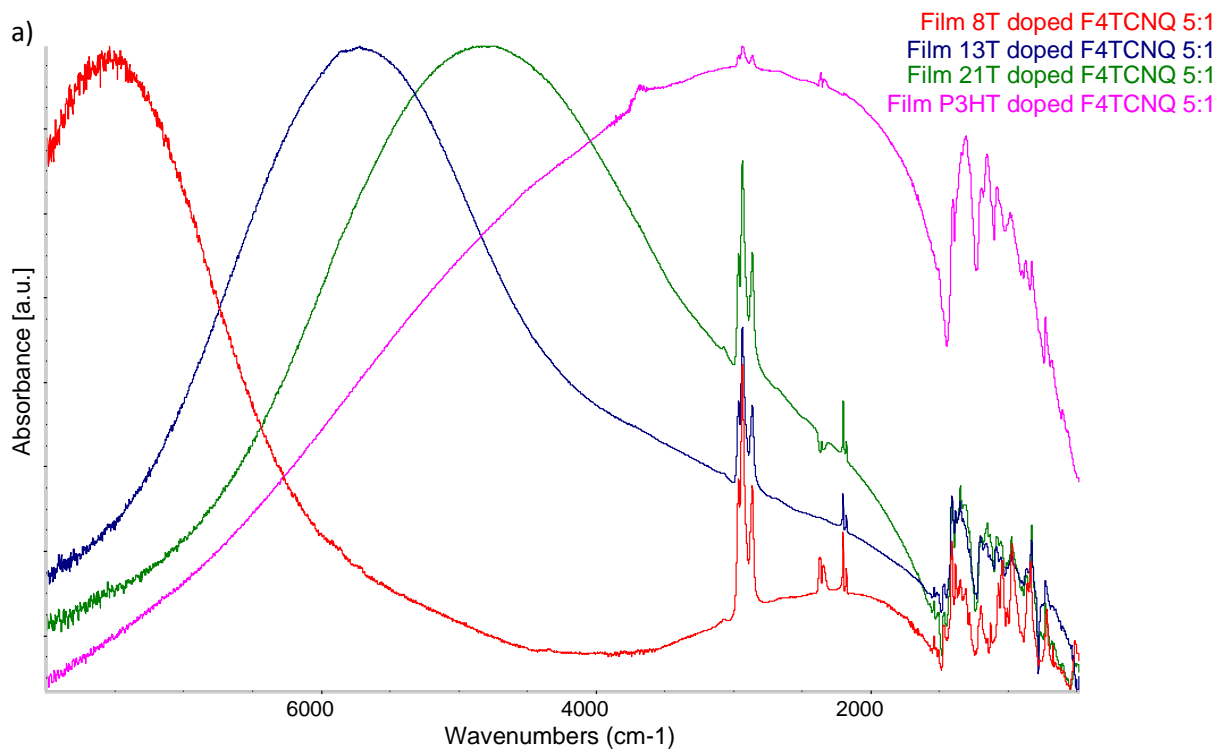


Figure 59: $C\equiv N$ stretching modes of 8T (red line), 13T (blue line) and 21T (green line) in solution doped 5:1 with F_4TCNQ compared to $C\equiv N$ modes of F_4TCNQ in chloroform solution (light green line).

The solutions were then deposited on a KBr substrate obtaining thin films of doped oligothiophenes and the results are shown in Figure 60. A first observation that can be done looking at the regions α , β and γ of the spectra is that the 8T is the most different from the polymer, while increasing the number of thiophene units the pattern becomes more similar to the one obtained for P3HT. Indeed, the 21T shows a pattern in the α region very close to the band P_s attributed to the polaron in the polymer.

On the contrary, 8T doped film shows some similarities with the rraP3HT doped film since in both cases the band in the region α is shifted to higher wavenumber in respect with the polaron band P_s , similarly to the case of rraP3HT, as shown in Figure 61. This could suggest that CTCs are formed in the film after doping. Looking at the stretching of the $C\equiv N$ groups (Figure 62) the band at 2205 cm^{-1} assigned to the CTC can't be seen,

but it can be noticed that the band of the F₄TCNQ anion is slightly shifted towards higher wavenumbers as seen for doped P3DT film. On the other hand, the presence of the two bands related to the dopant anion implies a complete charge transfer that, looking at the region α , may be attributed to the presence of some ICTs, namely polaronic structures. In fact, some IR features of the polaron can be recognized also in the 8T doped film, as highlighted in Figure 61. From this observation, it can be concluded that the oligomer with 8 thiophene unit is able to form ICTs at the solid state upon doping, but only in a very small quantity since also CTCs are present. This also confirms that the extension of the polaron is smaller than 8 thiophene units, as theoretically predicted.



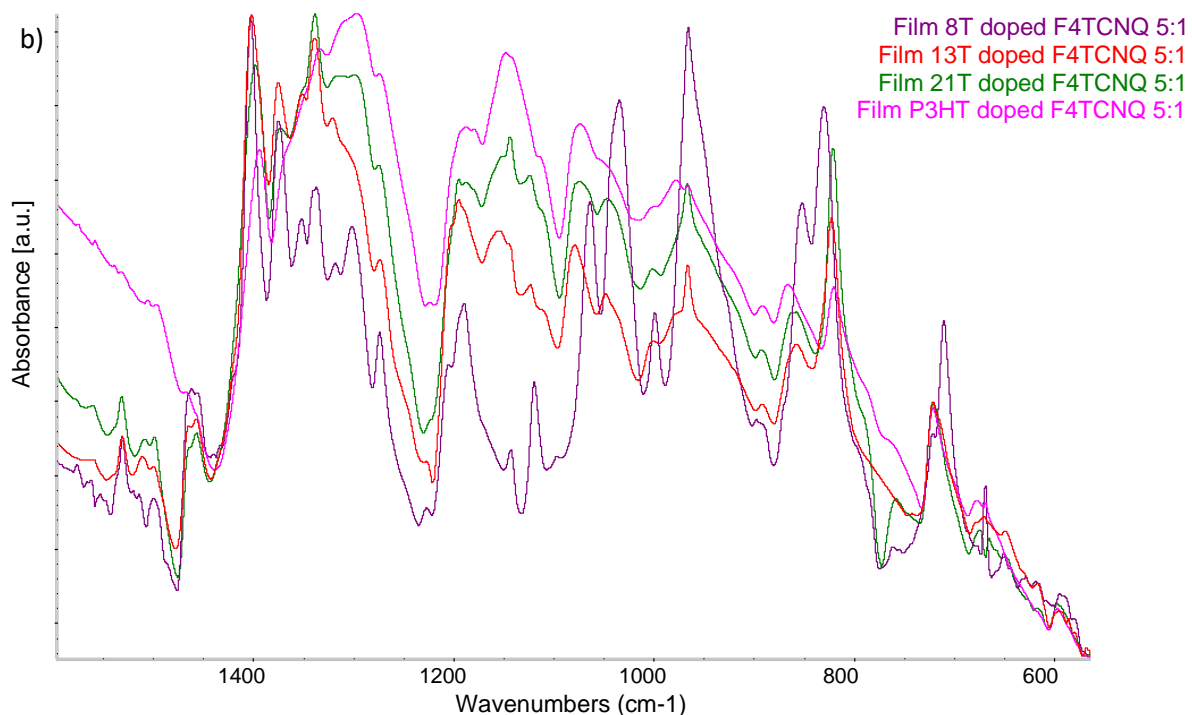


Figure 60: FT-IR spectra of 8T (red line), 13T (blue line) and 21T (green line) films doped 5:1 with F₄TCNQ compared to P3HT film doped 5:1 with F₄TCNQ a) from 8000 cm⁻¹ to 400 cm⁻¹ ; b) from 1600 cm⁻¹ to 600 cm⁻¹.

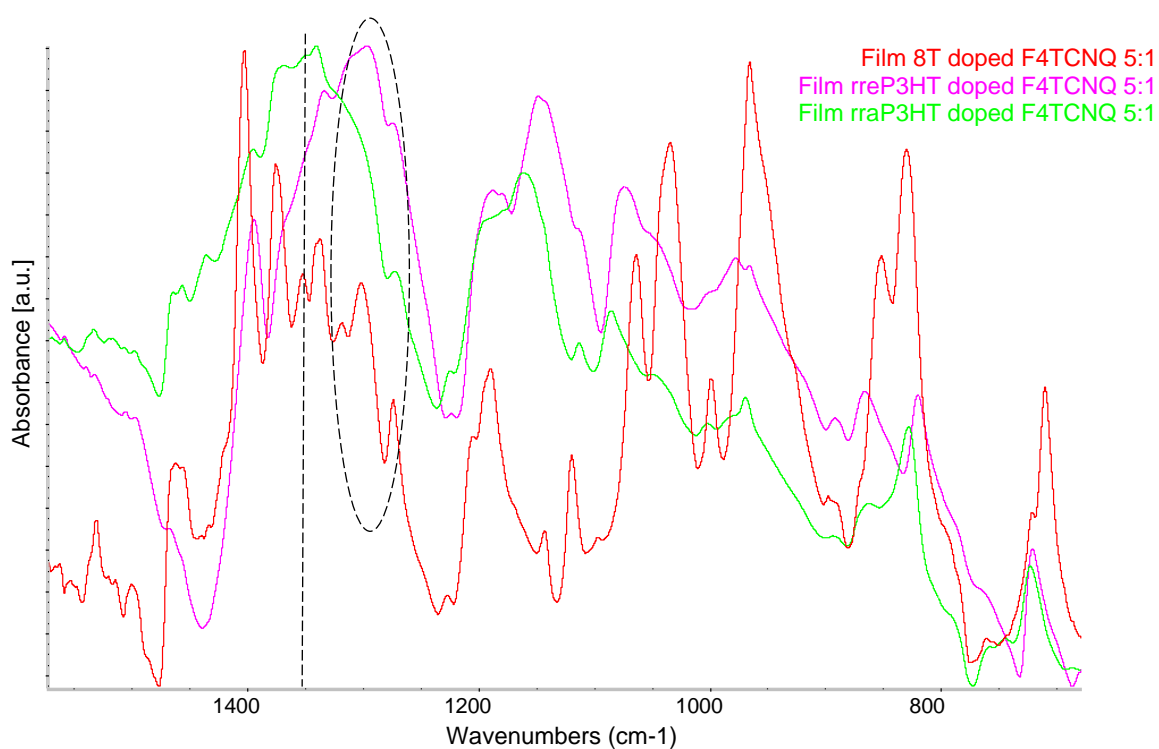


Figure 61: FT-IR spectra of 8T (red line), P3HT (pink line) and rraP3HT (green line) films doped 5:1 with F₄TCNQ from 1600 cm⁻¹ to 700 cm⁻¹. The black dotted line indicates the

centre of the band in the region α , while the black dotted circle highlights the polaron IR features.

As the length of the backbone increases the band P_s increases in intensity and the IR pattern becomes closer to the one of P3HT. In conclusion, these results confirm that, as it could be expected, increasing the number of thiophene units, the behavior of the oligomer becomes more similar to the one of the polymer.

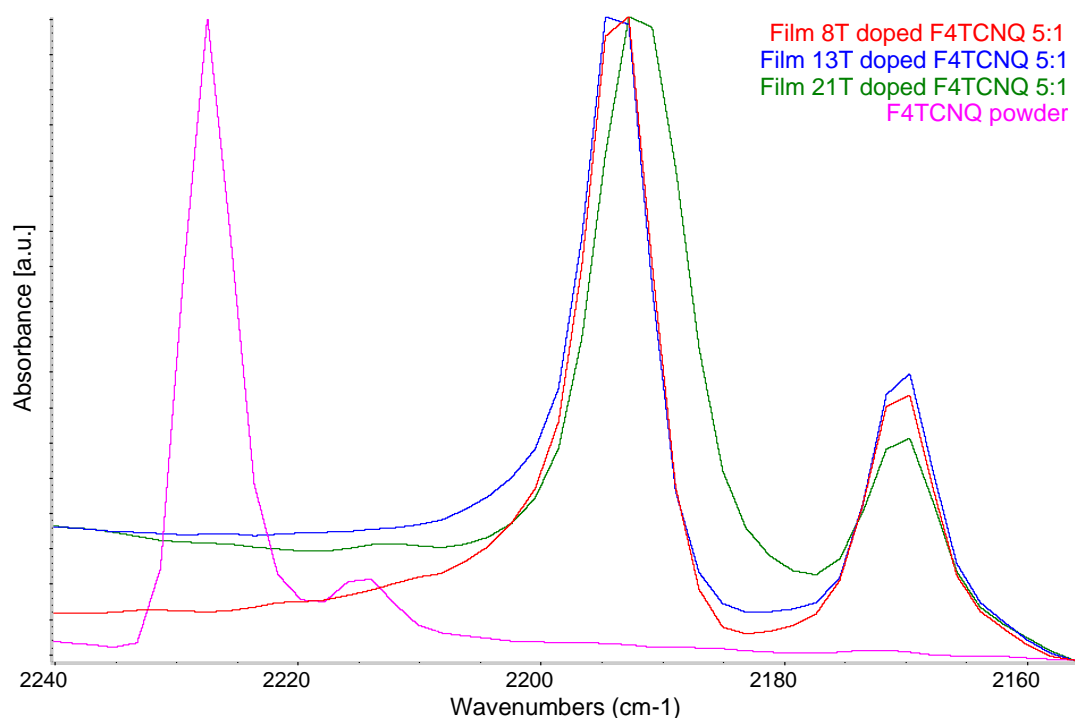


Figure 62: C≡N modes of 8T (red line), 13T (blue line) and 21T (green line) film doped 5:1 with F₄TCNQ compared to C≡N modes of F₄TCNQ film (pink line).

In addition, the oligomer 13T was doped with a lower doping ratio, 10:1, to see if some of the previously observed features varies by changing the level of doping, as seen for P3HT in solution. The results obtained are shown in Figure 63 and Figure 64.

In solution the two IR pattern in the α region are very similar. The only difference is an increase in the intensity of the bands in the 5:1 in respect with the 10:1, but the frequencies of the peaks remain the same, thus suggesting that the same species is present at both doping ratios. When the solution is casted into a thin film the two levels of doping show, again, very similar IR spectra. Also, here it can be seen that the 5:1 is more doped than the 10:1, as expected. In fact, the presence of a higher amount of ICTs in the higher doping ratio case is proven by the comparison of the IR spectra normalized in the IR_{AV} region. Indeed, the 10:1 sample shows a stronger band at 1450

cm^{-1} , corresponding to the peak of the pristine molecule (see Figure 64). Regarding other features, no significant differences can be seen in the two doping levels.

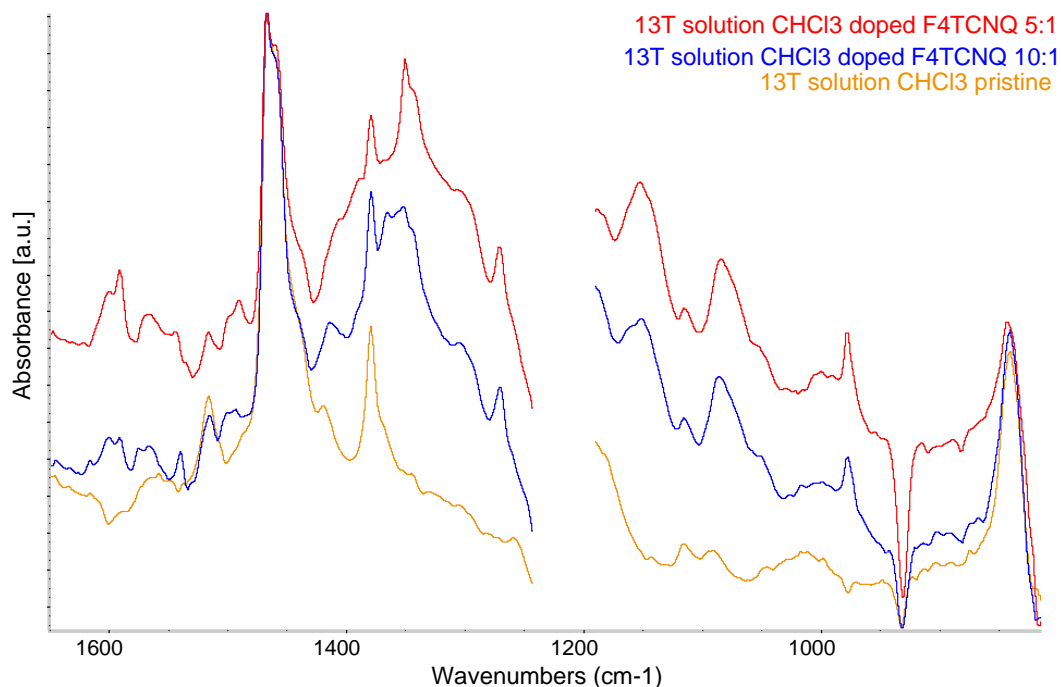


Figure 63: FT-IR spectra of the oligomer 13T pristine in solution (brown line), doped F_4TCNQ in solution with a ratio 10:1 (blue line) and 5:1 (red line).

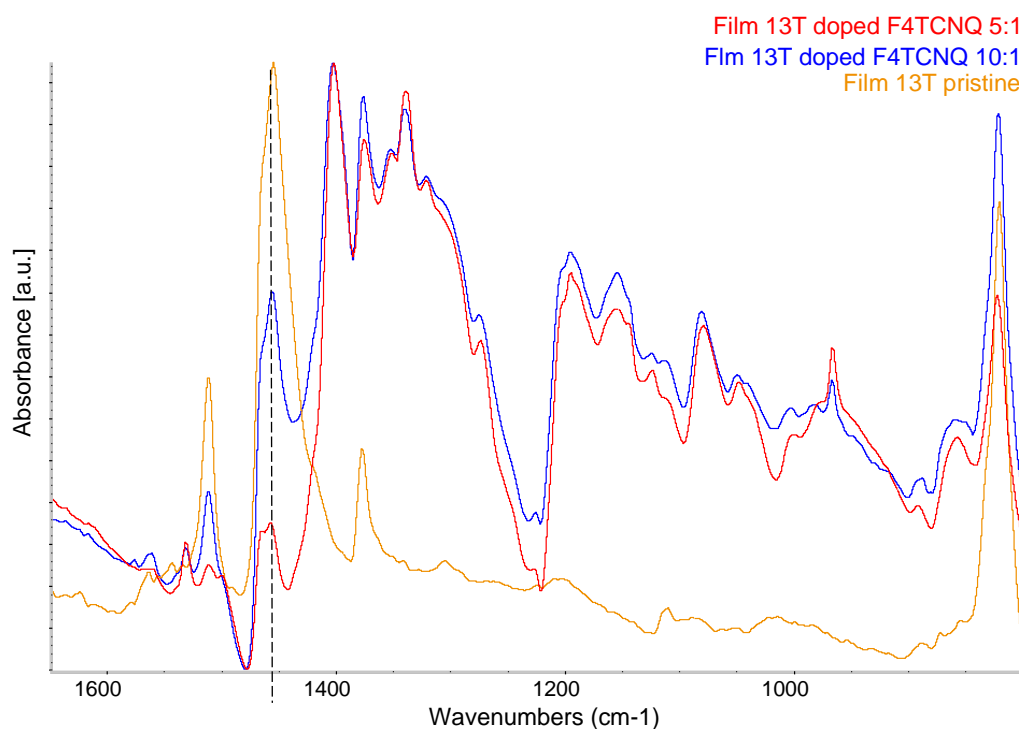


Figure 64: FT-IR spectra of the oligomer 13T film pristine (brown line), doped F_4TCNQ with a ratio 10:1 (blue line) and 5:1 (red line); the black dotted line highlights the band of pristine polymer.

Another difference among the oligomers is the energy gap (E_g) between the HOMO and the LUMO that depends on their length. This E_g decreases going from shorter to longer oligomers. The reason of this decrease is related to an increase in the conjugation length when more monomer units are added to form the oligomer. For this reason increasing n in the $(3HT)_n$ an increase in the wavelength of the lower energy electronic transition can be seen in the spectra, as showed in Figure 65. [39]

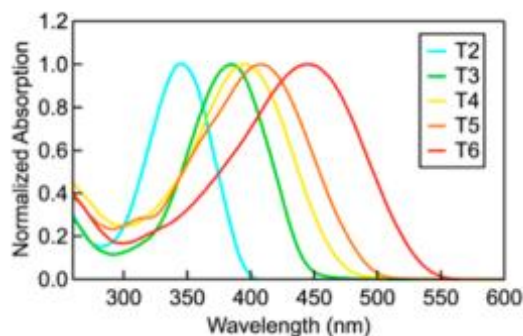


Figure 65: Solution UV-vis absorption spectra of T2-T6 dissolved in DCM. [40]

A shift of the electronic transitions between the energy states formed in the gap due to the presence of charged species, as explained in Chapter 1, can be seen also in the doped films, as highlighted by the black arrow in Figure 66. It can be noticed that in the 8T this band is at lower wavenumbers, then it increases in the 13T and in the 21T up to the polymer where this band is at much higher wavenumbers and is also much broader than in oligomers.

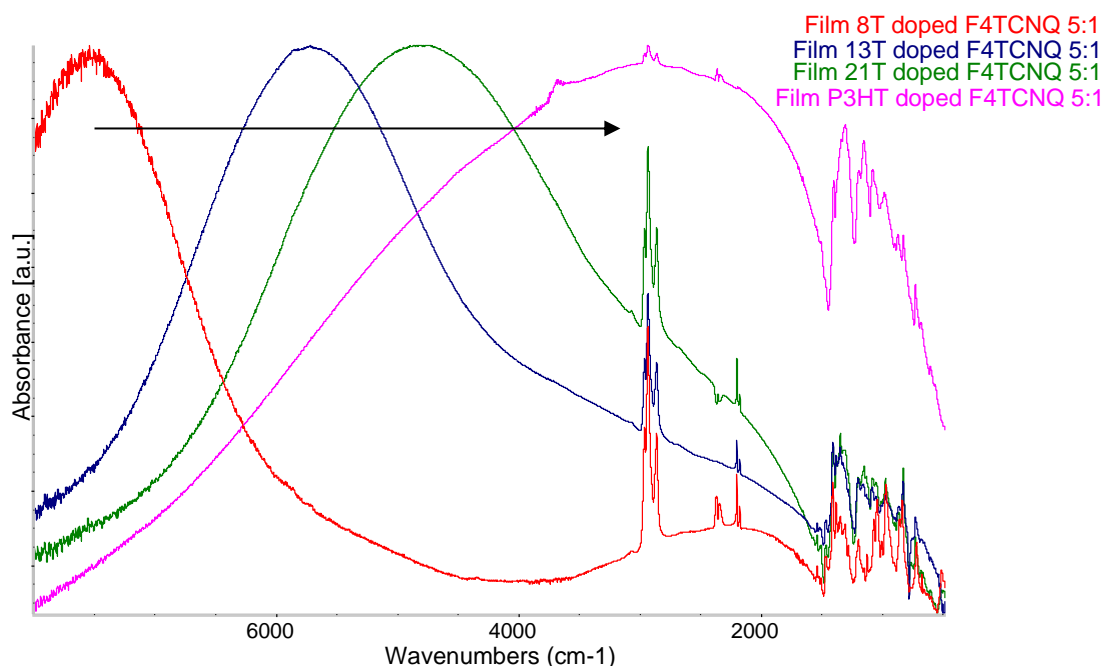


Figure 66: FT-IR spectra of 8T (red line), 13T (blue line) and 21T (green line) films doped 5:1

with F₄TCNQ compared to P3HT film doped 5:1 with F₄TCNQ (pink line). The black arrow highlights the shift of the electronic transitions.

3.1.4 IR spectra of P3HT and rraP3HT doped by iodine vapours

In order to achieve a better understanding of the doping mechanism, an alternative doping process was explored. Doping by vapour is often used to dope conjugated polymers since is much easier and faster than doping in solution, however it's not a precise and stable method, as it will be demonstrated in this chapter.

Thin films of P3HT can be doped simply exposing them to iodine vapours. A pristine film of the regioregular polymer was deposited on a KBr substrate and then exposed to iodine vapours for 2 minutes to get a highly doped film. This was done by closing the sample in a small container with iodine. After this, the process of de-doping was monitored by leaving the sample for some time at room temperature and/or heating it. The results are shown in Figure 67. The IR pattern that was obtained with P3HT film doped in solution (P_s), assigned to the polaron_{OA} phase, is similar to the one obtained in this case (P_v) but the band in region α is a bit broader in the vapour doped film. This may suggest that the two different doping techniques act in a similar way. However, after vapour doping, the system rapidly starts evolving: the intensity of the bands decreases much faster than in case of films doped from solution. Not only a decrease in intensity can be seen but also a change in the IR pattern, suggesting that more components are initially present. Within 5 minutes the band P_v moves towards higher wavenumbers. After this first change the situation seems more stable and no more changes in the pattern can be seen up to 30 minutes after deposition. By subtracting the spectrum of the film just after doping from that after 30 minutes the component that first leave the system, so the most unstable one, can be highlighted. From Figure 70, it can be seen that this less stable component that rapidly disappear from the spectra is similar to the pattern I observed for doped P3HT in solution at low doping ratio (25:1).

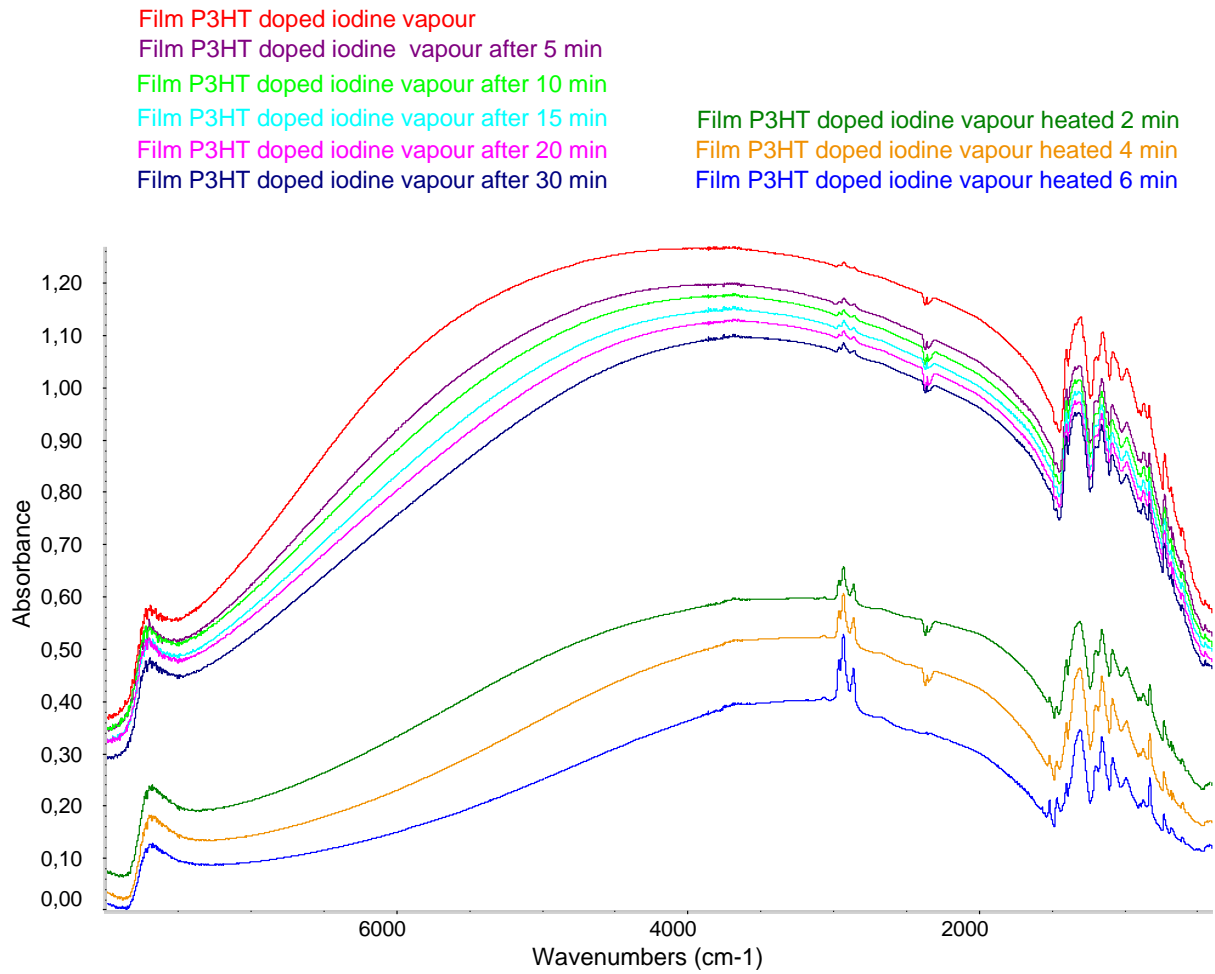


Figure 67: FT-IR spectra of film P3HT doped with iodine in vapour phase evolution in time (from doping to 30 minutes after doping) and after heating the film for 2, 4 and 6 minutes (respectively green, orange and blue lines).

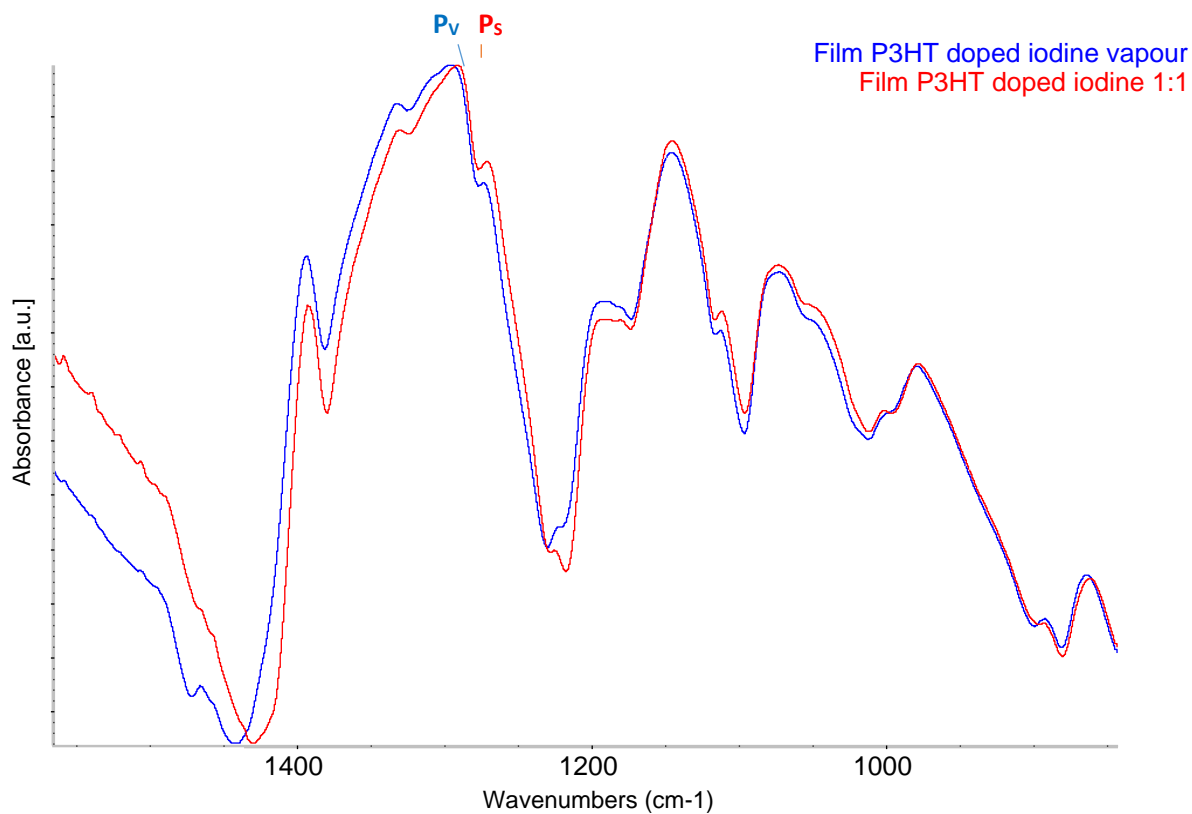
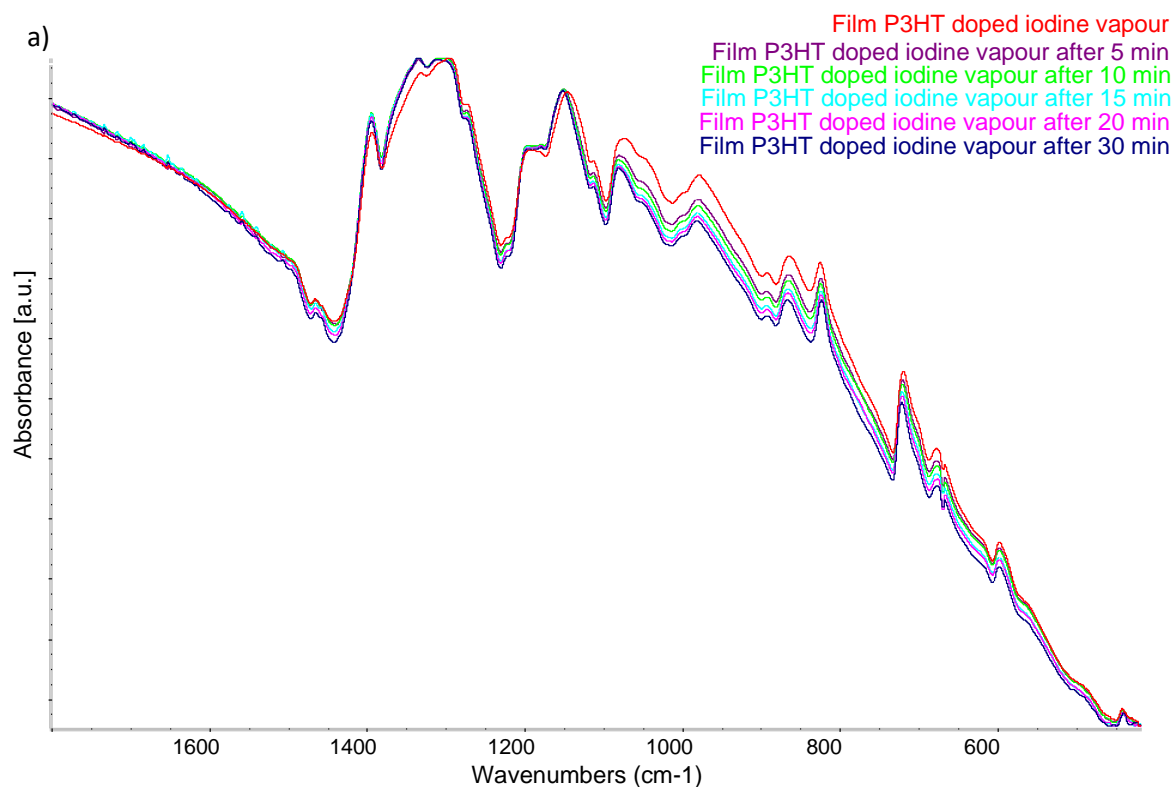


Figure 68: comparison between IR spectra in the range $1500 \text{ cm}^{-1} - 900 \text{ cm}^{-1}$ of P3HT thin film doped by iodine vapours (blue line) and P3HT thin film deposited by solution doped 1:1 (red line).



68

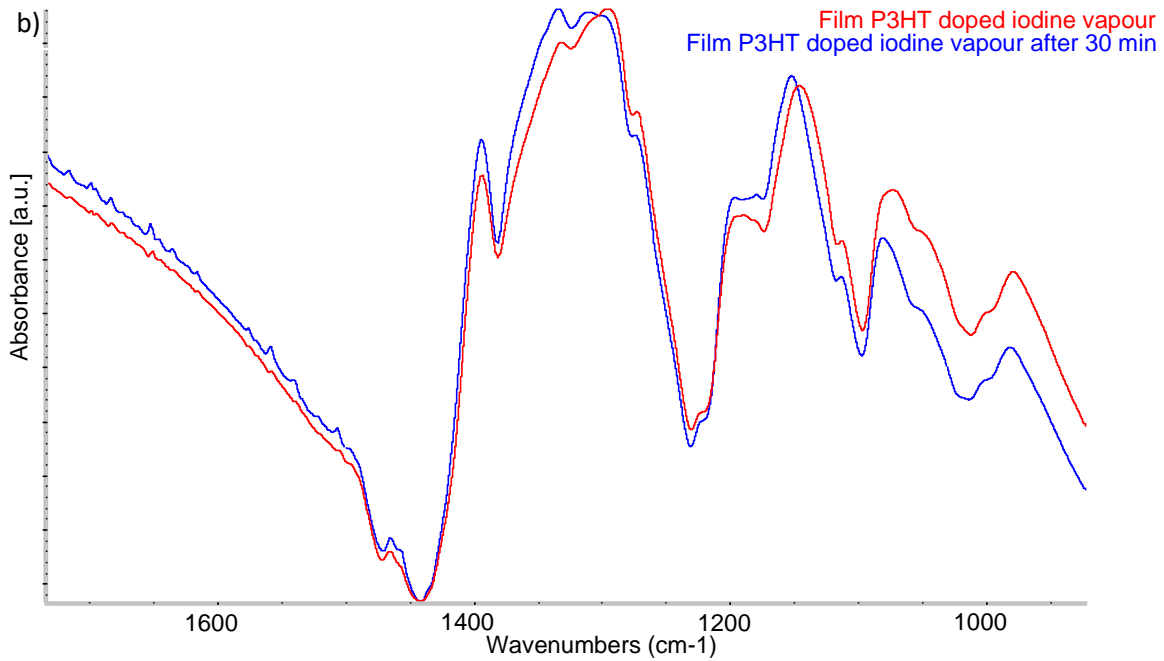


Figure 69: IR spectra in the range 1700 cm⁻¹ – 900 cm⁻¹ of a) P3HT thin film doped by iodine vapours evolution in time leaving them at room temperature; b) comparison P3HT thin film after doping by vapour (red line) and after 30 minutes (blue line).

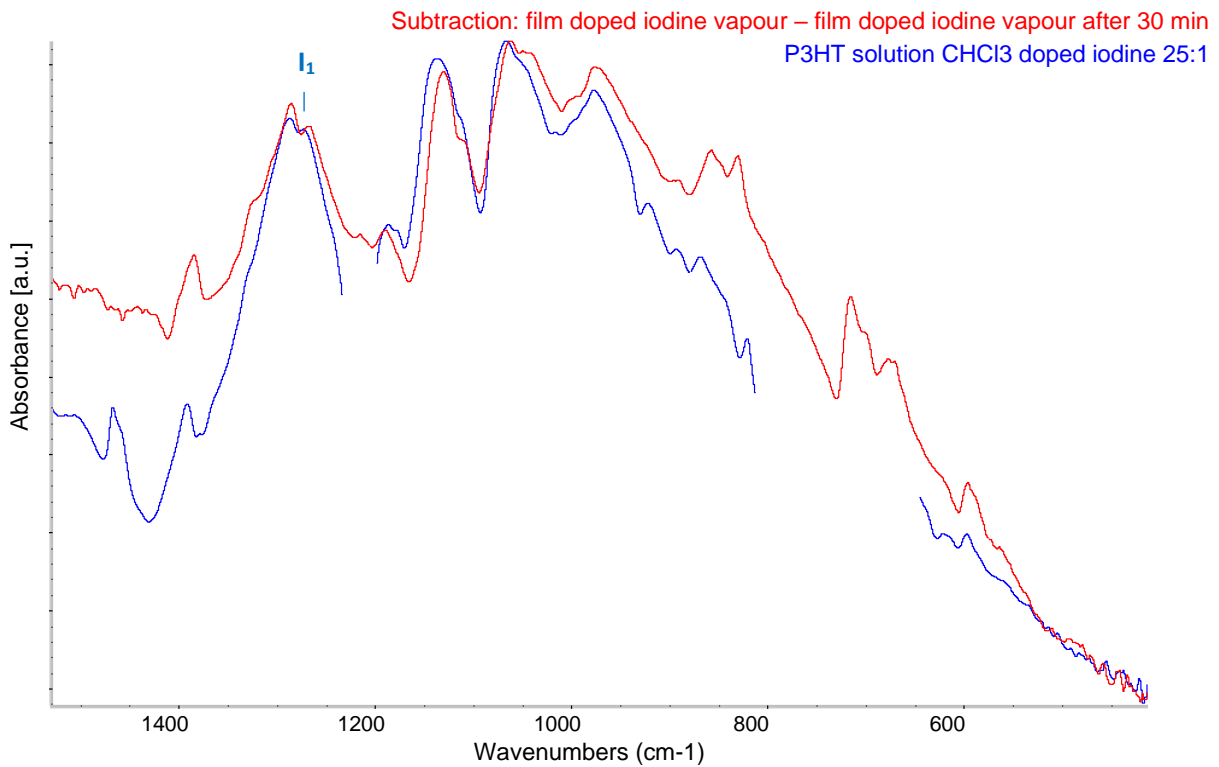
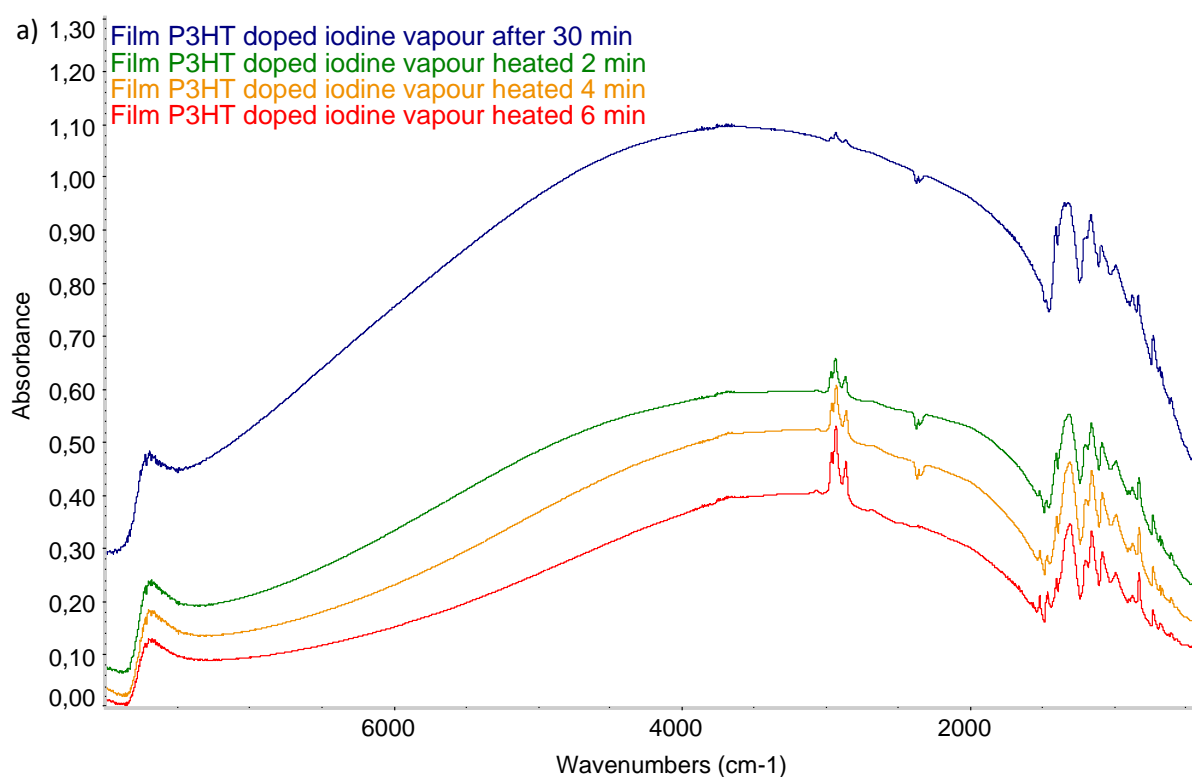


Figure 70: comparison between the first component that disappear in time (red line: subtraction spectra between the film doped with iodine vapors – film doped iodine vapors after 30 min) and the component I seen in the doped P3HT solution 25:1 (blue line).

Since the film seems to have reached a new equilibrium condition some minutes after doping, to promote further changes, energy was given to the system in form of heat. The results are shown in Figure 71. Another change in the IR pattern can be observed: the band P_v moves towards lower wavenumbers. As before, by subtracting the spectrum of the film after 30 minutes from that of the film heated for 6 minutes the component at high wavenumbers that leaves the system when energy is supplied can be identified. If this component is compared to the P3HT doped solutions, a similarity can be observed with the 1:1 level of doping where the band in region α is at higher wavenumber, as showed in Figure 73. Finally, the component that still remains in the IR spectra of the film even after heating (Figure 74), so the most stable component, if compared to the film obtained from the doped solutions, is very similar to the features attributed to the polaron_OA at the solid state showing the characteristic band P_s . This analysis of the de-doping process confirms the presence of different polymer-dopant species in the vapour-doped system. As in case of doping in solution 3 components are identified: one at lower wavenumbers (I) that is the first one which spontaneously disappears, one at higher wavenumbers (C), that disappear after giving thermal energy to the film, and the last one, the most stable that corresponds to the polaron_OA at solid state.



| Polarons in P3HT: unravelling vibrational fingerprints of ordered and disordered doped phases in solids and solutions. IR and Raman study of the polymers and oligomers.

70

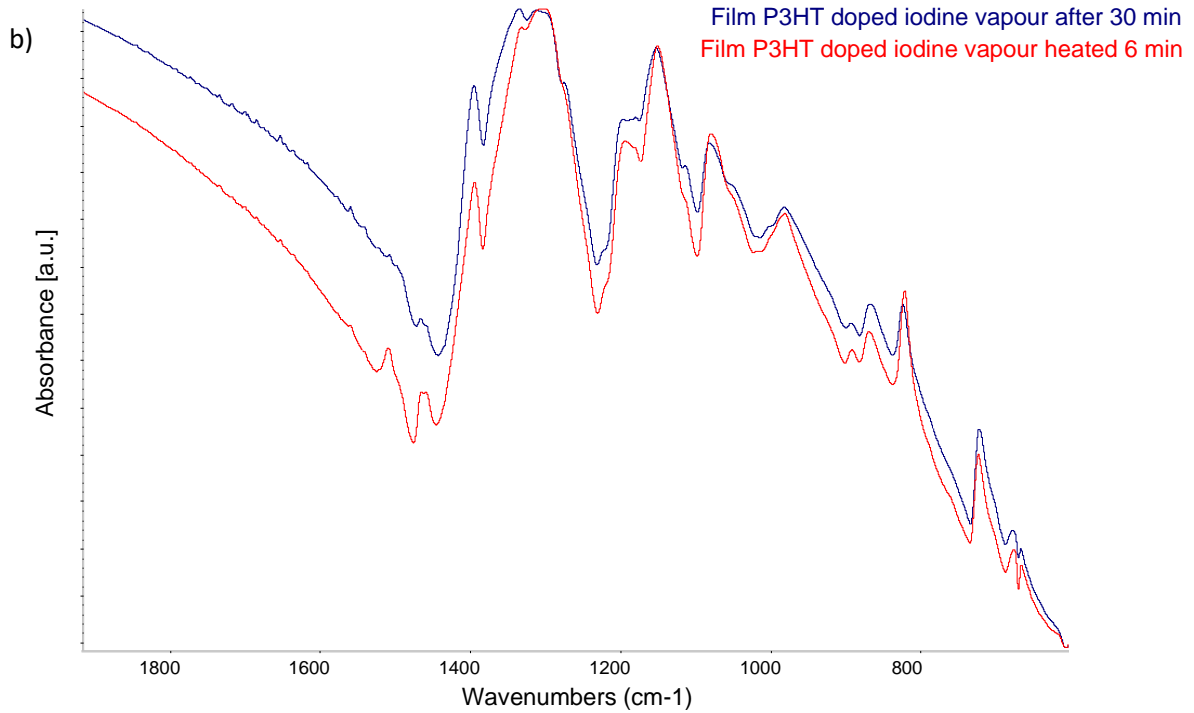


Figure 71: IR spectra in the range $1700\text{ cm}^{-1} - 700\text{ cm}^{-1}$ of a) film P3HT doped with iodine vapors after 30 minutes (blue line) and after heating the film for 2, 4 and 6 minutes (respectively green, orange and red lines); b) comparison between P3HT thin film doped by vapors after 30 minutes (blue line) and after heating for 6 minutes (red line).

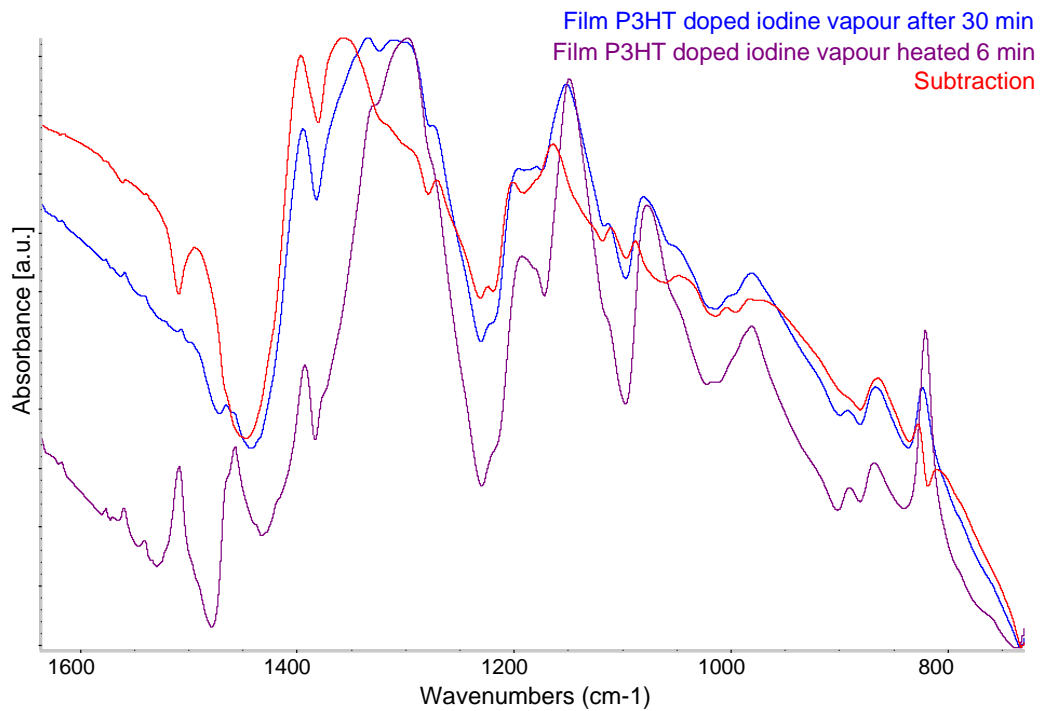


Figure 72: FT-IR spectra of P3HT thin film doped by vapors after 30 minutes (blue line), same film after heating it for 6 minutes (purple line) and the subtraction spectra between the film

doped with iodine vapors after 30 min – film doped iodine vapors after heating 6 min (red line).

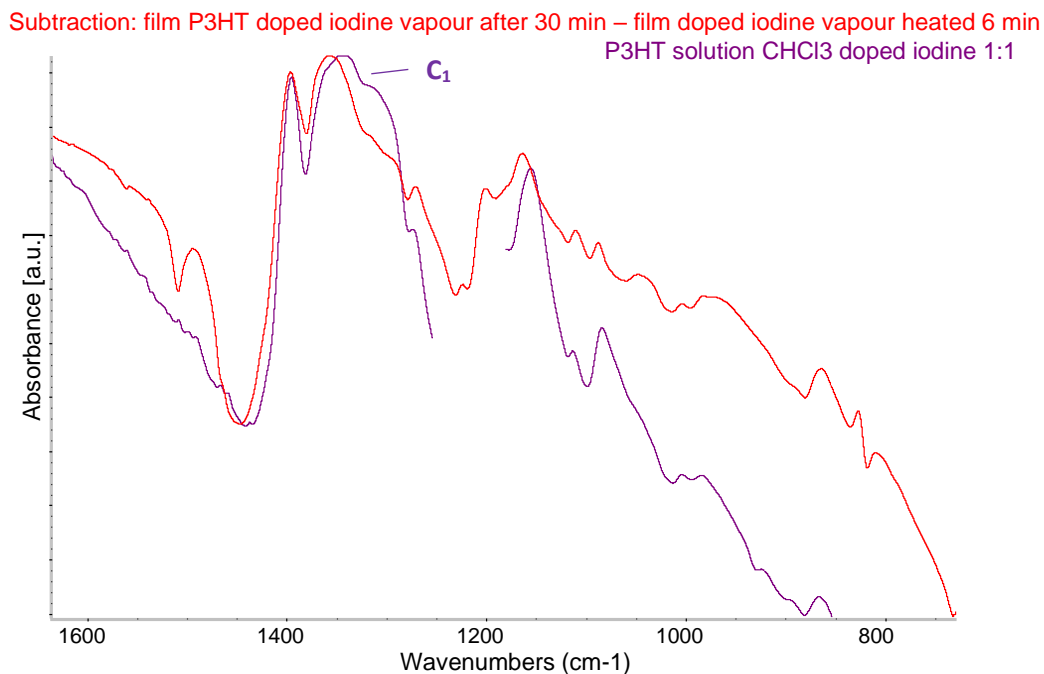


Figure 73: comparison between FT-IR spectra of P3HT doped in solution 1:1 (blue line) with the subtraction spectra between the film doped with iodine vapors after 30 min – film doped iodine vapors after heating 6 min (red line).

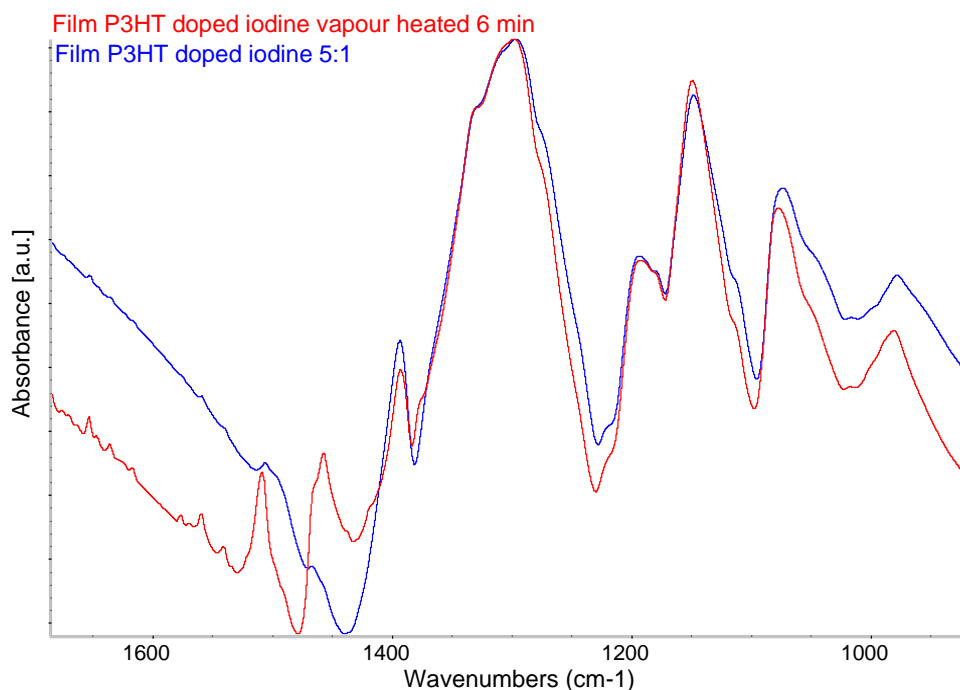
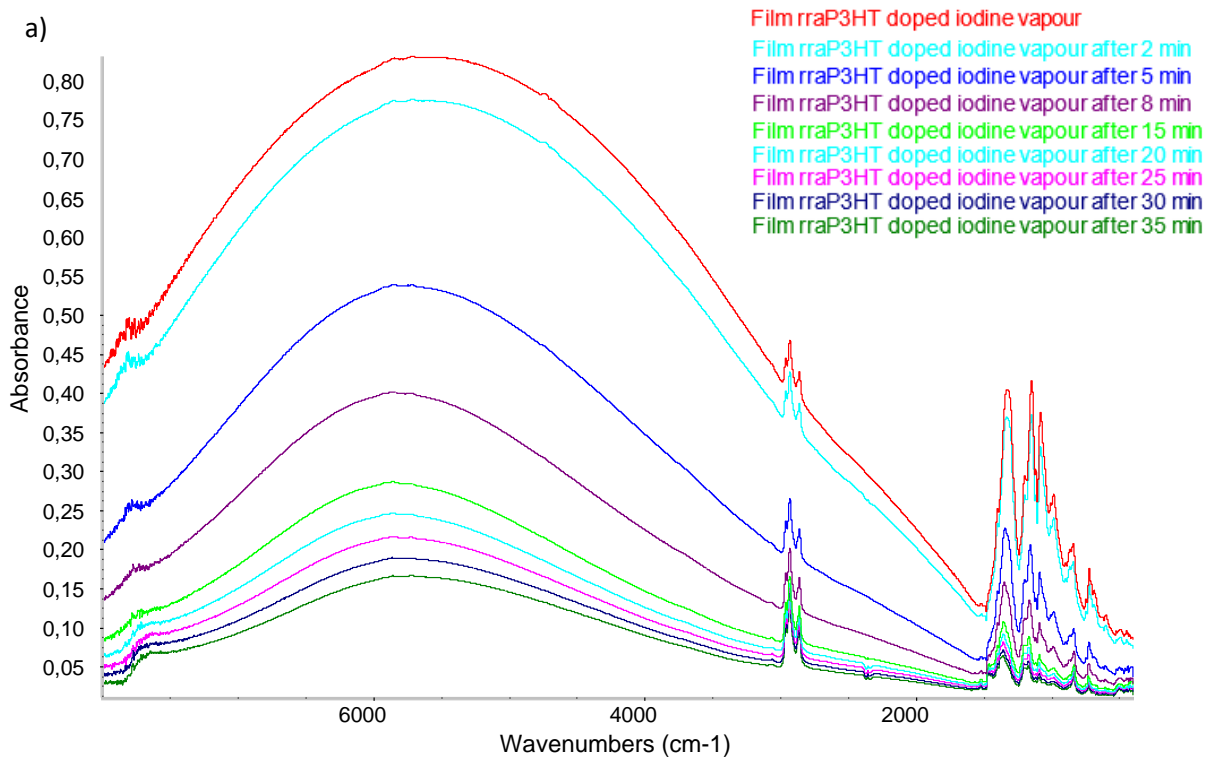


Figure 74: comparison between IR spectra in the range 1500 cm⁻¹ – 900 cm⁻¹ of P3HT film doped by iodine vapour (red line) and P3HT film deposited by solution doped 5:1 (blue line).

Also rraP3HT films can be doped by exposing them to iodine vapour. As done previously with the regioregular polymer the film was doped for 2 minutes and then the evolution of the IR spectra was monitored in time. The results obtained for the de-doping sequence are shown in Figure 75 and Figure 76. Differently from P3HT the process is faster, in particular at the beginning the spectra show many changes in just few minutes. After one hour the sample was heated to see if a complete de-doping could be obtained and, as shown in Figure 77, the spectra of rraP3HT film was almost equal to the pristine one. This is another difference from P3HT that, after heating it for 6 minutes, evolves to the stable configuration of the polaron_{OA} and still shows doped IR features. This suggests that vapour doping of rraP3HT is less stable than doping of P3HT.



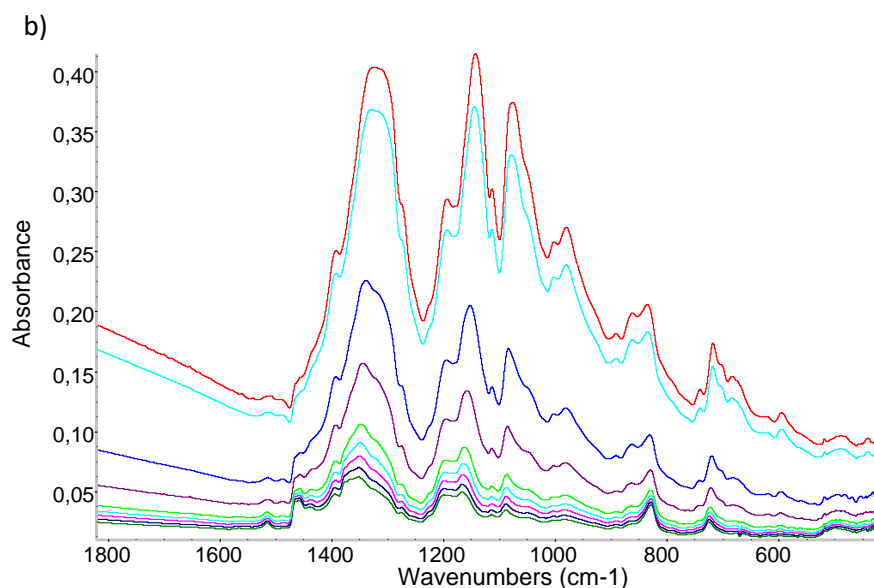
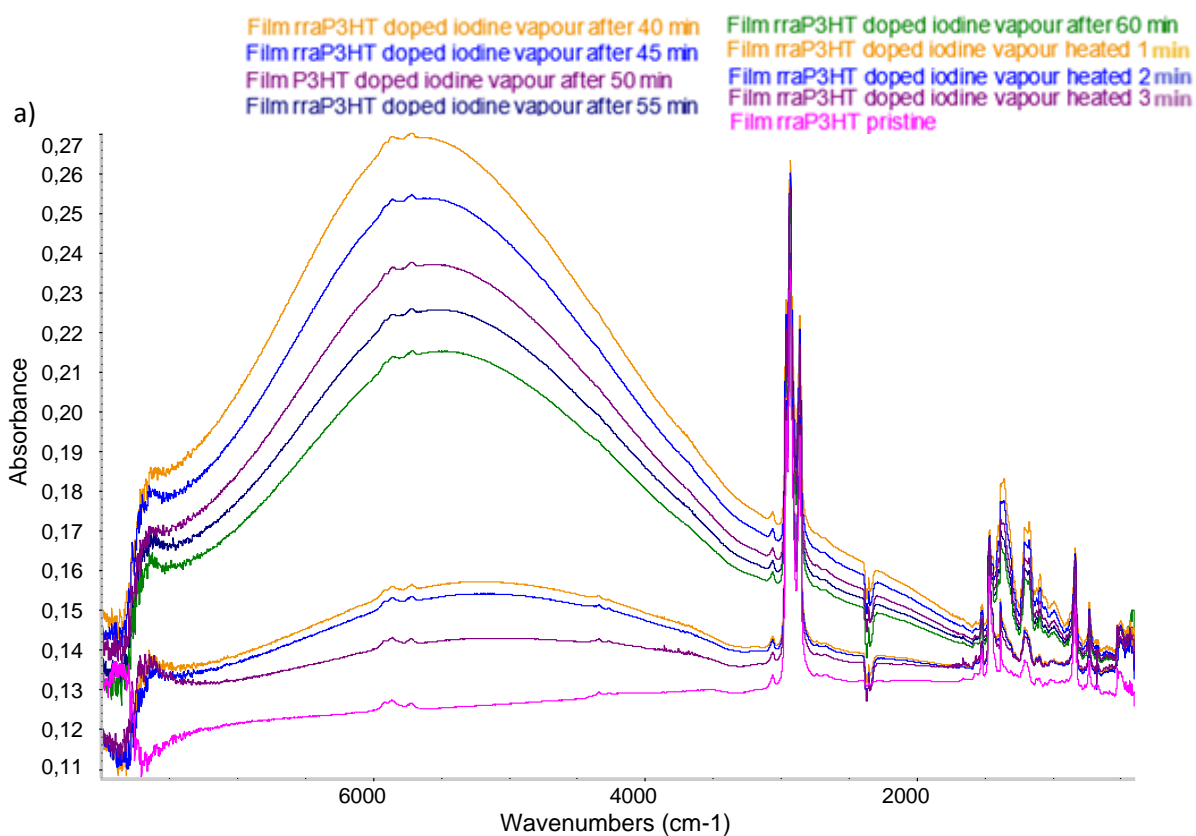


Figure 75: FT-IR spectra of rraP3HT film doped with iodine in vapour phase evolution in time (from doping to 35 minutes after doping) a) from 8000 cm^{-1} to 400 cm^{-1} , b) from 1800 cm^{-1} to 400 cm^{-1} .



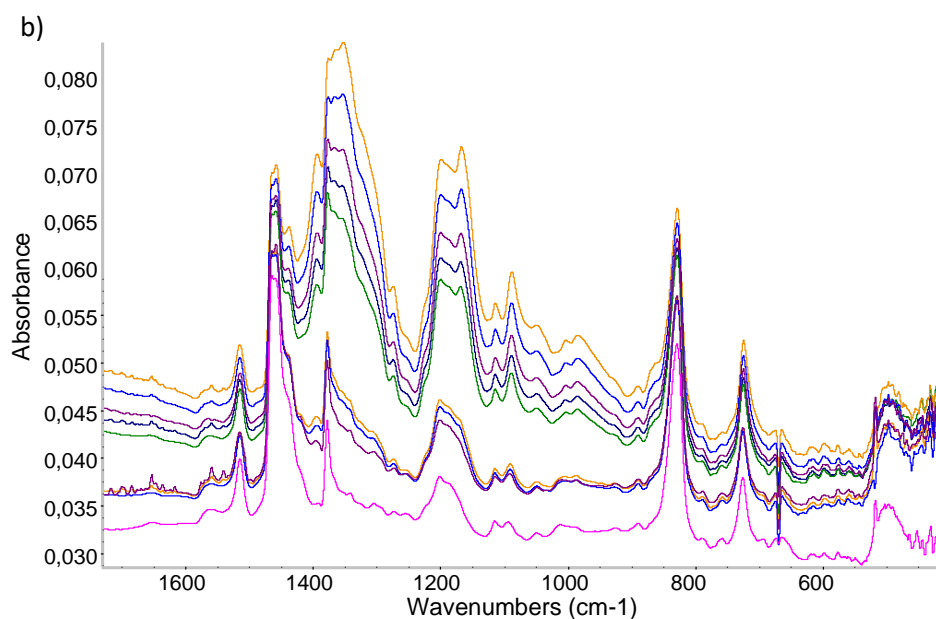


Figure 76: FT-IR spectra of rraP3HT film doped with iodine in vapour phase evolution in time (from 35 minutes after doping to 60 minutes after doping) and after heating the film for 1, 2 and 3 minutes (respectively orange, blue and purple lines) a) from 8000 cm^{-1} to 400 cm^{-1} , b) from 1800 cm^{-1} to 400 cm^{-1} .

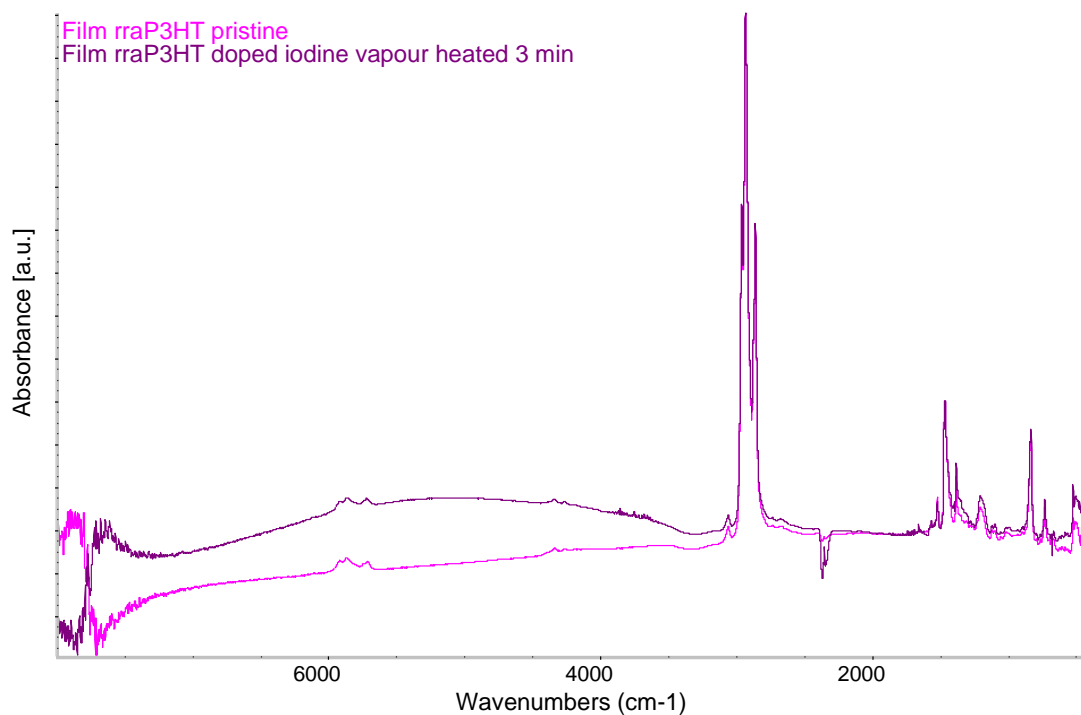


Figure 77: IR spectra of rraP3HT film doped by iodine vapour for 2 minutes collected after 60 minutes and heated for 3 minutes (purple line) compared to the pristine film (pink line).

Comparing the spectra obtained for rraP3HT with the signature of the polaron_{OA} (P_s band) it can be confirmed that, even doping by vapour, rraP3HT is not able to form ordered polarons domains, as showed in Figure 78. However, the spectra obtained is different from the one of the same polymer doped in solution and then deposited (Figure 79). Comparing the bands in region α to the IR pattern that was previously attributed to the CTC it can be noticed that they are very similar. This may suggest that when a film of regio-random polymer is exposed to iodine vapour it mainly forms charge transfer complexes.

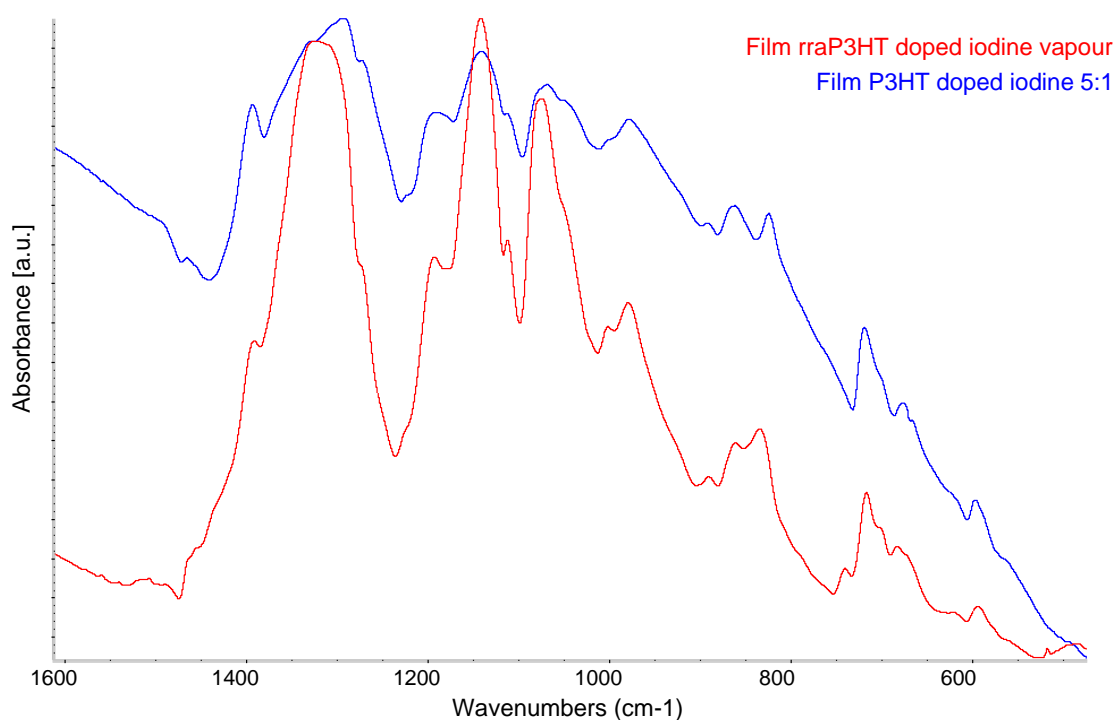


Figure 78: IR spectra in the region between 1600 cm^{-1} and 600 cm^{-1} of rraP3HT film doped by iodine vapour for 2 minutes (red line) compared to P3HT doped iodine 5:1 by solution (blue line).

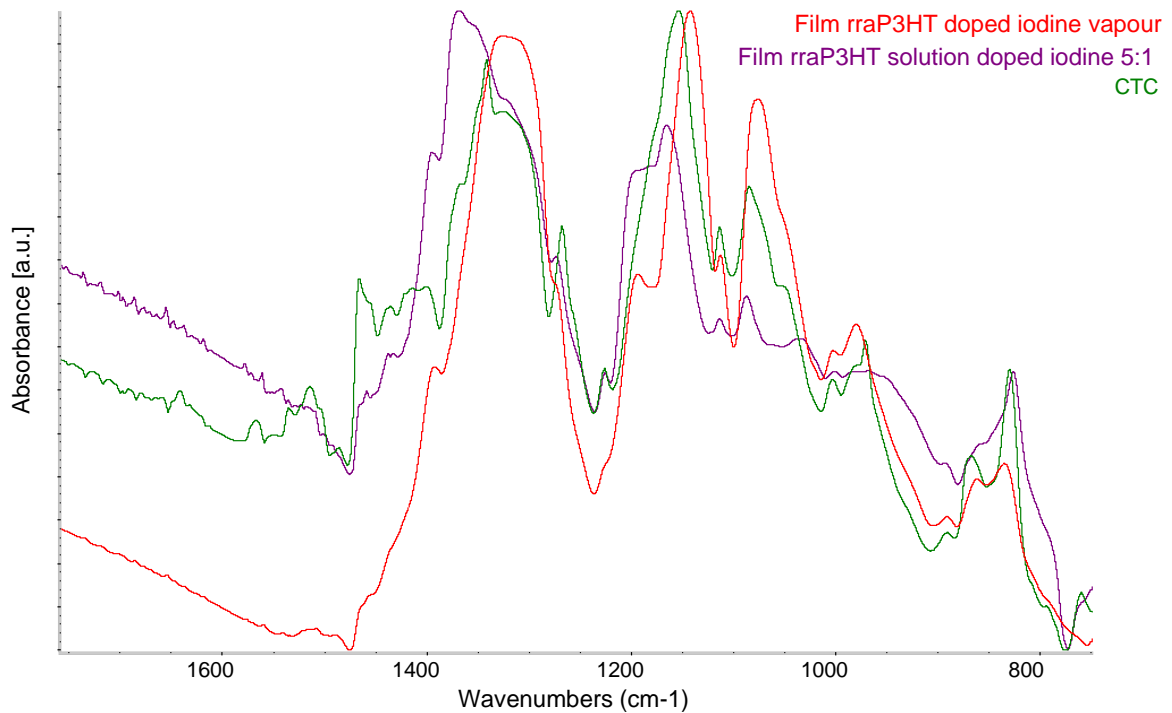


Figure 79: IR spectra in the region between 1600 cm^{-1} and 800 cm^{-1} of rraP3HT film doped by iodine vapour for 2 minutes (red line) compared to rraP3HT doped iodine 5:1 by solution (purple line) and the IR spectra of the charged transfer complex (green line).

In conclusion, the process of doping by vapour generates less stable complexes since the spectra evolve more rapidly with respect to those of solid samples doped in solution. For P3HT the results obtained at the end of the process, are the same as the one obtained with doping in solution. In both cases the spectral feature P_s of the polaron_{OA} structure is obtained. In addition, monitoring the process of de-doping, the presence of three different components in the polymer/dopant system, similar to the ones observed in solutions at different concentrations, was confirmed.

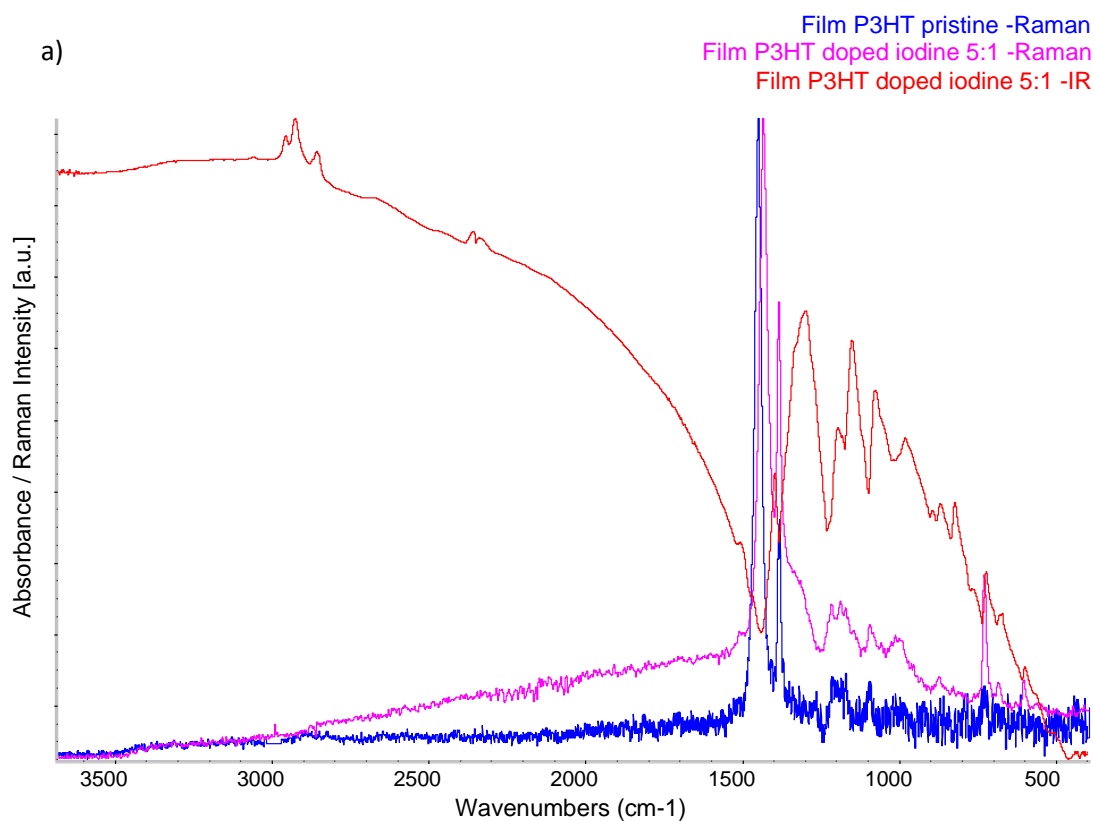
On the contrary, for the case of rraP3HT doping in solution and by vapour exposure led to different results. In case of doping by vapour the charged species are unstable and, differently from doping in solution, only CTC seems are detected.

3.2 FT-Raman spectroscopy

In this section are reported the results of the analysis carried out by FT-Raman spectroscopy of:

- doped P3HT in solution at three doping ratios with iodine and F₄TCNQ and thin films deposited from the previous solutions;
- doped rraP3HT in solution at doping ratio 5:1 with iodine and F₄TCNQ and thin film deposited from the previous solution;
- doped P3DT in solution at doping ratio 5:1 with iodine and F₄TCNQ and thin film deposited from the previous solution;
- doped 8T, 13T, 21T in solution at doping ratio 5:1 with iodine and F₄TCNQ and thin films deposited from the previous solutions.

3.2.1 FT-Raman spectra of doped regioregular P3HT in solution



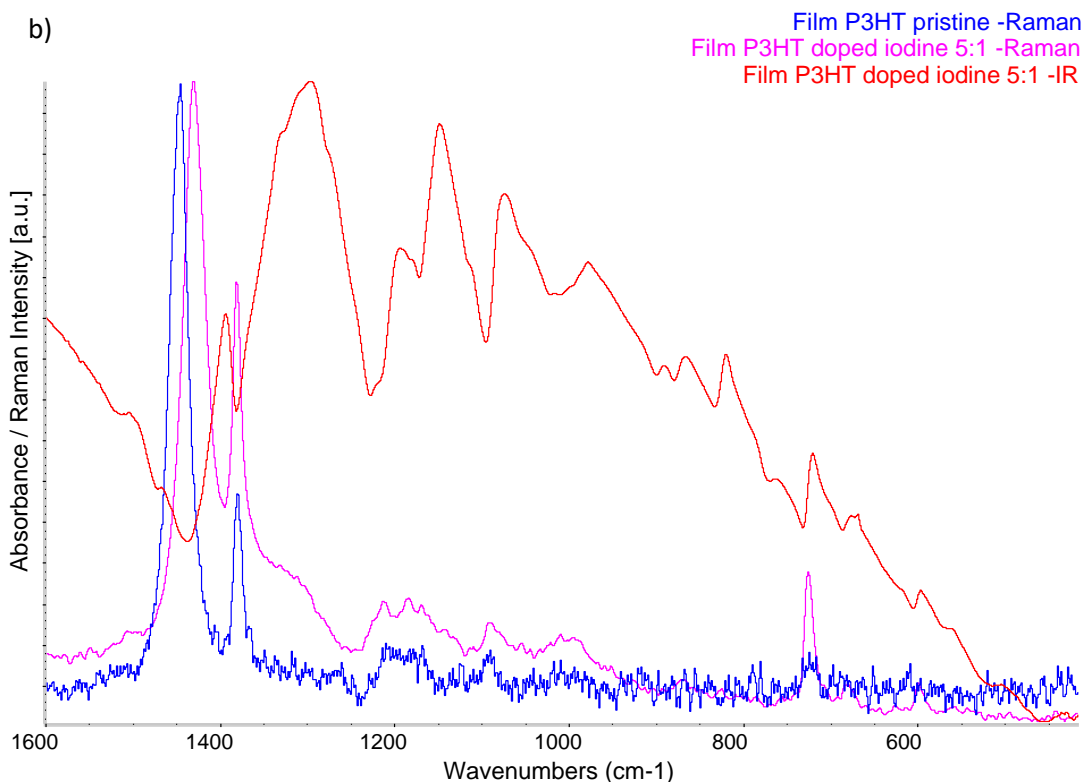


Figure 80: P3HT in solid state (film): FT-Raman spectrum of the pristine sample (blue line), FT-Raman spectrum (pink line) and IR spectrum (red line) of iodine doped 5:1 P3HT a) from 3700 cm^{-1} to 400 cm^{-1} b) from 1600 cm^{-1} to 400 cm^{-1}

The figure above (Figure 80) shows the Raman spectrum of P3HT solid film obtained from solutions in the most representative doping ratio 5:1, at which in the IR was seen that the formation of a stable phase like the OA one, was possible even in solution. In the doped samples the intense Raman band (associated to the ECC vibration by analogy with the pristine case) is shifted towards lower frequency of about 10 cm^{-1} and is broader with respect to the ECC Raman band of the pristine sample. It can be noticed that no intense bands are observed in the spectral range of the IRAV bands seen in the IR spectra. Recalling what happens in the case of doped polyacetylene, we can hypothesize that the Raman spectra show preferentially vibrational transitions of the neutral segments of the polymer chain, that consist of CC bonds with low polarization and showing CC stretching modes with Raman intensity much higher in respect with the charged regions. However, this does not imply that with Raman spectroscopy we are not able to see the effect of doping: in all cases the doped samples, both in solution and in film, will show distinguishable situations compared to the pristine case. For this reason, Raman spectroscopy is a useful tool to investigate the doping process, in particular if complemented by IR spectroscopic analysis. For this reason, it's important to correctly understand the origin of the observed bands and of their frequency shift with respect to the case of the pristine material.

The fact that the Raman spectra of doped samples are different from the pristine ones suggest that the presence of polarons induce on the neutral segments of the polymer chain some effects even if they are not directly affected by the charge transfer process. The most evident effect, both for solid films (for example, Figure 80 and also for the cases at different dopant concentrations, which demonstrate the persistence of the effect regardless of the type and amount of dopant), and in solution (that will be discussed later), is the shift of the ECC frequency ν_1 . Changes in the frequency of this vibration can be due to:

- i. Increase in the length of the chain – namely of the conjugation length - as shown by comparison of Raman spectra between the polymer and oligomers with increasing length. However, at difference from the case of polyenes and polyacetylene, this effect is almost negligible in P3HT;
- ii. Planarization of the polymer chain, as seen when going from liquid solution to solid sample;
- iii. Conformational change of the side chains. This rather subtle effect has been pointed out by means of DFT calculations on molecular models: a shift of approximately 10 cm^{-1} is obtained when the side chains arrange themselves transplanar within the backbone plane, in contrast to the typical crystalline structure of P3HT, where the chains arrange themselves out-of-plane; [19]
- iv. Change in the force constants of the CC bonds in the thiophene ring, that is directly related to the charge distribution and the structure of the rings. This is the reason why IRAV vibrations, that are ECC-like modes of the thiophene rings that host the polaron, have much lower frequency.

Based on the previous observations we can make the following hypothesis to explain the shift of the ECC frequency in the Raman spectra of doped P3HT:

- For the samples in solution, where we will see a significant shift in respect to the pristine case, we will have an effect of the planarization (effect ii.), that could also confirm the hypothesis that in solution clusters of doped polymer are formed.
- For the solid samples (shown on Figure 80) the lowering of the frequency can't be attributed to a planarization of the backbone since it is already planar in the pristine polymer and we can consider the effect of the lateral chains (effect iii.), however this could be not enough to justify the whole shift in frequency observed. Another reason could be that the neutral rings close to the polaron have geometry and force constants slightly modified due to the presence of the defect (effect iv.). In fact, despite we usually adopt a simplified description of polarons with a well-defined length, it is not

possible to achieve a clear separation between the perturbed domain and the unperturbed domains.

- For both solid and liquid samples there is also the possibility of the presence of undoped chains, in particular in the low doping cases (25:1).

Furthermore, there are notable effects of the structure in the intrinsic (absolute) Raman intensities: in the analysis of the spectra is important to consider that in Raman spectroscopy the varying activity of different species (and different normal modes) can selectively highlight certain specific molecules or domains in the polymer, while not showing others. The fact that a region with a specific structure is detected by the spectra means that it is present, but not necessarily it is the most abundant. For example, neutral segments with planar geometry will have much higher Raman intensity of ECC modes, while planar segments but partially polarized (segments close to the polaron) could have ECC-like bands with lower intensity, and so it could be difficult to detect them. This observation will help us discussing the highly doped samples (1:1), that have an intrinsically lower Raman intensity (see Figure 81). This finding indicates that, in absence of neutral domains, the spectra can show only vibrations of highly perturbed segments. In addition, in some cases the spectra of highly doped samples are structured: there isn't a neutral species that dominates with its collective ECC.

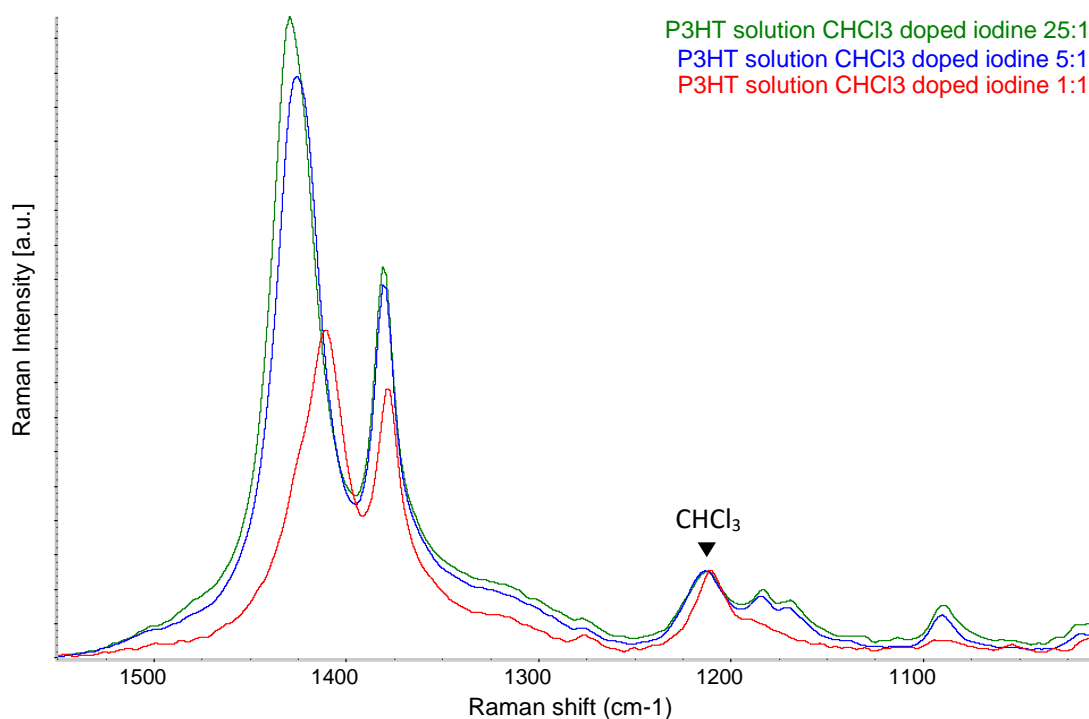


Figure 81: FT-Raman spectra of P3HT solution in CHCl₃ doped iodine 25:1 (green line), 5:1 (blue line) and 1:1 (red line) normalized in respect with the band at 1200 cm⁻¹ attributed to CHCl₃ vibrations.

In conclusion, the complex scenario illustrated above, complies with the experimental evidence from the Raman spectra of doped polyacetylene, suggesting that charged defects have a very weak Raman activity. For this reason, the Raman spectra of doped P3HT will be dominated by the response of polymer segments not affected or scarcely affected by the charge transfer, namely i) polymer chains which are not doped at all ii) almost neutral regions adjacent to polaron defects or iii) extended neutral segments between to two polaron defects.

A possible description of the different features observed in the Raman spectra of doped P3HT is schematically represented in Figure 82. In the lower doping case, the situation can be represented by few polarons (blue rectangles), which have a size of around five P3HT monomer units, far from each other (Figure 82, case i). Portions of the chain next to the defect (blue dotted rectangles) which are neutral but still perturbed by the presence of the polaron and extended neutral unperturbed segments are also present. Figure 82, case ii shows a higher polaron density, where polarons are separated by short neutral, perturbed domains. We will assign to these segments the Raman band observed at 1430 cm^{-1} for 5:1 samples. Instead, in the case i, with polarons far from each other, the long sequences of neutral thiophenes are supposed to give origin to the ECC mode vibration (ν_1) at 1445 cm^{-1} , as for the pristine polymer. Notice that the 1445 cm^{-1} band should co-exist with the band at 1430 cm^{-1} (like case ii), possibly giving rise to a structured broader band peaked at intermediate frequency (1435 cm^{-1} see Figure 82, case i). Moreover, the component at 1445 cm^{-1} (same frequency of the solid pristine material) could be ascribed to the presence of non-doped polymer chains (not described in Figure 82). When the dopant concentration is very high there are almost all polarons close one to each other, without unperturbed thiophene units in between, and so a band tentatively ascribed to the ring at the polarons interface appear at 1410 cm^{-1} , observed for the polymer doped with F_4TCNQ (see spectrum of 1:1 F_4TCNQ doped P3HT, Figure 84).

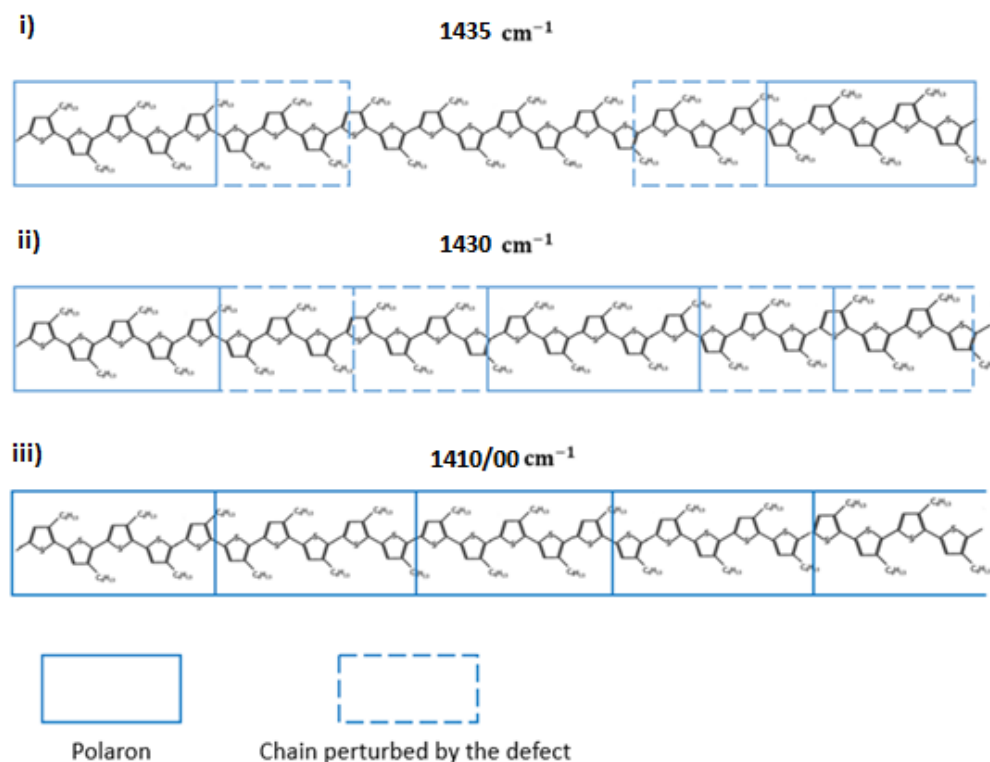


Figure 82: schematic representation of the three different components observed in the FT-Raman spectra at i) $1435 = 1445 + 1430 \text{ cm}^{-1}$, ii) 1430 cm^{-1} and iii) $1410\text{-}1400 \text{ cm}^{-1}$. The blue rectangle and the dotted ones represent respectively the extension of the polaron and the extension of the portion of neutral polymer chain perturbed by the defect.

In the following, we will present and discuss in detail the Raman spectra obtained by casting from solution at different concentration ratios and with different dopant molecules.

The comparison between the FT-Raman spectra of the film casted from the three different iodine doped solutions is reported in Figure 83. These spectra are focused on the spectral range $1500\text{-}1300 \text{ cm}^{-1}$, where the peak corresponding to the ECC vibration modes (ν_1) can be seen. From this result it can be noticed that the film with 5:1 and 1:1 doping ratio converge both to the peak at 1430 cm^{-1} , while the 25:1, the ν_1 band shifts to 1435 cm^{-1} and becomes broader. Looking at the films from $F_4\text{TCNQ}$ doped P3HT case (Figure 84) it can be observed that the 25:1 and 5:1 show a trend like the iodine doped solutions and films, while, in the highly doped case (1:1) some differences can be seen. In this last case, the intensities are very low overall and the band ν_1 at 1430 cm^{-1} if presents, is a weak shoulder of the peak at 1410 cm^{-1} .

The case of P3HT doped $F_4\text{TCNQ}$ 1:1 can be explained considering a higher content of ICTs with respect to I_2 doped samples. The idea is that $F_4\text{TCNQ}$ do not leave the system when the solution is deposited to form the film, while this happens for the more mobile

iodine. As a result, the film of F₄TCNQ doped P3HT 1:1 does not show the 1430 cm⁻¹ band, but only the 1410 cm⁻¹ feature, typical of very crowded polaron defects. This may suggest that the system does not rearrange when deposited since, as it will be showed later, the same ECC frequency is observed in the 1:1 F₄TCNQ doped solution.

The broad, structured ν_1 band of the 1:25 case observed at 1435 cm⁻¹ could be reasonably ascribed to the convolution of the Raman signal of slightly perturbed segments close to the polaron, which concur to a 1430 cm⁻¹ transition and the long sequences of unperturbed rings which behave as the pristine samples (model i, Figure 82), or to some pristine domain which concur to a 1445 cm⁻¹ transition.

In conclusion, we ascribe the Raman line at 1430 cm⁻¹, observed in most of the solid samples, to the presence of regions slightly perturbed by the polarons. Lower frequency features, like those observed in the 1:1 case of F₄TCNQ doped sample, are ascribed to Raman modes involving the polarons on highly doped chains. Features at higher frequency come by the very few segments not perturbed by the charge defects.

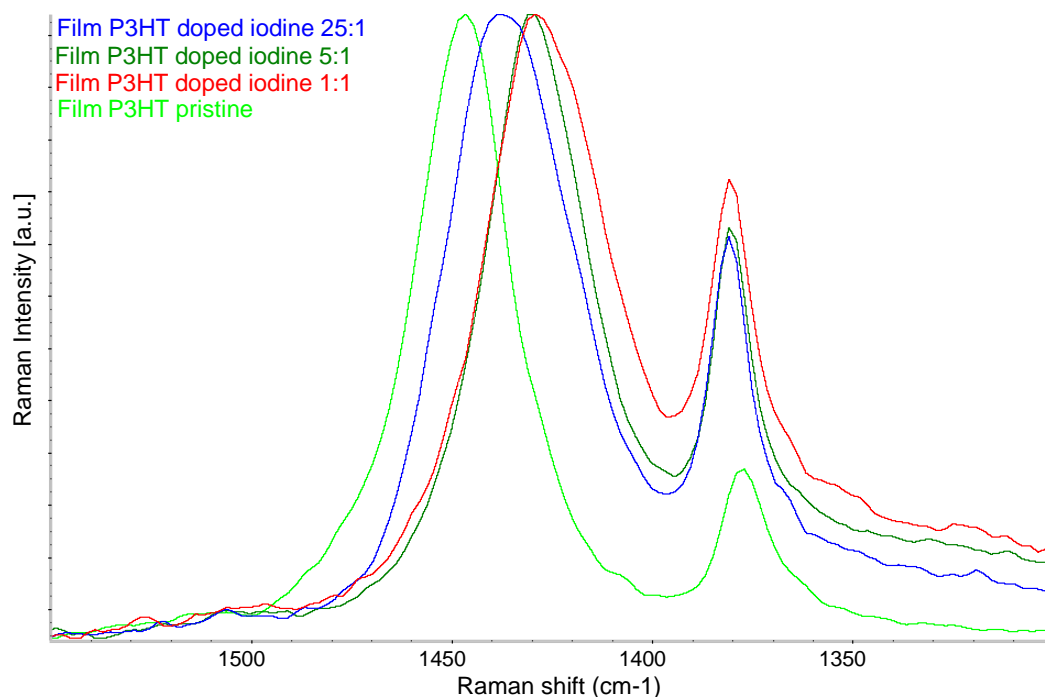


Figure 83: FT-Raman spectra in the region between 1550 cm⁻¹ and 1300 cm⁻¹ of film from P3HT iodine doped solution 25:1 (blue line); 5:1 (dark green line) and 1:1 (red line) compared to P3HT pristine film (light green line).

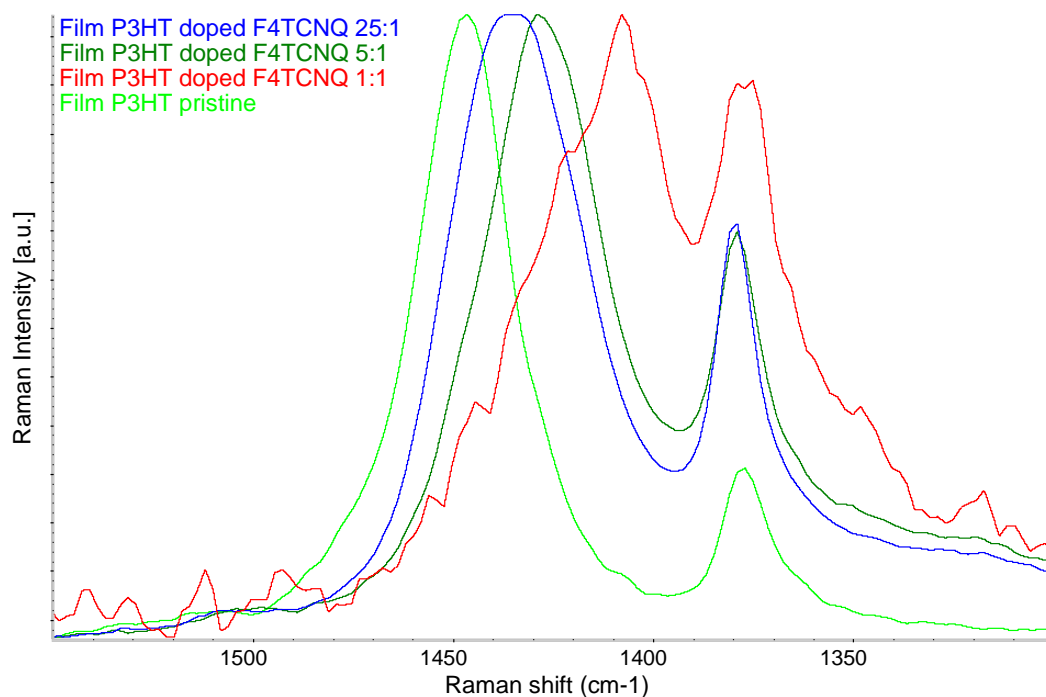


Figure 84: FT-Raman spectra in the region between 1550 cm^{-1} and 1300 cm^{-1} of film from P3HT F_4TCNQ doped solution 25:1 (blue line); 5:1 (dark green line) and 1:1 (red line) compared to P3HT pristine film (light green line).

Doping	Pristine	25:1	5:1	1:1
I_2	1445 cm^{-1}	1435 cm^{-1}	1430 cm^{-1}	1430 cm^{-1}
F_4TCNQ	1445 cm^{-1}	1435 cm^{-1}	1430 cm^{-1}	1410 cm^{-1}

Table 6: peak frequencies of the band ν_1 for the pristine P3HT film and the three doped films with I_2 and F_4TCNQ .

In Figure 85 and Figure 86 are reported the spectra of P3HT solutions, doped respectively with I_2 and F_4TCNQ compared to the pristine polymer in solution. Since, as previously seen, in pristine P3HT the wavenumber decreases when going from liquid to solid state, the doped solutions are more like the pristine film (Figure 87) suggesting that the doping promotes a sort of planarization and straightening of the polymer backbone. Furthermore, it can be noticed that, as for the IR spectra in solution, there is a dependence on the doping ratio: the band changes its position depending on the doping level. Three main components seem to be present: one with ν_1 at 1445 cm^{-1}

(pristine polymer or segments), 1430 cm^{-1} , and the last one at 1410 cm^{-1} . Looking at the iodine doped solutions (Figure 85) it can be observed that in the lowest doping level, 25:1, the band is centred at 1430 cm^{-1} . When increasing the doping to 5:1 the band moves to 1425 cm^{-1} : probably in this case, the band is the convolution of both the component at 1430 cm^{-1} and 1410 cm^{-1} . Finally, in the highest doping level there is a significant shift down to 1410 cm^{-1} with a shoulder at around 1430 cm^{-1} . Comparing these results with the $F_4\text{TCNQ}$ doped solutions it can be seen that the spectra of samples 25:1 and 5:1 are very similar to the iodine doped ones, but some differences can be spotted out when looking at the 1:1 solution. In this case the band is much broader for the $F_4\text{TCNQ}$ doped sample and is composed by different peaks: 1400 cm^{-1} , 1410 cm^{-1} and 1430 cm^{-1} . This much complex band structure seen in the highly doped case could be due to the fact that, being the Raman intensity lower, as previously discussed, we are able to see more components that in other cases we weren't able to observe because the abundant neutral species dominate the Raman spectra.

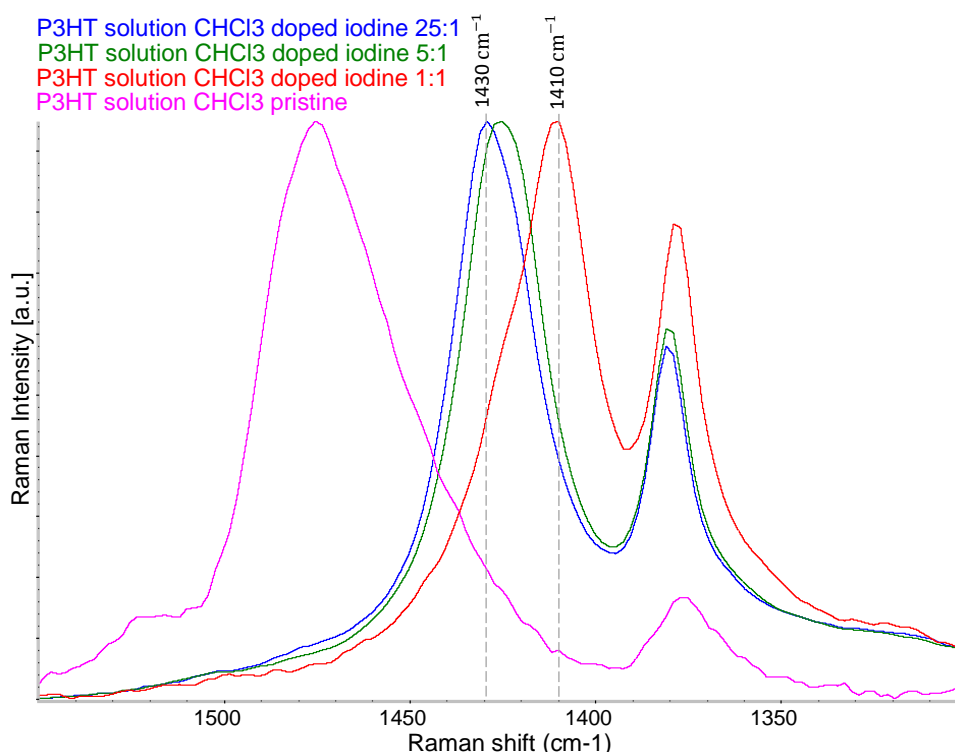


Figure 85: FT-Raman spectra in the region between 1550 cm^{-1} and 1300 cm^{-1} of iodine doped P3HT solutions 25:1 (blue line); 5:1 (green line) and 1:1 (red line) compared to P3HT pristine in solution of CHCl_3 (pink line). The two dotted lines highlight the components at 1430 cm^{-1} and 1410 cm^{-1} .

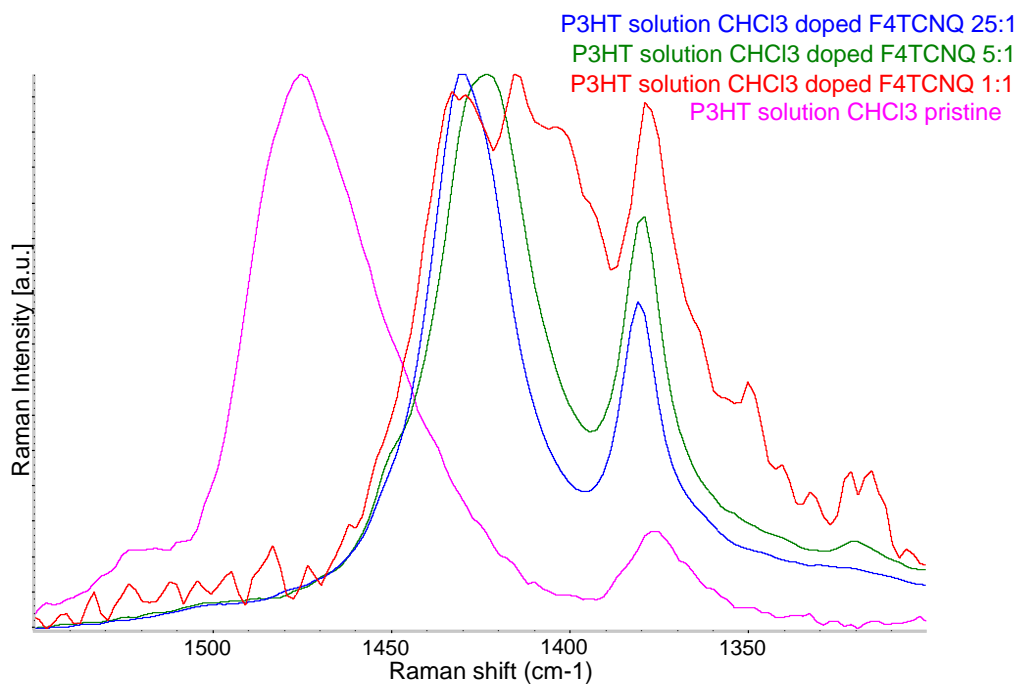


Figure 86: FT-Raman spectra in the region between 1550 cm⁻¹ and 1250 cm⁻¹ of F₄TCNQ doped P3HT solutions 25:1 (blue line); 5:1 (green line) and 1:1 (red line) compared to P3HT pristine in solution with CHCl₃ (pink line).

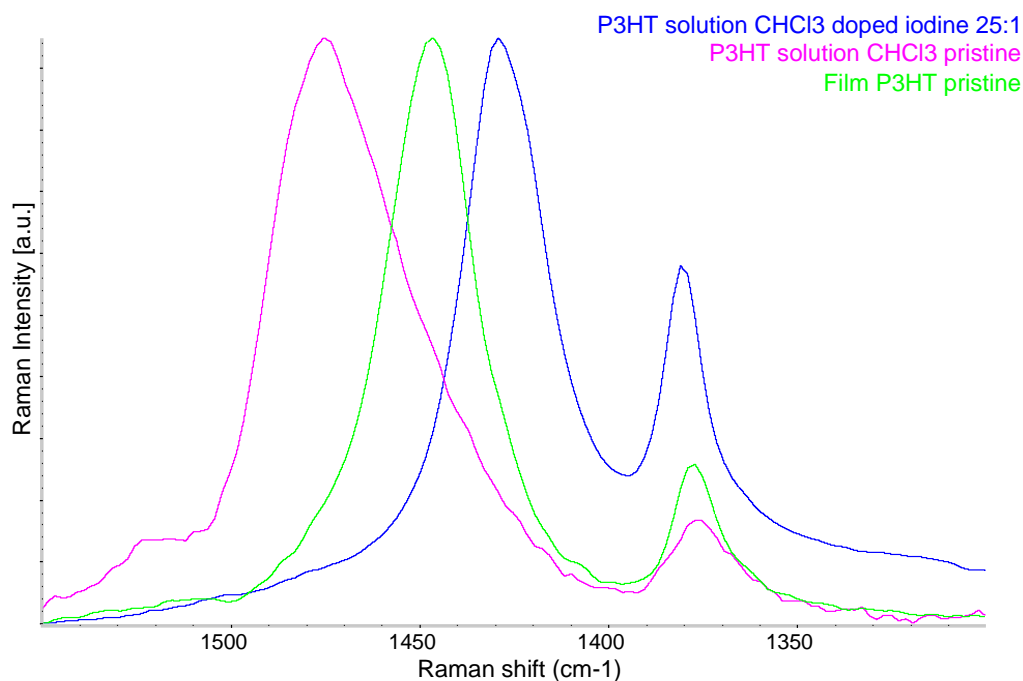


Figure 87: FT-Raman spectra in the region between 1550 cm⁻¹ and 1250 cm⁻¹ of F₄TCNQ doped P3HT solutions 25:1 (blue line) compared to P3HT pristine in solution with CHCl₃ (pink line) and in solid film (light green line).

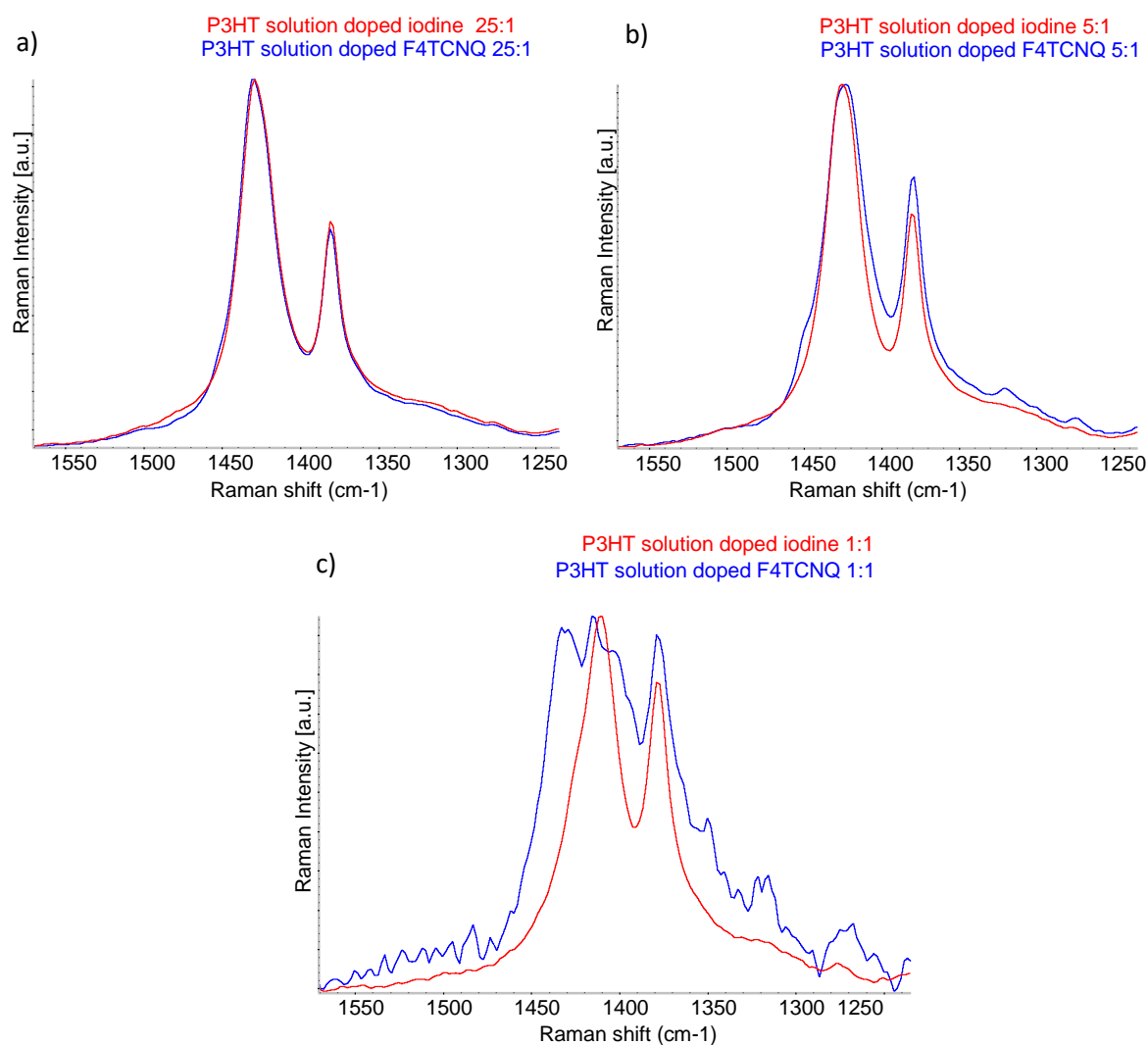


Figure 88: FT-Raman spectra in the region between 1550 cm^{-1} and 1250 cm^{-1} comparison of iodine doped (red lines) and F_4TCNQ doped (blue lines) P3HT solutions 25:1 (a); 5:1 (b) and 1:1 (c).

Doping	Pristine	25:1	5:1	1:1
I_2	1475 cm^{-1}	1430 cm^{-1}	1425 cm^{-1}	1410 cm^{-1} 1430 cm^{-1} sh
F_4TCNQ	1475 cm^{-1}	1430 cm^{-1}	1425 cm^{-1}	1430 cm^{-1} 1410 cm^{-1} 1400 cm^{-1}

Table 7: frequencies of the band ν_1 for the pristine P3HT solution and the three doped solutions with I_2 and F_4TCNQ .

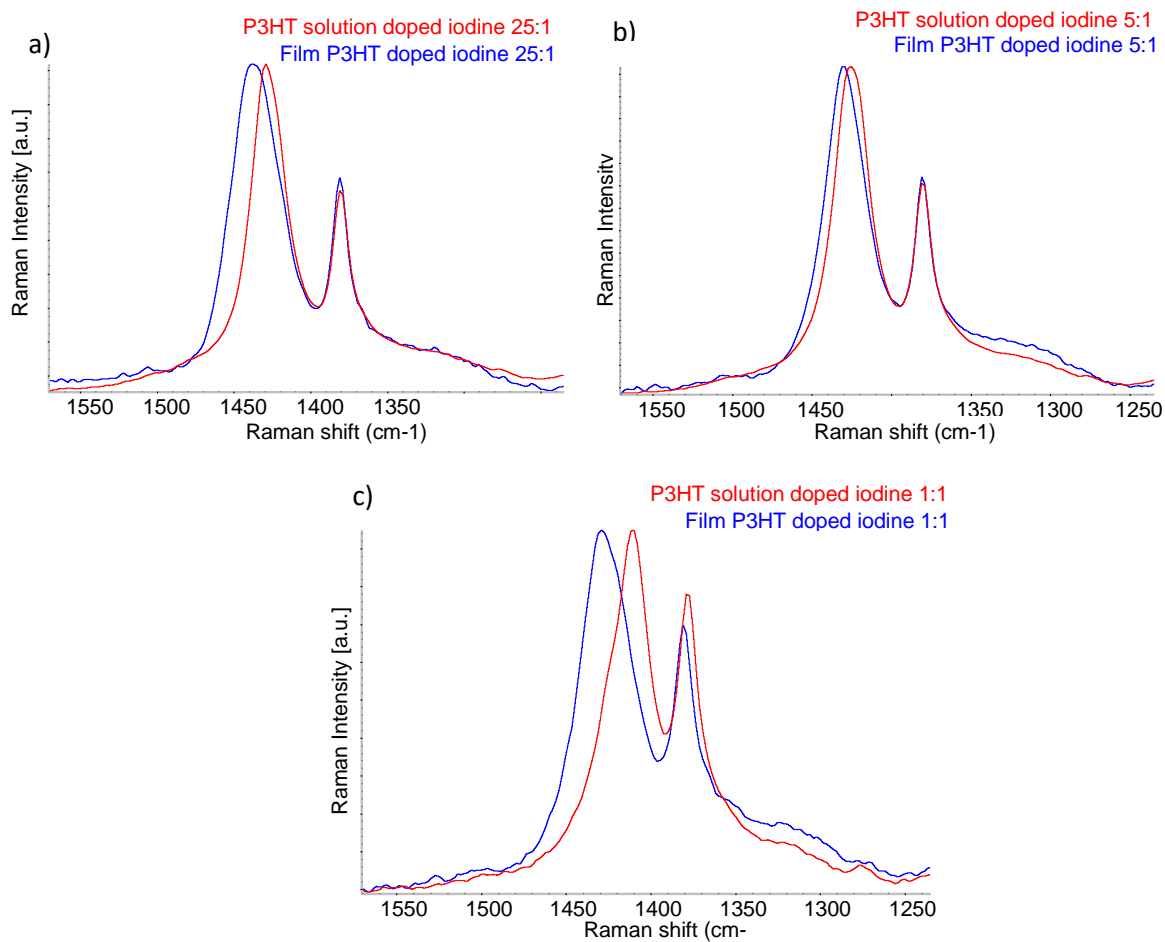
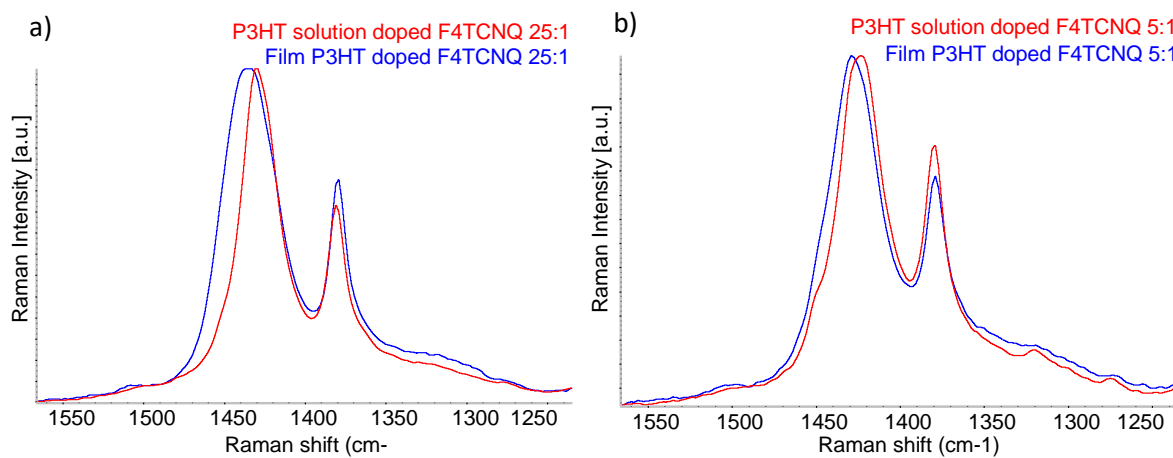


Figure 89: FT-Raman spectra in the region between 1550 cm^{-1} and 1250 cm^{-1} comparison of iodine doped P3HT solutions (red lines) and film (blue lines) 25:1 (a); 5:1 (b) and 1:1 (c).



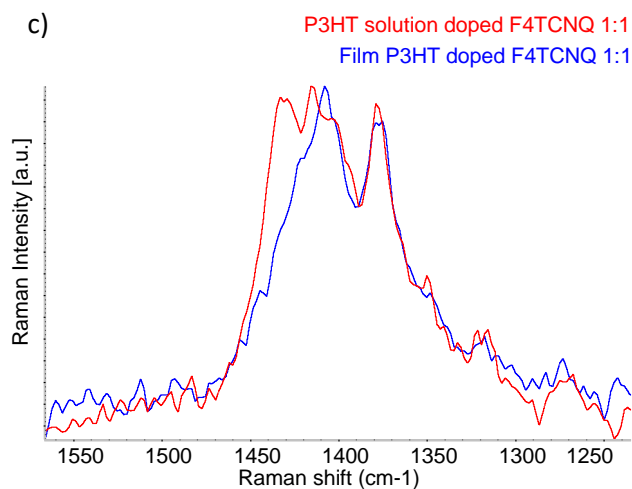


Figure 90: FT-Raman spectra in the region between 1550 cm^{-1} and 1250 cm^{-1} comparison of F_4TCNQ doped P3HT solutions (red lines) and film (blue lines) 25:1 (a); 5:1 (b) and 1:1 (c).

As shown in the figures above (Figure 89 and Figure 90) the comparison between solid and solution samples shows similar features but with some differences: the bands of the samples in solution are less broad and appears at lower frequencies. This could be because in solution the long neutral segments of the chains between two polarons are distorted and not planar. Due to this higher disorder the Raman intensity given by these neutral segments decrease and so the planar segments close to the polarons dominates the spectra, for this reason the bands are less broad in solution. As in the IR we observe that the most stable doping ratio is the 5:1 since the difference between solid and liquid sample is smaller than in the other two cases, the 25:1 and 1:1, that in the IR showed very different IRAV features in respect to the polaron_{OA} phase in solution.

3.2.2 Influence of the backbone conformation and the side alkyl chains in the doping process

Previously the influence of conformation and length of the backbone and side chains length was examined by IR spectroscopy. In this section the same investigation is done with FT-Raman spectroscopy analyzing the same samples of rraP3HT, P3DT and the oligothiophenes (8T, 13T, 21T).

3.2.2.1 FT-Raman spectra of doped regiorandom P3HT: role of the backbone.

The FT-Raman spectra of pristine rraP3HT in solution and in film are reported in Figure 91. Regio random P3HT behaves differently from P3HT. Because of a higher conformational disorder of the backbone the band ν_1 is observed at higher frequency both in solid state and in solution. In particular it can be noticed that the sample in solution shows a band at 1483 cm^{-1} , while in solid film the peak is only slightly shifted to 1475 cm^{-1} , as in the case of P3HT in solution.

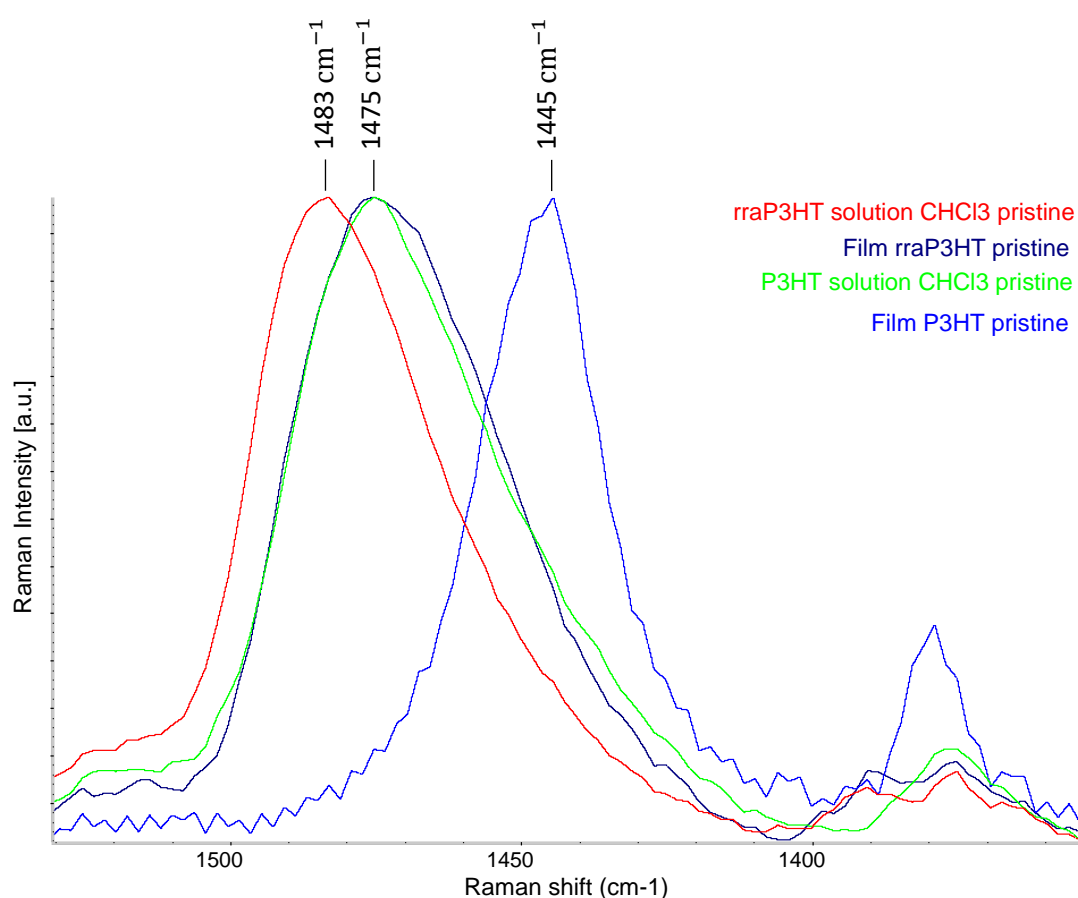


Figure 91: FT-Raman spectra in the region between 1530 cm^{-1} and 1350 cm^{-1} of pristine rraP3HT in solution with chloroform (red line) and in solid film (dark blue line) compared to pristine rraP3HT in solution with chloroform (green line) and in solid film (light blue line).

Since, as previously seen, rraP3HT in solution can't be doped by iodine in this chapter we will focus on the doping with F₄TCNQ only. The spectrum with doping ratio 5:1, is reported in Figure 92. The peak ν_1 can be seen at a frequency of 1442 cm^{-1} , while in pristine rraP3HT the same peak is at higher frequency, around 1475 cm^{-1} . This shift in the wavenumber from pristine to doped solution suggests, as seen also in the IR

spectroscopy, that some changes are induced by the doping process. However, also by the Raman spectra it can be confirmed that the interaction dopant-polymer is not in the form of polaron_{OA} phase since the component at 1430 cm^{-1} is not present in the spectra. On the other hand, planar sequences of neutral thiophene rings cannot develop, due to the conformational disorder. The presence of a band at 1442 cm^{-1} could be due to the few regioregular sequences that may be present in the solution, since the intensity of this band seems to be quite low.

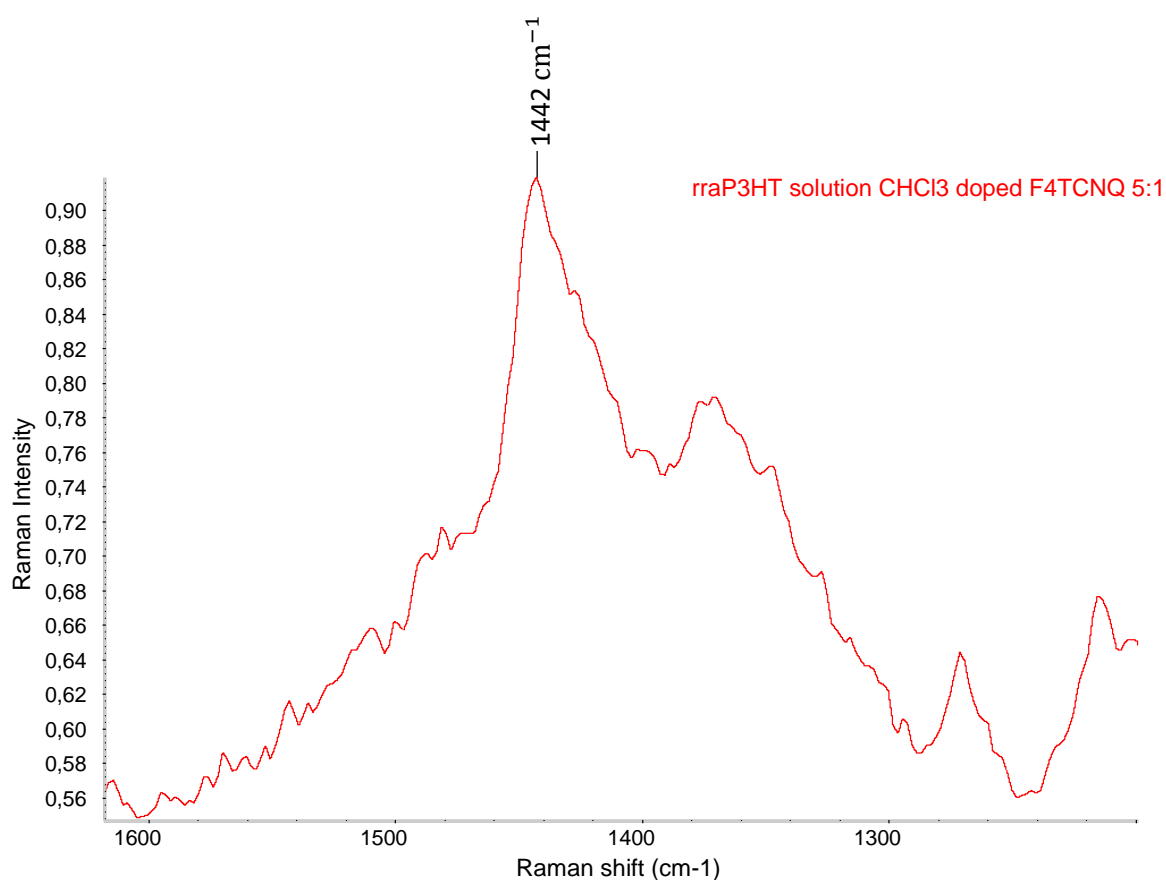


Figure 92: FT-Raman spectra in the region between 1600 cm^{-1} and 1200 cm^{-1} of rraP3HT doped F₄TCNQ 5:1 in solution.

When the solution is deposited in a thin film the Raman spectra, shown in Figure 93, confirms again the inability of rraP3HT to form a polaron_{OA} phase even in solid state. In fact, the signature of this phase present in P3HT at 1430 cm^{-1} can't be seen, since in rraP3HT planar segments close to the polaron (cases i and ii in Figure 82) can't exist. In this case we observe a band at 1405 cm^{-1} , close to the one previously associated to a more disordered situation as in the highly doped (1:1) case of regioregular P3HT. As in solution, there could be some regioregular segments as a

small band can be seen at 1442 cm^{-1} , but no pristine signal can be seen meaning that there are no longer undoped chains.

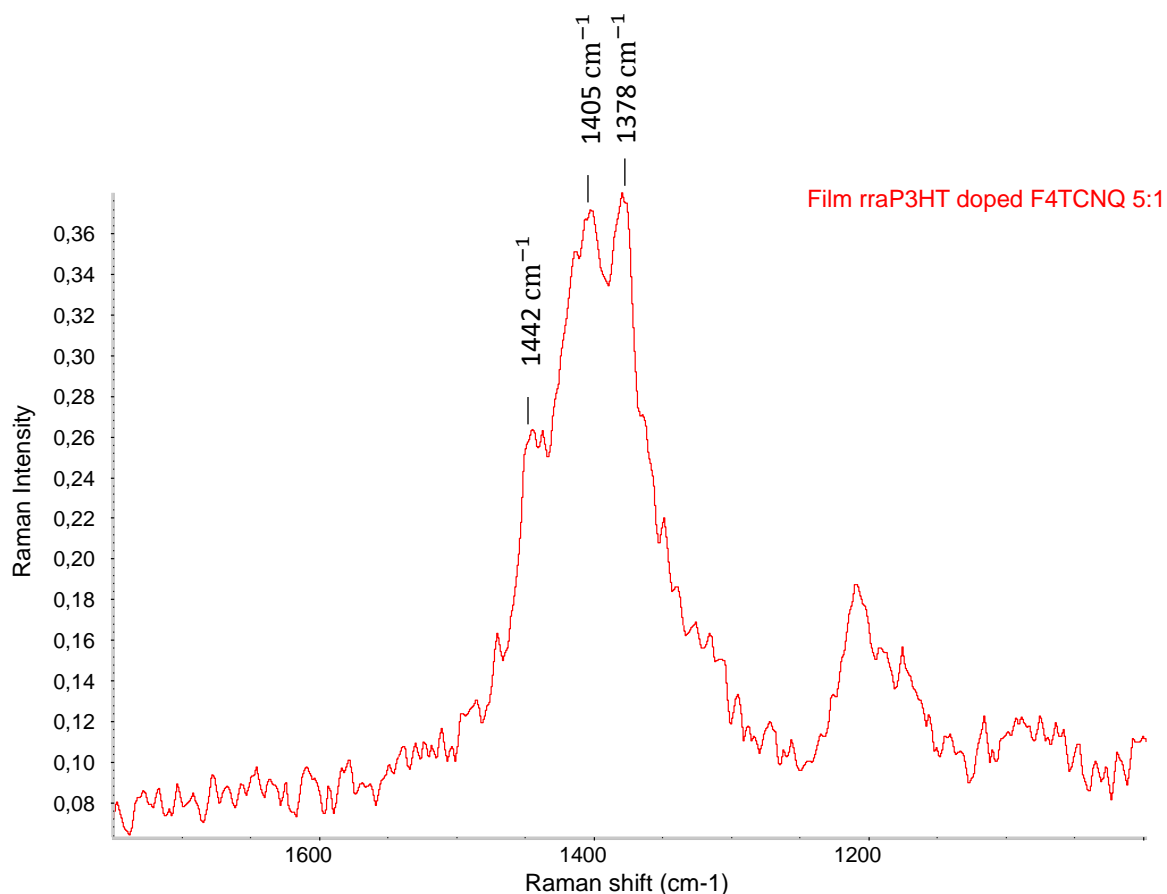


Figure 93: FT-Raman spectra in the region between 1700 cm^{-1} and 1000 cm^{-1} of rraP3HT film doped F4TCNQ 5:1 in solution.

In conclusion FT-Raman spectroscopy confirms that the effect of a disordered backbone is to hinder the formation of an ordered polaronic phase (polaron_{OA}) both in solution and in film. In addition, some suggestion of planarization of some sequence as consequence of the doping can be derived from the observation of the shift of the band ν_1 .

3.2.2.2 FT-Raman spectra of doped P3DT: role of the lateral alkyl chains.

FT-Raman spectra of pristine P3DT both in solution with chloroform and deposited in solid film are shown in Figure 94. It can be noticed that the behavior of P3DT is almost the same of P3HT. In fact, the band ν_1 goes from 1475 cm^{-1} in solution to 1445 cm^{-1} in solid film.

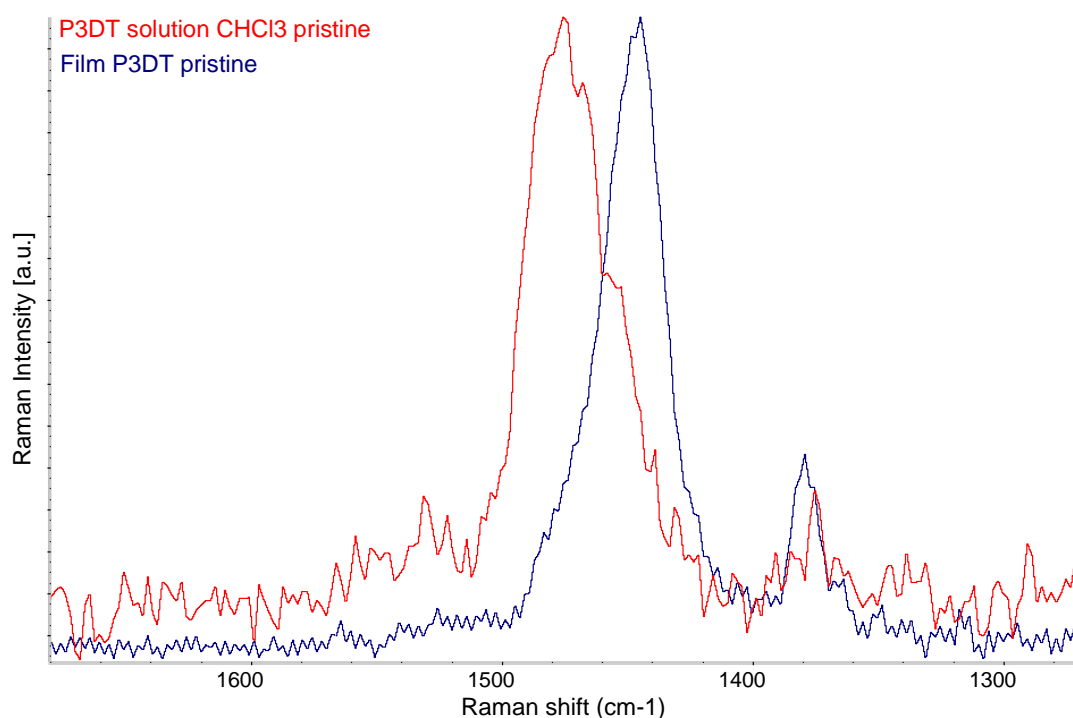


Figure 94: FT-Raman spectra in the region between 1650 cm^{-1} and 1300 cm^{-1} of pristine P3DT in solution with chloroform (red line) and in solid film (blue line).

As for rraP3HT, the doping was done using F₄TCNQ as dopant at a doping ratio of 5:1. The FT-Raman spectra of doped P3DT in solution is reported in Figure 95. The overall intensity is very low compared to the level of the noise, thus suggesting that most of the thiophene rings are affected by the doping. The peak ν_1 can be seen at a frequency of 1400 cm^{-1} , close to the wavenumber associated to a more disordered configuration like in rraP3HT and in the highly doped case. Also, some pristine polymer can be seen due to the presence of a component at 1440 cm^{-1} . This confirms that, as seen from the IR spectra, P3DT doped in solution behaves differently from P3HT doped with the same doping ratio (5:1) where the band was observed at 1425 cm^{-1} and no pristine signal was present.

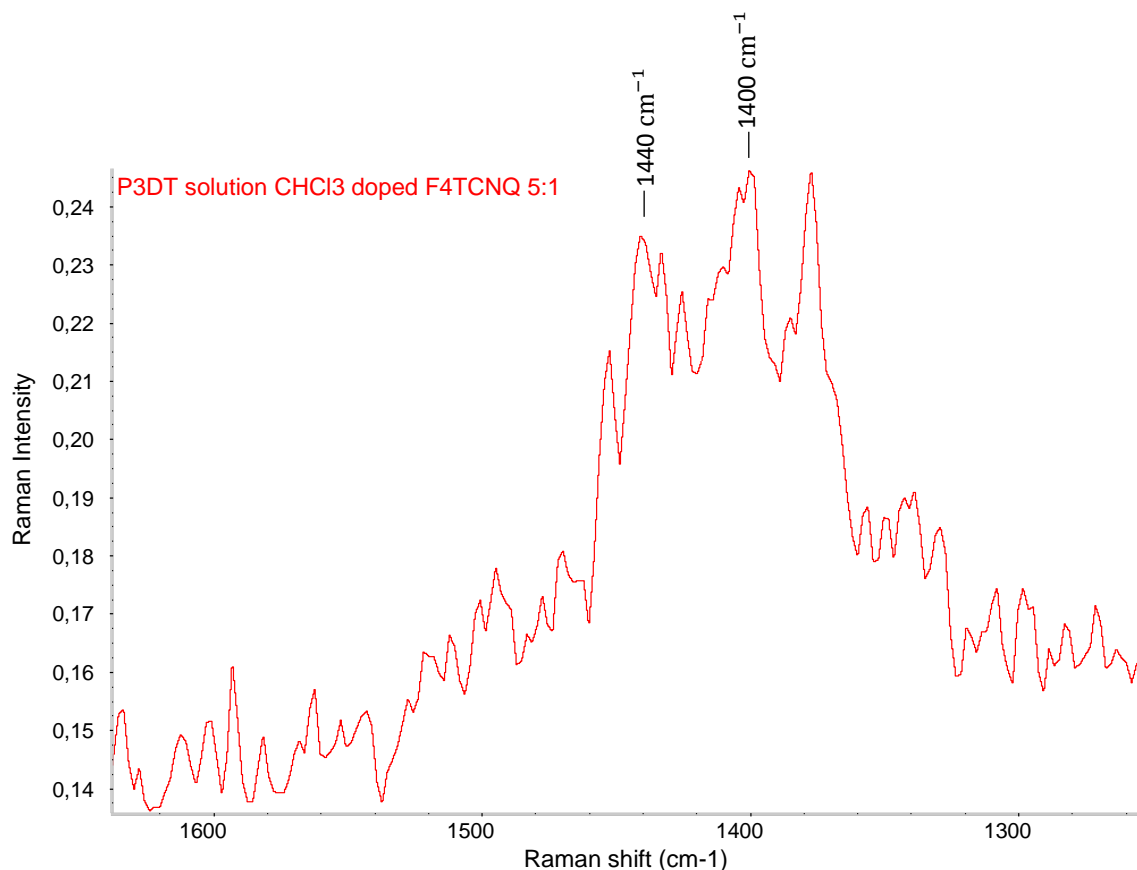


Figure 95: FT-Raman spectra of P3DT solution doped F₄TCNQ 5:1.

When the solution is deposited the spectrum shows a broad peak with both the components 1410 cm^{-1} and 1430 cm^{-1} seen in the Raman spectra of P3HT (see Figure 96). By the analysis of the IR spectroscopy, we concluded that longer alkyl chains hinder the formation of a prevailing ordered polaronic structure, however, by doping with F₄TCNQ, a small amount of ordered polaron_{OA} phase was supposed to be present. The appearance of the component at 1430 cm^{-1} in the FT-Raman spectra of P3DT doped film may confirm this last hypothesis.

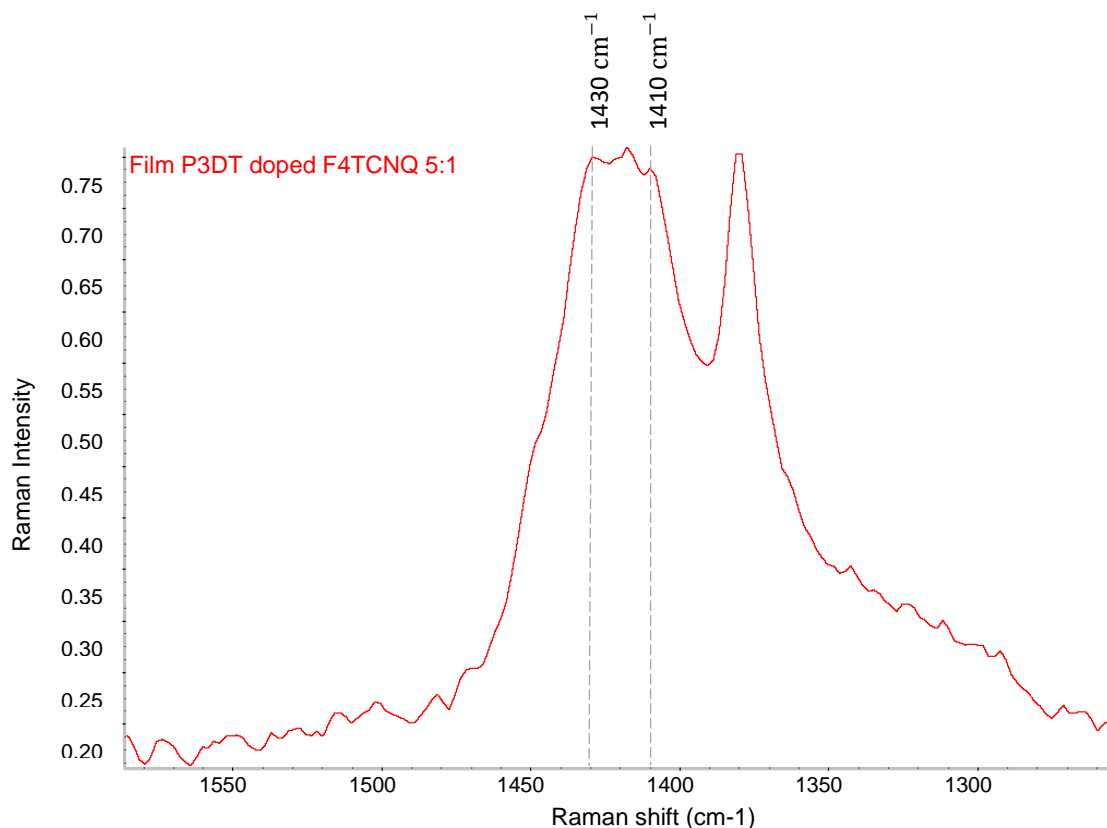


Figure 96: FT-Raman spectra of P3DT film doped F₄TCNQ in solution 5:1.

3.2.2.3 FT-Raman spectra of doped oligothiophenes: role of the backbone length.

In Figure 97 are reported the FT-Raman spectra of pristine oligothiophene (8T, 13T, 21T) in CHCl₃ solution. It can be noticed that all the three samples show the band ν_1 at high wavenumbers, 1475 cm⁻¹. When the same solutions are deposited into thin film the band shift to 1445 cm⁻¹, except for the 8T where the same band appears at 1448 cm⁻¹ as reported in Figure 98.

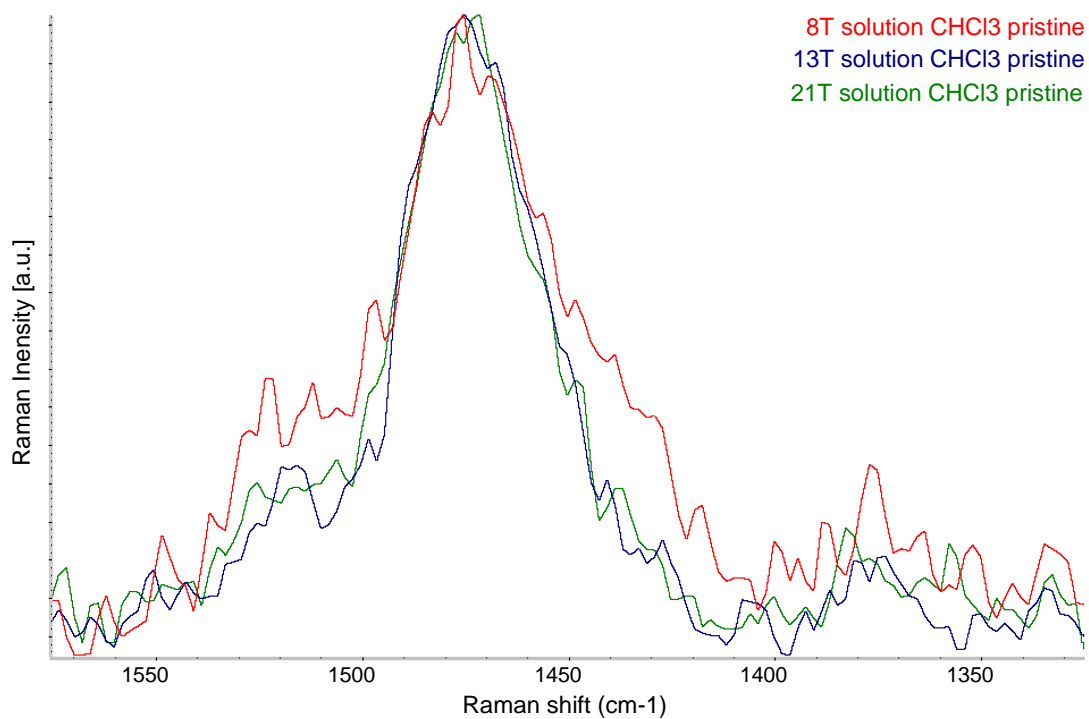


Figure 97: FT-Raman spectra of pristine oligothiophenes in solution: 8T (red line), 13T (blue line) and 21T (green line).

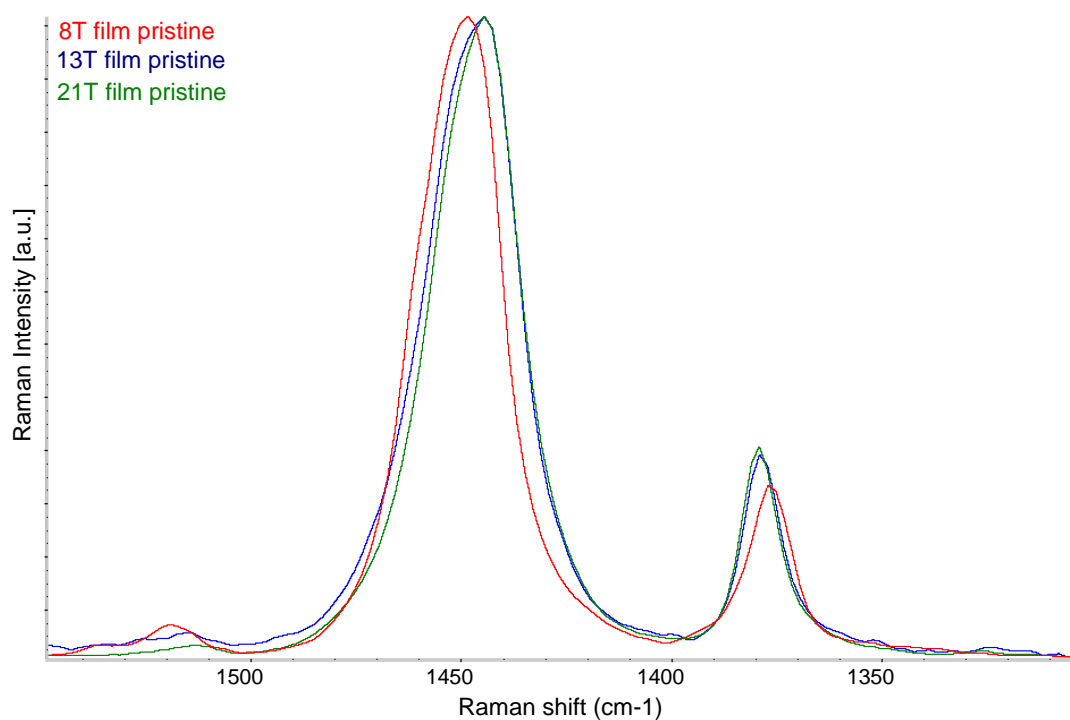


Figure 98: FT-Raman spectra of pristine oligothiophenes films: 8T (red line), 13T (blue line) and 21T (green line).

The FT-Raman spectra of the three different oligomers in solution doped F₄TCNQ with a ratio 5:1 are reported in Figure 99 and Figure 100. These spectra confirm that the behavior of doped oligothiophenes in solution is different from P3HT. Comparing the doped spectra with the pristine ones a shift towards lower wavenumber can be seen, from 1475 cm⁻¹ to 1442 cm⁻¹, as seen in the doped rraP3HT in solution. This change is induced by the doping process, and it may be due to a planarization and straightening of the backbone. Again FT-Raman spectroscopy confirms what was observed in the IR spectra: in solution the OTs behaves more like the regiorandom polymer than like the regioregular one.

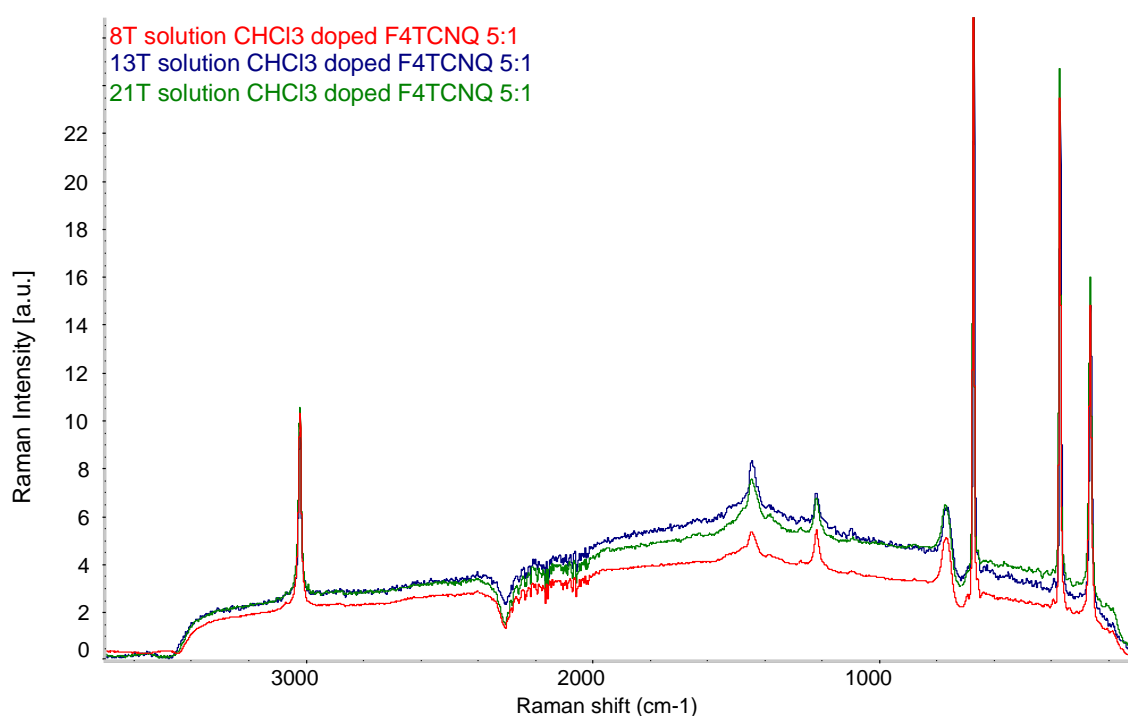


Figure 99: FT-Raman spectra of oligothiophenes doped F₄TCNQ 5:1 in solution: 8T (red line), 13T (blue line) and 21T (green line).

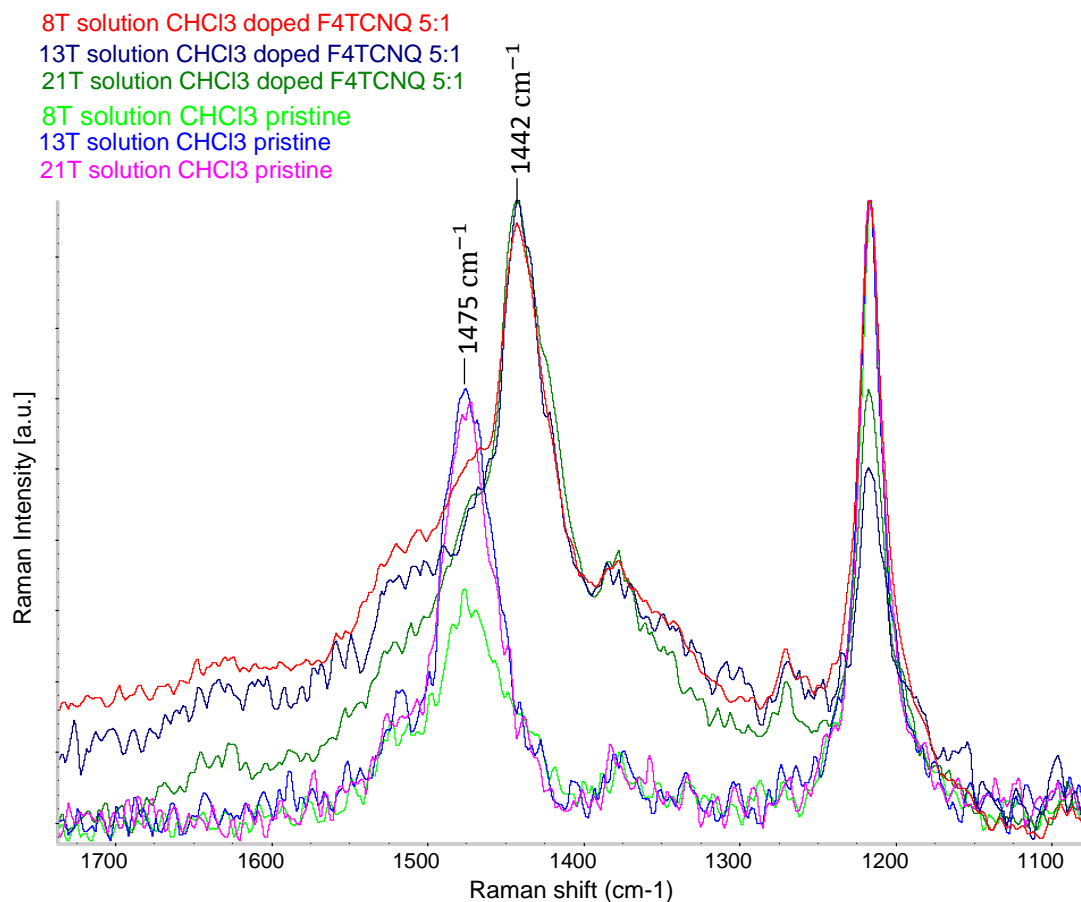


Figure 100: FT-Raman spectra of oligothiophenes in solution pristine 8T (light green line), 13T (blue line) and 21T (pink line) compared to oligothiophenes doped F₄TCNQ 5:1 in solution 8T (red line), 13T (dark blue line) and 21T (dark green line). The peak at 1200 cm⁻¹ is due to the presence of chloroform.

The Raman spectra of the films obtained by deposition of the previous solutions are shown in Figure 101. It can be noticed that the band ν_1 shifts to 1430 cm⁻¹, the signal attributed to the regions adjacent to the polarons in the polaron_{OA} phase seen in the P3HT doped films, that, in case of oligomers, coincide with the terminal rings. These bands have a very low intensity in case of the oligomers. This may confirm what previously seen with the IR spectroscopy: in solid state the oligomers are able to form polarons when interacting with F₄TCNQ. However, some chains of the OTs remain undoped since in all the spectra a component at 1445 cm⁻¹ can be seen. In the spectra of 8T a third component at 1400 cm⁻¹ can be seen, as observed also for the rraP3HT doped film.

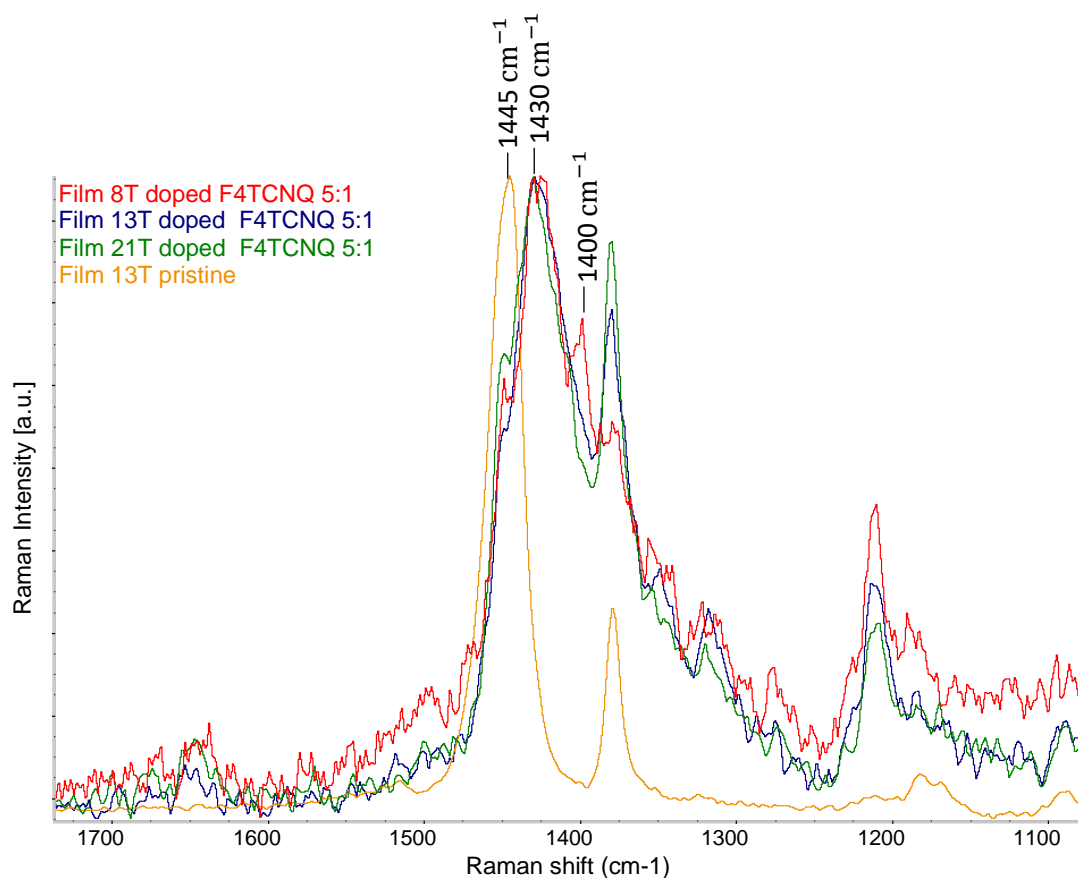


Figure 101: FT-Raman spectra of film of doped F₄TCNQ 5:1 in solution 8T (red line), 13T (blue line) and 21T (green line) compared to 13T film pristine (brown line).

In conclusion, IR spectroscopy suggested that, in solid film, increasing the number of thiophene units, the behavior of the oligomer becomes more similar to the one of the polymer, since the band P_s (associated to the ordered polaron phase) increases in intensity. With Raman spectroscopy we were able to confirm the possibility of these oligothiophenes to form polaron_{OA} phases.

| Polarons in P3HT: unravelling vibrational fingerprints of ordered and disordered doped phases in solids and solutions. IR and Raman study of the polymers and oligomers.

100

Sample n°	Material description	FT-IR Region α	comments	C≡N stretching modes of the counter ion	comments	FT-Raman	comments
1	P3HT pristine solution CHCl ₃	1377 cm ⁻¹		-	-	1474 cm ⁻¹	
2	P3HT pristine solid film	1377 cm ⁻¹		-	-	1445 cm ⁻¹	
3	P3HT + I ₂ 25:1 solution CHCl ₃	1392 cm ⁻¹ (A) 1270 cm ⁻¹ (I ₁)	Low wavenumber component I	-	-	1430 cm ⁻¹	Narrow band
4	P3HT + I ₂ 5:1 solution CHCl ₃	1393 cm ⁻¹ (A) 1300 cm ⁻¹ (P ₁)	Medium wavenumber component P	-	-	1425 cm ⁻¹	Made by 1430 and 1410 components
5	P3HT + I ₂ 1:1 solution CHCl ₃	1393 cm ⁻¹ (A) 1340 cm ⁻¹ (C ₁)	High wavenumber component C	-	-	1410 cm ⁻¹	Also a small shoulder at 1430 cm ⁻¹ is present
6	P3HT + I ₂ 25:1 solid film deposited from sample 3	1392 cm ⁻¹ (A) 1295 cm ⁻¹ (P _S)	Polaron at solid state (polaron_OA)	-	-	1435 cm ⁻¹	Broad band
7	P3HT + I ₂ 5:1 solid film deposited from sample 4	1392 cm ⁻¹ (A) 1295 cm ⁻¹ (P _S)	Polaron at solid state (polaron_OA)	-	-	1430 cm ⁻¹	Sharp band
8	P3HT + I ₂ 1:1 solid film deposited from sample 5	1391 cm ⁻¹ (A) 1292 cm ⁻¹ (P _S)	Polaron at solid state (polaron_OA)	-	-	1430 cm ⁻¹	Broad band
9	P3HT + I ₂ solid film doped by vapour	1392 cm ⁻¹ (A) 1292 cm ⁻¹ (P _V)	The band P _V is broader than the band P _S in samples 6, 7 and 8	-	-	-	The system evolves too fast to record the spectra
10	P3HT + F ₄ TCNQ 25:1 solution CHCl ₃	1391 cm ⁻¹ (A) 1269 cm ⁻¹ (I ₁)	Low wavenumber component I	2213 cm ⁻¹ (N ₁) 2194 cm ⁻¹ (A _D) 2173 cm ⁻¹ (A ₂)	Both neutral and anionic species of the dopant are present	1430 cm ⁻¹	
11	P3HT + F ₄ TCNQ 5:1 solution CHCl ₃	1392 cm ⁻¹ (A) 1297 cm ⁻¹ (P ₁)	Medium wavenumber component P	2194 cm ⁻¹ (A _D) 2171 cm ⁻¹ (A ₂)	Only anionic species of the dopant seem to be present	1425 cm ⁻¹	
12	P3HT + F ₄ TCNQ 1:1 solution CHCl ₃	1392 cm ⁻¹ (A) 1300 cm ⁻¹ (P ₁) 1340 cm ⁻¹ (C ₁)	Broad band with both P ₁ and C ₁ components	2213 cm ⁻¹ (N ₁) 2196 cm ⁻¹ (A _D) 2170 cm ⁻¹ (A ₂)	Both neutral and anionic species of the dopant are present	1430 cm ⁻¹ 1410 cm ⁻¹ 1400 cm ⁻¹	Broad band with different peaks
13	P3HT + F ₄ TCNQ 25:1 solid film deposited from sample 10	1393 cm ⁻¹ (A) 1296 cm ⁻¹ (P _S)	Polaron at solid state (polaron_OA)	2195 cm ⁻¹ (A _D) sh 2189 cm ⁻¹ (A _S) 2171 cm ⁻¹ (A ₂)	The band A _D can be seen as a small shoulder of band A _S	1435 cm ⁻¹	
14	P3HT + F ₄ TCNQ 5:1 solid film deposited from sample 11	1393 cm ⁻¹ (A) 1296 cm ⁻¹ (P _S)	Polaron at solid state (polaron_OA)	2195 cm ⁻¹ (A _D) w 2186 cm ⁻¹ (A _S) 2167 cm ⁻¹ (A ₂)	A weak band A _D can be seen	1430 cm ⁻¹	
15	P3HT + F ₄ TCNQ 1:1 solid film	1392 cm ⁻¹ (A) 1296 cm ⁻¹ (P _S)	Polaron at solid state (polaron_OA)	2197 cm ⁻¹ (A _D) w 2185 cm ⁻¹ (A _S) 2167 cm ⁻¹ (A ₂)	A weak band A _D can be seen	1410 cm ⁻¹	Broad band

	deposited from sample 12						
16	rraP3HT pristine solution CHCl ₃	1377 cm ⁻¹	Same as pristine rreP3HT	-	-	1483 cm ⁻¹	
17	rraP3HT pristine solid film	1377 cm ⁻¹	Same as pristine rreP3HT	-	-	1475 cm ⁻¹	Similar to pristine rreP3HT in solution
18	rraP3HT + I ₂ solid film doped by vapour	1393 cm ⁻¹ (A) 1320 cm ⁻¹ (C)		-	-	-	The system evolves too fast to record the spectra
19	rraP3HT + F ₄ TCNQ 5:1 solution CHCl ₃	1393 cm ⁻¹ (A) 1335 cm ⁻¹ (C)	The spectra obtained is of doped rraP3HT with C component	2227 cm ⁻¹ (S) 2211 cm ⁻¹ (N) 2195 cm ⁻¹ (A _D) sh	There is the presence of solid F ₄ TCNQ (band S)	1442 cm ⁻¹	A small shoulder can be seen at 1475 cm ⁻¹
20	rraP3HT + F ₄ TCNQ 5:1 solid film deposited from sample 19	1394 cm ⁻¹ (A) 1340 cm ⁻¹ (C ₁)	The spectra obtained is of doped rraP3HT film with C component	2227 cm ⁻¹ (S) 2205 cm ⁻¹ (CTC) sh 2191 cm ⁻¹ (A _S) 2170 cm ⁻¹ (A ₂)	There is the presence of solid F ₄ TCNQ (band S) and evidence of CTC	1405 cm ⁻¹	A small shoulder can be seen at 1442 cm ⁻¹
21	rreP3DT pristine solution CHCl ₃	1377 cm ⁻¹	Same as pristine rreP3HT	-	-	1475 cm ⁻¹	Same as pristine rreP3HT
22	rreP3DT pristine solid film	1377 cm ⁻¹	Same as pristine rreP3HT	-	-	1445 cm ⁻¹	Same as pristine rreP3HT
23	rreP3DT + F ₄ TCNQ 5:1 solution CHCl ₃	1395 cm ⁻¹ (A) 1342 cm ⁻¹ (C)		2211 cm ⁻¹ (N ₁) 2194 cm ⁻¹ (N ₂)	Only neutral F ₄ TCNQ molecules	1440 cm ⁻¹ 1400 cm ⁻¹	Broad band with two main peaks
24	rreP3DT + F ₄ TCNQ 5:1 solid film deposited from sample 23	1395 cm ⁻¹ (A) 1326 cm ⁻¹	Broad band	2194 cm ⁻¹ (A _D) 2169 cm ⁻¹ (A ₂)		1430 cm ⁻¹ 1420 cm ⁻¹ 1410 cm ⁻¹	Broad band with three main peaks
25	8T solution CHCl ₃ pristine	1377 cm ⁻¹	Same as pristine rreP3HT	-	-	1475 cm ⁻¹	Very weak band
26	8T solid film pristine	1377 cm ⁻¹	Same as pristine rreP3HT	-	-	1448 cm ⁻¹	Narrow band
27	8T + I ₂ 5:1 solution CHCl ₃	1345 cm ⁻¹	Broad and weak band	2211 cm ⁻¹ (N ₁) 2192 cm ⁻¹ (N ₂)	Only neutral F ₄ TCNQ molecules	1442 cm ⁻¹ 1475 cm ⁻¹	Very weak band
28	8T + I ₂ 5:1 solid film deposited from sample 27	1402 cm ⁻¹ (A) 1330 cm ⁻¹	Broad band with both components C ₁ and P ₅ (weak)	2193 cm ⁻¹ (A _D) 2170 cm ⁻¹ (A ₂)		1445 cm ⁻¹ 1430 cm ⁻¹ 1400 cm ⁻¹	Broad band with three main peaks
29	13T solution CHCl ₃ pristine	1377 cm ⁻¹	Same as pristine rreP3HT	-	-	1475 cm ⁻¹	Very weak band
30	13T solid film pristine	1377 cm ⁻¹	Same as pristine rreP3HT	-	-	1445 cm ⁻¹	Narrow band
31	13T + I ₂ 5:1 solution CHCl ₃	1345 cm ⁻¹	Broad and weak band	2211 cm ⁻¹ (N ₁) 2192 cm ⁻¹ (N ₂) w	Only neutral F ₄ TCNQ molecules are present	1442 cm ⁻¹ 1475 cm ⁻¹	Very weak band

| Polarons in P3HT: unravelling vibrational fingerprints of ordered and disordered doped phases in solids and solutions. IR and Raman study of the polymers and oligomers.

102

32	13T + I ₂ 5:1 solid film deposited from sample 31	1402 cm ⁻¹ (A) 1329 cm ⁻¹	Broad band with both components C ₁ and P ₅ (medium)	2193 cm ⁻¹ (A _D) 2170 cm ⁻¹ (A ₂)		1445 cm ⁻¹ 1430 cm ⁻¹	
33	13T + I ₂ 10:1 solution CHCl ₃	1345 cm ⁻¹	Broad and weak band	2211 cm ⁻¹ (N ₁) 2192 cm ⁻¹ (N ₂) w	Only neutral F ₄ TCNQ molecules are present	1442 cm ⁻¹ 1475 cm ⁻¹	Very weak band
34	13T + I ₂ 10:1 solid film deposited from sample 33	1402 cm ⁻¹ (A) 1328 cm ⁻¹	Broad band with both components C ₁ and P ₅ (medium)	2193 cm ⁻¹ (A _D) 2170 cm ⁻¹ (A ₂)		1445 cm ⁻¹ 1428 cm ⁻¹	
35	21T solution CHCl ₃ pristine	1377 cm ⁻¹	Same as pristine rreP3HT	-	-	1475 cm ⁻¹	Very weak band
36	21T solid film pristine	1377 cm ⁻¹	Same as pristine rreP3HT	-	-	1445 cm ⁻¹	Narrow band
37	21T + I ₂ 5:1 solution CHCl ₃	1345 cm ⁻¹	Broad and weak band	2210 cm ⁻¹ (N ₁) 2192 cm ⁻¹ (N ₂) w	Only neutral F ₄ TCNQ molecules are present	1442 cm ⁻¹ 1475 cm ⁻¹	Very weak band
38	21T + I ₂ 5:1 solid film deposited from sample 37	1398 cm ⁻¹ (A) 1316 cm ⁻¹	Broad band with both components C ₁ and P ₅ (high)	2191 cm ⁻¹ (A _S) 2170 cm ⁻¹ (A ₂)		1445 cm ⁻¹ 1430 cm ⁻¹	

Table 8: summary table with all the wavenumbers of the bands in region α of the IR spectra, wavenumbers of the bands corresponding to the C \equiv N stretching vibrations of F₄TCNQ and band ν_1 in the Raman spectra with comments.

4 Conclusions and future developments

The aim of this study was a deep characterization of doped poly(3-hexylthiophene-2,5-diyl) exploiting IR and Raman spectroscopy. This work was driven by the objective of unravelling the mechanisms of the chemical doping of P3HT and the characterization of the various charged defects which form in different environments.

To achieve this, P3HT was doped with I₂ and F₄TCNQ in chloroform solutions with three different polymer/dopant molar ratios.

The novelty of this work is the monitoring of the doping process both in solution and in solid state of the same doped samples leading to the identification of several, and so far unknown features of the doping process. Moreover, the direct comparison between IR and Raman data allowed the identification of the origin of the vibrational transitions observed in the spectra.

Several additional experiments were conducted on model molecules (P3HT oligomers) and two different polymers (regiorandom P3HT and P3DT), which allow to support and validate structure/property relationships developed in this framework.

Three different kinds of charged defects were observed and characterized in doped P3HT samples:

- i) the ordered polaron phase (called polaron_OA);
- ii) the disordered polaron phase;
- iii) the charge transfer complex (CTC).

The phases i) and ii) are both integer charge transfer complexes (ICTs) between the polymer and the dopant species but the first one is present where the structure of the doped polymer chains can adopt an ordered crystalline architecture, while the second one is observed in more disordered cases, as for instance in P3DT. Case (iii) corresponds to the formation of charge transfer dimers, which differs from ICT defects (polarons) because of the fractional charge transferred. Since CTC are typical of very disordered phases, they are more localized than polarons and feature specific interactions between the dopant molecule and the polymer segment forming the dimer.

- For P3HT a stable doping condition was achieved: the 5:1 doping ratio that allows to obtain an ordered polaron phase both in solution and in solid sample.
- All the solid state samples deposited from solutions at different molar ratios, showing distinct spectroscopic features, evolve toward a common pattern assigned to the polaron_OA phase, which has a characteristic “universal” signature in the infrared spectrum.
- Finally, this study confirmed what was already observed in polyacetylene: Raman spectroscopy shows preferentially vibrational transitions of the neutral segments of the polymer chain. The conformation of these segments is affected by the presence of the adjacent polarons which are hosted on the same polymer chain, thus showing clear evidences of the doping in the Raman spectrum.

These findings open the possibility of further research on the doping process of P3HT and of other “conducting” polymers.

Since we identified two different ICT complexes it could be useful to complement the spectroscopic studies with measurements of the sample conductivity to understand if one of the two polaron phases is better than the other. This could be an important understanding for the technological application of OSC films. In addition, the possibility to dope the P3HT directly in solution with a precise dopant ratio and being able to monitor through IR spectroscopy the level of doping, could be a very useful tool to optimize materials to make organic electronic devices with the desired properties.

Bibliography

- [1] T. L. Stott and M. O. Wolf, "Electronic interactions in metallated polythiophenes: What can be learned from model complexes," *Coordination Chemistry Reviews*, vol. 246, no. 1–2. Elsevier, pp. 89–101, 2003. doi: 10.1016/S0010-8545(03)00114-0.
- [2] A. E. Mansour *et al.*, "Understanding the evolution of the Raman spectra of molecularly p-doped poly(3-hexylthiophene-2,5-diyl): Signatures of polarons and bipolarons," *Physical Chemistry Chemical Physics*, vol. 24, no. 5, pp. 3109–3118, Feb. 2022, doi: 10.1039/d1cp04985b.
- [3] P. J. Donohoo-Vallett and A. E. Bragg, " π -delocalization and the vibrational spectroscopy of conjugated materials: Computational insights on Raman frequency dispersion in thiophene, furan, and pyrrole oligomers," *Journal of Physical Chemistry B*, vol. 119, no. 8, pp. 3583–3594, Feb. 2015, doi: 10.1021/jp512693e.
- [4] A. J. Heeger, S. Kivelson, J. R. Schrieffer, and W.-P. Su, "Solitons in conducting polymers," 1988.
- [5] X. Guo, M. Baumgarten, and K. Müllen, "Designing π -conjugated polymers for organic electronics," *Progress in Polymer Science*, vol. 38, no. 12. pp. 1832–1908, Dec. 2013. doi: 10.1016/j.progpolymsci.2013.09.005.
- [6] D. T. Duong, C. Wang, E. Antono, M. F. Toney, and A. Salleo, "The chemical and structural origin of efficient p-type doping in P3HT," *Org Electron*, vol. 14, no. 5, pp. 1330–1336, May 2013, doi: 10.1016/J.ORGEL.2013.02.028.
- [7] G. Louarn *et al.*, "Raman spectroscopic studies of regioregular poly(3-alkylthiophenes)," *Journal of Physical Chemistry*, vol. 100, no. 30, pp. 12532–12539, Jul. 1996, doi: 10.1021/JP960104P/ASSET/IMAGES/LARGE/JP960104PFB16A.JPEG.
- [8] M. T. Dang, L. Hirsch, G. Wantz, M. T. Dang, + L Hirsch, and G. Wantz, "P3HT:PCBM, Best Seller in Polymer Photovoltaic Research," *Advanced Materials*, vol. 23, no. 31, pp. 3597–3602, Aug. 2011, doi: 10.1002/ADMA.201100792.
- [9] A. Rubino, A. Camellini, and I. Kriegel, "(INVITED) Stable solution emission of 2,3,5,6-Tetrafluoro-7,7,8,8-tetracyanoquinodimethane," *Optical Materials: X*, vol. 11, p. 100081, Aug. 2021, doi: 10.1016/J.OMX.2021.100081.
- [10] M. T. Fontana, D. A. Stanfield, D. T. Scholes, K. J. Winchell, S. H. Tolbert, and B. J. Schwartz, "Evaporation vs Solution Sequential Doping of Conjugated Polymers: F4TCNQ Doping of Micrometer-Thick P3HT Films for Thermoelectrics," *Journal of Physical Chemistry C*, vol. 123,

- no. 37, pp. 22711–22724, Sep. 2019, doi:
10.1021/ACS.JPCC.9B05069/ASSET/IMAGES/LARGE/JP9B05069_0009.JPEG.
- [11] M. Arvind *et al.*, “Quantitative Analysis of Doping-Induced Polarons and Charge-Transfer Complexes of Poly(3-hexylthiophene) in Solution,” *Journal of Physical Chemistry B*, vol. 124, no. 35, pp. 7694–7708, Sep. 2020, doi:
10.1021/ACS.JPCB.0C03517/ASSET/IMAGES/LARGE/JPOC03517_0008.JPEG.
- [12] Y. Lu, J. Y. Wang, and J. Pei, “Achieving Efficient n-Doping of Conjugated Polymers by Molecular Dopants,” *Acc Chem Res*, vol. 54, no. 13, pp. 2871–2883, Jul. 2021, doi:
10.1021/ACS.ACCOUNTS.1C00223/ASSET/IMAGES/LARGE/AR1C00223_0011.JPEG.
- [13] P. Pingel and D. Neher, “Comprehensive picture of p-type doping of P3HT with the molecular acceptor F4TCNQ,” *Phys Rev B Condens Matter Mater Phys*, vol. 87, no. 11, p. 115209, Mar. 2013, doi: 10.1103/PHYSREVB.87.115209/FIGURES/7/MEDIUM.
- [14] C. Enengl *et al.*, “Doping-Induced Absorption Bands in P3HT: Polarons and Bipolarons,” *ChemPhysChem*, vol. 17, no. 23, pp. 3836–3844, Dec. 2016, doi: 10.1002/cphc.201600961.
- [15] E. C. Wu *et al.*, “Counterion Control and the Spectral Signatures of Polarons, Coupled Polarons, and Bipolarons in Doped P3HT Films,” *Adv Funct Mater*, vol. 33, no. 19, May 2023, doi: 10.1002/adfm.202213652.
- [16] G. Huseynova, J. Lee, J. H. Lee, and J. H. Lee, “Charge generation efficiency of electrically doped organic semiconductors,” *Mater Today Energy*, vol. 21, Sep. 2021, doi:
10.1016/j.mtener.2021.100709.
- [17] D. A. Stanfield, Y. Wu, S. H. Tolbert, and B. J. Schwartz, “Controlling the Formation of Charge Transfer Complexes in Chemically Doped Semiconducting Polymers,” *Chemistry of Materials*, vol. 33, no. 7, pp. 2343–2356, Apr. 2021, doi: 10.1021/acs.chemmater.0c04471.
- [18] J. Yin, Z. Wang, D. Fazzi, Z. Shen, and C. Soci, “First-Principles Study of the Nuclear Dynamics of Doped Conjugated Polymers,” *Journal of Physical Chemistry C*, vol. 120, no. 3, pp. 1994–2001, Jan. 2016, doi: 10.1021/acs.jpcc.5b11764.
- [19] L. Brambilla *et al.*, “Regio-regular oligo and poly(3-hexyl thiophene): Precise structural markers from the vibrational spectra of oligomer single crystals.,” *Macromolecules*, vol. 47, no. 19, pp. 6730–6739, Oct. 2014, doi: 10.1021/ma501614c.
- [20] A. Arrigoni, L. Brambilla, C. Castiglioni, and C. Bertarelli, “Conducting electrospun nanofibres: monitoring of Iodine 2 doping of P3HT through Infrared (IRAV) and Raman (RaAV) 3 polarons spectroscopic features,” *Nanomaterials 2022*, vol. 12, 2022, doi: 10.3390/xxxxx.
- [21] C. Castiglioni, M. Tommasini, and G. Zerbi, “Raman spectroscopy of polyconjugated molecules and materials: Confinement effect in one and two dimensions,” *Philosophical Transactions of the Royal Society A: Mathematical, Physical and Engineering Sciences*, vol. 362, no. 1824, pp. 2425–2459, Nov. 2004, doi: 10.1098/rsta.2004.1448.
- [22] B. Horovitz, H Gutfreund, and M. Weger, “PHYSICAL REVIEW B, VOLUME 17, NUMBER 6, 15 MARCH 1978 ”Infrared and Raman activities of organic linear conductors* The self-energies of the phase and amplitude modes are.”

- [23] G. Zerbi, M. Gussoni, and C. Castiglioni, "Vibrational Spectroscopy of Polyconjugated Aromatic Materials with Electrical and Non Linear Optical Properties," *Conjugated Polymers*, pp. 435–507, 1991, doi: 10.1007/978-94-011-3476-7_10.
- [24] L. Brambilla *et al.*, "Infrared and multi-wavelength Raman spectroscopy of regio-regular P3HT and its deuterio derivatives," *Journal of Raman Spectroscopy*, vol. 49, no. 3, pp. 569–580, Mar. 2018, doi: 10.1002/jrs.5301.
- [25] L. Brambilla, J. S. Kim, B. J. Kim, V. Hernandez, J. T. Lopez Navarrete, and G. Zerbi, "Poly(3-hexylthiophene-2.5-diyl): Evidence of different polymer chain conformations in the solid state from a combined study of regioregularity control and Raman spectroscopy," *J Mol Struct*, vol. 1221, p. 128882, Dec. 2020, doi: 10.1016/J.MOLSTRUC.2020.128882.
- [26] L. C. T. Shoute, N. Pekas, Y. Wu, and R. L. McCreery, "Redox driven conductance changes for resistive memory," *Appl Phys A Mater Sci Process*, vol. 102, no. 4, pp. 841–850, Mar. 2011, doi: 10.1007/s00339-011-6268-5.
- [27] J. Yamamoto and Y. Furukawa, "Electronic and Vibrational Spectra of Positive Polarons and Bipolarons in Regioregular Poly(3-hexylthiophene) Doped with Ferric Chloride," *Journal of Physical Chemistry B*, vol. 119, no. 13, pp. 4788–4794, Apr. 2015, doi: 10.1021/jp512654b.
- [28] D. Liu *et al.*, "Control Aggregation of P3HT in Solution for High Efficiency Doping: Ensuring Structural Order and the Distribution of Dopants," *Chinese Journal of Polymer Science (English Edition)*, vol. 41, no. 5, pp. 811–823, May 2023, doi: 10.1007/s10118-023-2939-x.
- [29] Carlo Saporiti, Chiara Castiglioni, and Daniele Fazzi, "Structure and properties of the polaron in doped poly(3-alkyl thiophenes): DFT modeling of the vibrational spectra.," *Politecnico di Milano*, Milano, 2023.
- [30] K. E. Watts, B. Neelamraju, E. L. Ratcliff, and J. E. Pemberton, "Stability of Charge Transfer States in F4TCNQ-Doped P3HT," *Chemistry of Materials*, vol. 31, no. 17, pp. 6986–6994, Sep. 2019, doi: 10.1021/acs.chemmater.9b01549.
- [31] D. A. Stanfield, Z. Mehmedović, and B. J. Schwartz, "Vibrational Stark Effect Mapping of Polaron Delocalization in Chemically Doped Conjugated Polymers," *Chemistry of Materials*, vol. 33, no. 21, pp. 8489–8500, Nov. 2021, doi: 10.1021/ACS.CHEMMATER.1C02934/ASSET/IMAGES/LARGE/CM1C02934_0004.JPEG.
- [32] M. Meneghetti and C. Pecile, "Charge–transfer organic crystals: Molecular vibrations and spectroscopic effects of electron–molecular vibration coupling of the strong electron acceptor TCNQF4," *J Chem Phys*, vol. 84, no. 8, pp. 4149–4162, Apr. 1986, doi: 10.1063/1.450086.
- [33] B. Neelamraju, K. E. Watts, J. E. Pemberton, and E. L. Ratcliff, "Correlation of Coexistent Charge Transfer States in F 4 TCNQ-Doped P3HT with Microstructure," *Journal of Physical Chemistry Letters*, vol. 9, no. 23, pp. 6871–6877, Dec. 2018, doi: 10.1021/ACS.JPCLETT.8B03104/ASSET/IMAGES/LARGE/JZ-2018-03104Q_0005.JPEG.
- [34] M. Arvind, "Regarding the Role of Aggregation and Structural Order on the Mechanism of Molecular Doping of Semiconducting Polymers: From Solutions to Films Dissertation", doi: 10.25932/publishup-50060.

- [35] "Poly(3-decylthiophene-2,5-diyl) regioregular, average Mw ~42,000, average Mn ~30,000 | 110851-65-5." <https://www.sigmaaldrich.com/IT/it/product/aldrich/495344> (accessed Aug. 18, 2023).
- [36] "P3ht | Sigma-Aldrich." https://www.sigmaaldrich.com/IT/it/search/p3ht?focus=products&page=1&perpage=30&sort=relevance&term=p3ht&type=product_name (accessed Aug. 18, 2023).
- [37] S. S. Zade, N. Zamoshchik, and M. Bendikov, "From short conjugated oligomers to conjugated polymers. Lessons from studies on long conjugated oligomers," *Acc Chem Res*, vol. 44, no. 1, pp. 14–24, Jan. 2011, doi: 10.1021/AR1000555.
- [38] S. F. Parker, J. E. Trevelyan, and H. Cavaye, "Vibrational spectra of neutral and doped oligothiophenes and polythiophene," *RSC Adv*, vol. 13, no. 8, pp. 5419–5427, Feb. 2023, doi: 10.1039/d2ra07625j.
- [39] D. Khlaifia *et al.*, "Unraveling the real structures of solution-based and surface-bound poly(3-hexylthiophene) (P3HT) oligomers: a combined theoretical and experimental study †," 2016, doi: 10.1039/c6ra03903k.
- [40] B. Capozzi, E. J. Dell, T. C. Berkelbach, D. R. Reichman, L. Venkataraman, and L. M. Campos, "Length-Dependent Conductance of Oligothiophenes," *J. Am. Chem. Soc.*, vol. 136, p. 38, 2014, doi: 10.1021/ja505277z.

List of Figures

Figure 1: Chemical structures of a) neutral P3HT, b) P3HT polaron [14].....	4
Figure 2: schematic representation of the energy level diagrams of pristine P3HT and positive polaron after chemical p-doping. The possible electronic transitions are highlighted by the blue arrows. The black arrow on the first localized state in the gap of the p-doped polymer represents an unpaired electron. [14].....	4
Figure 3: schematic representation of the different models to describe the charge transfer between P3HT and F ₄ TCNQ: a) integer charge transfer (ICT) where a hole electron is transferred resulting in a charged defect; b) charge transfer complex (CTC) in which there is a partial charge transfer between polymer and dopant. [13]	5
Figure 4: schematic representation of a) pristine P3HT crystal structures; b) ICT structure of doped P3HT where the dopant resides in the lamellar region; c) CTC structure where the dopant resides in the π -stacking of the polymer chains [17]	6
Figure 5: illustration of the three levels of doping a) low level of doping with one dopant molecule every 25 P3HT monomer unit; b) medium level of doping with one dopant molecule every 5 P3HT monomer unit; c) high level of doping with one dopant molecule for each P3HT monomer unit	9
Figure 6: Schematic illustration of the vibrational displacements associated to the collective ECC coordinate for polythiophene. Green and blue segments represent respectively simultaneous stretching and shrinking of the CC bonds [20]	10
Figure 7: FT-Raman spectra of liquid solution of P3HT in chloroform (red line) compared to solid P3HT thin film (purple line)	12
Figure 8: IR spectra of pristine P3HT solid film (red line) compared to pristine P3HT in chloroform solution (blue line)	13
Figure 9: >CH ₂ and -CH ₃ absorption of solid pristine P3HT (red line) and liquid solution of pristine P3HT (blue line)	14
Figure 10: IR spectra in the region between 1560 cm ⁻¹ and 1300 cm ⁻¹ of solid pristine P3HT (red line) and liquid solution of pristine P3HT (blue line)	14
Figure 11: Raman spectra (exciting laser 830 nm) of (a) neutral P3HT solid film and (b,c,d) P3HT film doped with an acetonitrile solution of FeCl ₃ . The doping level increases from (b) to (d). [27]	15

- Figure 12: IR absorption spectra of (a) pristine P3HT film and (b-e) P3HT film doped FeCl_3 by solution doping with increasing doping level from (b) to (e). [27]..... 16
- Figure 13: UV-Vis-NIR absorption spectra of P3HT undoped and doped F_4TCNQ solution in TCE with increasing doping level [28] 16
- Figure 14: B3LYP (blue line) and hybrid (CAM-B3LYP//B3LYP) (green line) approach IR spectra of the dodecamer of 3-ethyl thiophene compared to the experimental spectrum of P3HT doped by I2 (red line). [29]..... 17
- Figure 15: FT-IR spectra in the region between 1600 cm^{-1} and 900 cm^{-1} of solution of P3HT in CHCl_3 pristine (pink line) and doped with iodine in different molar ratios: 25:1 blue line, 5:1 green line, and 1:1 red line..... 20
- Figure 16: FT-IR spectra in the region between 1600 cm^{-1} and 900 cm^{-1} of solution of P3HT in CHCl_3 doped with iodine: 25:1 blue line, 5:1 green line, 1:1 red line. The grey, pink and green areas identify respectively the region α , β and γ of the spectra. 21
- Figure 17: FT-IR spectra of a) solution of P3HT in CHCl_3 pristine (brown line) and doped with iodine: 25:1 (blue line), 5:1 (green line), 1:1 (red line); b) solution of P3HT in CHCl_3 doped with iodine in the region between 1700 cm^{-1} – 500 cm^{-1} . The blue arrow highlights the signals of pristine P3HT. 22
- Figure 18: FT-IR spectra of a) solution of P3HT in CHCl_3 pristine (brown line) and doped with F_4TCNQ : 25:1 (blue line), 5:1 (green line), 1:1 (red line), b) solution of P3HT in CHCl_3 doped with F_4TCNQ in the region between 1600 cm^{-1} – 500 cm^{-1} . The blue arrow highlights the signals of pristine P3HT. 23
- Figure 19: FT-IR spectra of solution of P3HT in CHCl_3 doped with iodine (a) and F_4TCNQ (b): blue line 25:1; green line 5:1; red line 1:1; normalized in respect with the intensity of the CH stretching..... 24
- Figure 20: FT-IR spectra in the region between 1500 cm^{-1} – 500 cm^{-1} , comparison between P3HT solution doped with iodine (red lines) and doped with F_4TCNQ (blue lines): a) 25:1; b) 5:1 and c) 1:1..... 26
- Figure 21: Representation of the two vibrational modes of $\text{C}\equiv\text{N}$ stretching with B_{1u} and B_{2u} symmetry. The atomic displacement vectors are represented in the figure: compression of the $\text{C}\equiv\text{N}$ bonds is represented with red arrows, while the expansion with blue arrows. The green arrows represent the dipole moments of the two modes. [31] 26
- Figure 22: schematic representation of the morphology of P3HT doped F_4TCNQ – solution 25:1. The blue lines represent the amorphous polymer, red lines and light green dots are domains of crystalline polymer with incorporated dopant molecules

and dark green dots are neutral dopant molecules that are not interacting with the polymer chain. Figure adapted from ref. [6] 28

Figure 23: FT-IR spectra in the C≡N stretching region (from 2260 cm⁻¹ to 2160 cm⁻¹) of F4TCNQ in solution with CHCl₃ (red line) compared to solutions of F4TCNQ doped P3HT (blue line) a) 25:1; b) 5:1; c) 1:1..... 29

Figure 24: FT-IR spectra of 400 nm-thick (blue curves) and 110 nm-thick (red curves) doped P3HT samples. Continuous lines correspond to films treated by sequential solution doping with F4TCNQ; dotted lines correspond to vapor phase doping. Figure adapted from ref. [17] 29

Figure 25: graph representing the % of F4TCNQ neutral molecules (red) and anions (blue) for F4TCNQ-doped P3HT solutions in the three different doping levels..... 30

Figure 26: FT-IR spectra in the region between 1500 cm⁻¹- 500 cm⁻¹ of P3HT thin films doped 25:1 (blue lines), 5:1 (green lines) and 1:1 (red lines) with a) iodine, b) F4TCNQ..... 32

Figure 27: IR spectra of P3HT thin films from iodine (red line) and F4TCNQ (blue line) doped polymer solution 5:1 deposited on a KBr substrate. 33

Figure 28: FT-IR spectra in the region between 1600 cm⁻¹- 600 cm⁻¹ of P3HT in solution (blue lines) and film (red lines) doped 5:1 with a) iodine; b) F4TCNQ. 34

Figure 29: stretching bands of the CN groups of film casted from solution of P3HT doped F4TCNQ 25:1 (blue line), 5:1 (green line) and 1:1 (red line) compared to F4TCNQ in powder (pink line). The spectra are reported with a baseline correction..... 35

Figure 30: FT-IR spectra reported in common scale of thin film P3HT from iodine doped polymer solution 5:1 deposited on a KBr substrate measured at different times: just after casting (red lines); after 10 minutes (orange lines); after 30 minutes (blue lines) and after 60 minutes (light blue lines)..... 36

Figure 31: FT-IR spectra reported in common scale of thin films of P3HT from F4TCNQ doped polymer solution 5:1 measured at different times: just after casting (red lines); after 10 minutes (orange lines); after 30 minutes (blue lines) and after 60 minutes (light blue lines)..... 37

Figure 32: FT-IR spectra reported in common scale of thin film P3HT from F4TCNQ doped solution 5:1 deposited on a KBr substrate (red line) and the same film heated for 2 minutes (green line) 37

Figure 33: representation of the chemical structure of P3HT and rraP3HT. [11] 39

Figure 34: FT-IR spectra of pristine rraP3HT in solution (red line) and pristine (regioregular) P3HT in solution (blue line). 40

Figure 35: FT-IR spectra of rraP3HT in solution doped with iodine 5:1 (red line); doped with F₄TCNQ 5:1 (blue line) and pristine rraP3HT in solution (green line). 40

Figure 36: FT-IR spectra of rraP3HT in solution doped with F₄TCNQ 5:1 (red line) and pristine rraP3HT in solution (blue line). The black dotted line highlights the signal of pristine P3HT. 41

Figure 37: FT-IR spectra in the C≡N stretching region of rraP3HT in solution doped with iodine 5:1 (red line) compared to F₄TCNQ in solution (blue line) and in solid state (green line). 41

Figure 38: FT-IR spectra of rraP3HT film casted from solutions doped 5:1 iodine (red line) and F₄TCNQ (blue line) 5:1. 42

Figure 39: FT-IR spectra in region between 1800 cm⁻¹ and 600 cm⁻¹ of rraP3HT films casted from solutions doped iodine (red line) and F₄TCNQ (blue line) 5:1 compared to P3HT film casted from solution doped F₄TCNQ 5:1 (green line). 43

Figure 40: FT-IR spectra of the CN modes of film casted from solution of rraP3HT doped F₄TCNQ 5:1 (red line) compared to the CN modes of F₄TCNQ powder (blue line). The red arrow and the blue arrow highlight respectively the band attributed to the formation of the CTCs and the presence of neutral dopant molecule in the doped film. 44

Figure 41: FT-IR spectra of CN modes of film casted from solution of rraP3HT doped F₄TCNQ 5:1 immediately after deposition (red line); after 10 minutes (orange line); after 30 minutes (blue line); after 60 minutes (light blue line) and after heating it (green line). The red arrow points out the decreasing of the CTCs band at about 1205 cm⁻¹. 45

Figure 42: FT-IR spectra between 1800 cm⁻¹ and 700 cm⁻¹ of rraP3HT film doped F₄TCNQ in solution 5:1 right after casting (blue line), after heating (green line) and the subtraction spectra obtained by subtracting the spectrum of the heated film from that of the film after casting (red line). 45

Figure 43: FT-IR spectra between 1700 cm⁻¹ and 800 cm⁻¹ of P3HT iodine doped solution 1:1 (green line); P3HT F₄TCNQ doped solution 1:1 (blue line) compared to the CTC IR features obtained by the subtraction spectra of rraP3HT doped film after casting and the heated film (red line). 46

Figure 44: representation of the chemical structure of a) P3HT and b) P3DT. [35], [36] 47

Figure 45: comparison of FT-IR spectra of pristine P3DT (red lines) and P3HT (blue lines) in solution (a) and in film (b). 48

Figure 46: FT-IR spectra of P3DT solutions doped 5:1 with iodine (red line) and F₄TCNQ (blue line) compared to pristine P3DT in chloroform (green line). 48

Figure 47: FT-IR spectra of P3DT solutions doped 5:1 with iodine (red line) and F ₄ TCNQ (blue line) compared to pristine P3DT in chloroform (green line) in the IRAV region.	49
Figure 48: FT-IR spectra of P3DT solution doped 5:1 with F ₄ TCNQ (red line) and rraP3HT solution doped 5:1 with F ₄ TCNQ (blue line) in the IRAV region.	49
Figure 49: FT-IR spectra of P3DT films doped in solution 5:1 with iodine (red line) and F ₄ TCNQ (blue line) compared to pristine P3DT film (green line).	50
Figure 50: FT-IR spectra of P3DT films doped in solution 5:1 with iodine (red line) and F ₄ TCNQ (blue line) compared to rraP3HT film (light green line) and P3HT film (light blue line) in the IRAV region (between 1600 cm ⁻¹ and 600 cm ⁻¹).	51
Figure 51: FT-IR spectra of P3DT (red line), rraP3HT (blue line) and P3HT (pink line). The black arrow highlights the shift towards lower wavenumbers.	51
Figure 52: stretching modes of the CN groups of film casted from solution of P3DT doped F ₄ TCNQ 5:1 (blue line) compared to P3HT doped F ₄ TCNQ 25:1 solution (green line) and film (red line). The spectra are reported with a baseline correction.	52
Figure 53: stretching modes of the CN groups of film casted from solution of P3DT doped F ₄ TCNQ 5:1 (red line) compared to film of P3HT doped F ₄ TCNQ 25:1 (pink line), 5:1 (blue line) and 1:1 (green line). The spectra are reported with a baseline correction.	53
Figure 54: schematic representation of the doping ratio 5:1 in the different oligomers.	54
Figure 55: FT-IR spectra of P3HT (pink lines), 21T (green lines), 13T (blue lines) and 8T (red lines) pristine in solution (a) and in solid film (b).	55
Figure 56: FT-IR spectra of a) 8T in solution doped 5:1 with F ₄ TCNQ (red lines) compared to the pristine 8T in solution; b) 13T in solution doped 5:1 with F ₄ TCNQ (red lines) compared to the pristine 8T in solution; c) 21T in solution doped 5:1 with F ₄ TCNQ (red lines) compared to the pristine 8T in solution.	57
Figure 57: FT-IR spectra of 8T (red line), 13T (blue line) and 21T (green line) in solution doped 5:1 with F ₄ TCNQ compared to P3HT in solution doped 5:1 with F ₄ TCNQ (pink line).	58
Figure 58: FT-IR spectra of 8T (red line), 13T (blue line) and 21T (green line) in solution doped 5:1 with F ₄ TCNQ compared to rraP3HT in solution doped 5:1 with F ₄ TCNQ (light green line).	58
Figure 59: C≡N stretching modes of 8T (red line), 13T (blue line) and 21T (green line) in solution doped 5:1 with F ₄ TCNQ compared to C≡N modes of F ₄ TCNQ in chloroform solution (light green line).	59

Figure 60: FT-IR spectra of 8T (red line), 13T (blue line) and 21T (green line) films doped 5:1 with F4TCNQ compared to P3HT film doped 5:1 with F4TCNQ (pink line) a) from 8000 cm^{-1} to 400 cm^{-1} ; b) from 1600 cm^{-1} to 600 cm^{-1} 61

Figure 61: FT-IR spectra of 8T (red line), P3HT (pink line) and rraP3HT (green line) films doped 5:1 with F4TCNQ from 1600 cm^{-1} to 700 cm^{-1} . The black dotted line indicates the centre of the band in the region α , while the black dotted circle highlights the polaron IR features. 61

Figure 62: $\text{C}\equiv\text{N}$ modes of 8T (red line), 13T (blue line) and 21T (green line) film doped 5:1 with F4TCNQ compared to $\text{C}\equiv\text{N}$ modes of F4TCNQ film (pink line). 62

Figure 63: FT-IR spectra of the oligomer 13T pristine in solution (brown line), doped F4TCNQ in solution with a ratio 10:1 (blue line) and 5:1 (red line). 63

Figure 64: FT-IR spectra of the oligomer 13T film pristine (brown line), doped F4TCNQ with a ratio 10:1 (blue line) and 5:1 (red line); the black dotted line highlights the band of pristine polymer. 63

Figure 65: Solution UV-vis absorption spectra of T2-T6 dissolved in DCM. [40] 64

Figure 66: FT-IR spectra of 8T (red line), 13T (blue line) and 21T (green line) films doped 5:1 with F4TCNQ compared to P3HT film doped 5:1 with F4TCNQ (pink line). The black arrow highlights the shift of the electronic transitions. 64

Figure 67: FT-IR spectra of film P3HT doped with iodine in vapour phase evolution in time (from doping to 30 minutes after doping) and after heating the film for 2, 4 and 6 minutes (respectively green, orange and blue lines). 66

Figure 68: comparison between IR spectra in the range 1500 cm^{-1} – 900 cm^{-1} of P3HT thin film doped by iodine vapours (blue line) and P3HT thin film deposited by solution doped 1:1 (red line). 67

Figure 69: IR spectra in the range 1700 cm^{-1} – 900 cm^{-1} of a) P3HT thin film doped by iodine vapours evolution in time leaving them at room temperature; b) comparison P3HT thin film after doping by vapour (red line) and after 30 minutes (blue line). ... 68

Figure 70: comparison between the first component that disappear in time (red line: subtraction spectra between the film doped with iodine vapour – film doped iodine vapour after 30 min) and the component I seen in the doped P3HT solution 25:1 (blue line). 68

Figure 71: IR spectra in the range 1700 cm^{-1} – 700 cm^{-1} of a) film P3HT doped with iodine vapour after 30 minutes (blue line) and after heating the film for 2, 4 and 6 minutes (respectively green, orange and red lines); b) comparison between P3HT thin film doped by vapour after 30 minutes (blue line) and after heating for 6 minutes (red line). 70

- Figure 72: FT-IR spectra of P3HT thin film doped by vapour after 30 minutes (blue line), same film after heating it for 6 minutes (purple line) and the subtraction spectra between the film doped with iodine vapour after 30 min – film doped iodine vapour after heating 6 min (red line). 70
- Figure 73: comparison between FT-IR spectra of P3HT doped in solution 1:1 (blue line) with the subtraction spectra between the film doped with iodine vapour after 30 min – film doped iodine vapour after heating 6 min (red line). 71
- Figure 74: comparison between IR spectra in the range $1500\text{ cm}^{-1} - 900\text{ cm}^{-1}$ of P3HT film doped by iodine vapour (red line) and P3HT film deposited by solution doped 5:1 (blue line). 71
- Figure 75: FT-IR spectra of rraP3HT film doped with iodine in vapour phase evolution in time (from doping to 35 minutes after doping) a) from 8000 cm^{-1} to 400 cm^{-1} , b) from 1800 cm^{-1} to 400 cm^{-1} 73
- Figure 76: FT-IR spectra of rraP3HT film doped with iodine in vapour phase evolution in time (from 35 minutes after doping to 60 minutes after doping) and after heating the film for 1, 2 and 3 minutes (respectively orange, blue and purple lines) a) from 8000 cm^{-1} to 400 cm^{-1} , b) from 1800 cm^{-1} to 400 cm^{-1} 74
- Figure 77: IR spectra of rraP3HT film doped by iodine vapour for 2 minutes collected after 60 minutes and heated for 3 minutes (purple line) compared to the pristine film (pink line). 74
- Figure 78: IR spectra in the region between 1600 cm^{-1} and 600 cm^{-1} of rraP3HT film doped by iodine vapour for 2 minutes (red line) compared to P3HT doped iodine 5:1 by solution (blue line). 75
- Figure 79: IR spectra in the region between 1600 cm^{-1} and 800 cm^{-1} of rraP3HT film doped by iodine vapour for 2 minutes (red line) compared to rraP3HT doped iodine 5:1 by solution (purple line) and the IR spectra of the charged transfer complex (green line). 76
- Figure 80: P3HT in solid state (film): FT-Raman spectrum of the pristine sample (blue line), FT-Raman spectrum (pink line) and IR spectrum (red line) of iodine doped 5:1 P3HT a) from 3700 cm^{-1} to 400 cm^{-1} b) from 1600 cm^{-1} to 400 cm^{-1} 78
- Figure 81: FT-Raman spectra of P3HT solution in CHCl_3 doped iodine 25:1 (green line), 5:1 (blue line) and 1:1 (red line) normalized in respect with the band at 1200 cm^{-1} attributed to CHCl_3 vibrations. 80
- Figure 82: schematic representation of the three different components observed in the FT-Raman spectra at i) $1435 = 1445 + 1430\text{ cm}^{-1}$, ii) 1430 cm^{-1} and iii) $1410 - 1400\text{ cm}^{-1}$. The blue rectangle and the dotted ones represent respectively the extension of

the polaron and the extension of the portion of neutral polymer chain perturbed by the defect.	82
Figure 83: FT-Raman spectra in the region between 1550 cm^{-1} and 1300 cm^{-1} of film from P3HT iodine doped solution 25:1 (blue line); 5:1 (dark green line) and 1:1 (red line) compared to P3HT pristine film (light green line).....	83
Figure 84: FT-Raman spectra in the region between 1550 cm^{-1} and 1300 cm^{-1} of film from P3HT F4TCNQ doped solution 25:1 (blue line); 5:1 (dark green line) and 1:1 (red line) compared to P3HT pristine film (light green line).....	84
Figure 85: FT-Raman spectra in the region between 1550 cm^{-1} and 1300 cm^{-1} of iodine doped P3HT solutions 25:1 (blue line); 5:1 (green line) and 1:1 (red line) compared to P3HT pristine in solution of CHCl_3 (pink line). The two dotted lines highlight the components at 1430 cm^{-1} and 1410 cm^{-1}	85
Figure 86: FT-Raman spectra in the region between 1550 cm^{-1} and 1250 cm^{-1} of F4TCNQ doped P3HT solutions 25:1 (blue line); 5:1 (green line) and 1:1 (red line) compared to P3HT pristine in solution with CHCl_3 (pink line).	86
Figure 87: FT-Raman spectra in the region between 1550 cm^{-1} and 1250 cm^{-1} of F4TCNQ doped P3HT solutions 25:1 (blue line) compared to P3HT pristine in solution with CHCl_3 (pink line) and in solid film (light green line).....	86
Figure 88: FT-Raman spectra in the region between 1550 cm^{-1} and 1250 cm^{-1} comparison of iodine doped (red lines) and F4TCNQ doped (blue lines) P3HT solutions 25:1 (a); 5:1 (b) and 1:1 (c).	87
Figure 89: FT-Raman spectra in the region between 1550 cm^{-1} and 1250 cm^{-1} comparison of iodine doped P3HT solutions (red lines) and film (blue lines) 25:1 (a); 5:1 (b) and 1:1 (c).	88
Figure 90: FT-Raman spectra in the region between 1550 cm^{-1} and 1250 cm^{-1} comparison of F4TCNQ doped P3HT solutions (red lines) and film (blue lines) 25:1 (a); 5:1 (b) and 1:1 (c).	89
Figure 91: FT-Raman spectra in the region between 1530 cm^{-1} and 1350 cm^{-1} of pristine rraP3HT in solution with chloroform (red line) and in solid film (dark blue line) compared to pristine rreP3HT in solution with chloroform (green line) and in solid film (light blue line).	90
Figure 92: FT-Raman spectra in the region between 1600 cm^{-1} and 1200 cm^{-1} of rraP3HT doped F4TCNQ 5:1 in solution.	91
Figure 93: FT-Raman spectra in the region between 1700 cm^{-1} and 1000 cm^{-1} of rraP3HT film doped F4TCNQ 5:1 in solution.	92

Figure 94: FT-Raman spectra in the region between 1650 cm^{-1} and 1300 cm^{-1} of pristine P3DT in solution with chloroform (red line) and in solid film (blue line). 93

Figure 95: FT-Raman spectra of P3DT doped F_4TCNQ solution 5:1..... 94

Figure 96: FT-Raman spectra of P3DT film doped F_4TCNQ in solution 5:1. 95

Figure 97: FT-Raman spectra of pristine oligothiophenes in solution: 8T (red line), 13T (blue line) and 21T (green line). 96

Figure 98: FT-Raman spectra of pristine oligothiophenes films: 8T (red line), 13T (blue line) and 21T (green line)..... 96

Figure 99: FT-Raman spectra of oligothiophenes doped F_4TCNQ 5:1 in solution: 8T (red line), 13T (blue line) and 21T (green line). 97

Figure 100: FT-Raman spectra of oligothiophenes in solution pristine 8T (light green line), 13T (blue line) and 21T (pink line) compared to oligothiophenes doped F_4TCNQ 5:1 in solution 8T (red line), 13T (dark blue line) and 21T (dark green line). The peak at 1200 cm^{-1} is due to the presence of chloroform. 98

Figure 101: FT-Raman spectra of film of doped F_4TCNQ 5:1 in solution 8T (red line), 13T (blue line) and 21T (green line) compared to 13T film pristine (brown line)..... 99

List of Tables

Table 1: doping ratio and concentration of the solutions of pristine P3HT in CHCl ₃ and of I ₂ in CHCl ₃	8
Table 2: doping ratio and concentration of the solutions of pristine P3HT in CHCl ₃ and of F ₄ TCNQ in CHCl ₃	8
Table 3: wavenumbers of the three components I, C and P observed in the IR spectra of P3HT solution doped iodine/F ₄ TCNQ at the three doping ratio.....	21
Table 4: peaks corresponding to the C≡N stretching modes in neutral F ₄ TCNQ in CHCl ₃ and in the three P3HT doped solutions.	27
Table 5: height of the band N ₁ (corresponding to neutral F ₄ TCNQ) and A ₁ (corresponding to anion F ₄ TCNQ ⁻); % of F ₄ TCNQ and F ₄ TCNQ ⁻ for solution of F ₄ TCNQ-doped P3HT in the three different doping levels.....	30
Table 6: peak frequencies of the band ν_1 for the pristine P3HT film and the three doped films with I ₂ and F ₄ TCNQ.	84
Table 7: frequencies of the band ν_1 for the pristine P3HT solution and the three doped solutions with I ₂ and F ₄ TCNQ.	87
Table 8: summary table with all the wavenumbers of the bands in region α of the IR spectra, wavenumbers of the bands corresponding to the C≡N stretching vibrations of F ₄ TCNQ and band ν_1 in the Raman spectra with comments.....	102

Acknowledgments

I would like to express my sincere gratitude to my advisor and co-advisor, Prof. Luigi Brambilla and Prof. Chiara Castiglioni, for giving me the opportunity to carry out this thesis work individually, but always knowing I could rely on their valuable advice and help.

I would also like to thank my family without whom none of this would be possible. I am extremely grateful to my family for their love, encouragement, and understanding during this challenging journey.

I extend my appreciation to my friends and colleagues who provided me with encouragement and motivation when needed. Thanks for sharing with me all the most difficult and important moments of this five years.

Lastly, I would like to thank the reader for taking the time to delve into this thesis. Your interest and attention are truly appreciated.

